Study on the Role of Calcium in Photosynthetic Oxygen Evolution

Thesis Presented for the Degree of
Doctor of Philosophy in
the University of London
by

Christopher John Lockett

Department of Biology
University College London
London

October 1989

Acknowledgements

I would like to thank Dr Jonathan Nugent for his help and supervision during my research project, and to thank all my research colleagues for their help and encouragement.

I would also like to thank the SERC for funding my studentship and my attendance at the VIIIth international congress on photosynthesis in Stockholm.

Abstract

Three extrinsic polypeptides of molecular mass 17, 23, 33 kDa and 4 manganese ions associated with photosystem II are involved in the oxygen evolution process. Calcium and chloride ions are essential for oxygen evolution. If the 17 and 23 kDa polypeptides are depleted, mM concentrations of both ions have to be supplied for maximum oxygen evolution.

The depletion of calcium ions from preparations of oxygen evolving photosystem 2 was investigated. Calcium ions were found to be accessible to depletion when the 17 and 23 kDa polypeptides were depleted. Calcium depletion was monitored by observing the S_2 state multiline epr signal and measuring the rate of oxygen evolution. Calcium appeared to play an essential role in oxygen evolution. Strontium and vanadyl ions were the only divalent cations that partially replaced the role of calcium. When calcium ions were depleted in the S_0 state there was no formation of the S_2 state multiline epr signal and oxygen evolution was inhibited. Other calcium depletion methods inhibited oxygen evolution, but did not inhibit the formation of the S_2 state multiline epr signal. The role of the tyrosine D in oxygen evolution and the effect of calcium depletion on this component was investigated. D was found to have a role in reseting the oxygen evolving complex to the S_1 state in the dark. This did not occur after calcium depletion in the S_0 state.

CONTENTS

ABBREVIATIONS

ADP, adenosine diphosphate;

ATP, adenosine triphosphate;

Chl, chlorophyll;

D, the tyrosine residue 160 of the D2 polypeptide of PS2;

D1 and D2, reaction centre binding polypeptides of PS2;

DCMU, 3 - (3,4 - dichlorophenyl) - 1,1 - dimethylurea;

DMBQ, 2,6 - dimethylbenzoquinone;

DPC, 1,5 - diphenylcarbazide;

EPR, electron paramagnetic resonance;

EDTA, ethylenediaminetatraacetate;

EGTA, ethyleneglycol bis (B - aminoethyl ether) - N,N,N',N' - tetraacetic acid;

EXAFS, extended x - ray absorption fine structure;

LHC2, light harvesting complex of PS2;

Mes, 2 - (N - morpholino) ethanesulfonic acid;

$NADP^+$, oxidised nicotinamide adenine dinucleotide phosphate;

OEC, oxygen evolving complex;

OGP, n - octyl B - D glucopyranoside;

PEG, polyethylene glycol compound (m.w. 15,000 - 20,000);

PPBQ, phenyl - p - benzoquinone;

PS2, photosystem two;

Q_A, primary quinone electron acceptor of PS2;

Q_B, secondary quinone electron acceptor of PS2;

SDS, sodium dodecyl sulphate;

TEMED, tetramethyl - ethylene diamine;

Tris, tris (hydroxymethyl) aminomethane;

Z, the tyrosine residue 161 of the D1 polypeptide of PS2;

TABLE OF CONTENTS

CHAPTER 1 : INTRODUCTION

FIGURES

PLATES

CHAPTER 1

INTRODUCTION

1.1 The Photosynthetic Apparatus

Oxygenic photosynthesis is carried out by higher plants, algae and cyanobacteria. The photosynthetic apparatus of higher plants and algae is contained within chloroplasts (Fig. 1. a). The chloroplast organelle is formed by an inner and outer membrane. The thylakoid membranes (Fig. 1. b), within the chloroplast, consist of appressed (or stacked) granal and unstacked stromal regions. The stroma is the aqueous phase of the chloroplast containing a solution of enzymes involved in light independent carbon fixation.

Chloroplasts and cyanobacteria are thought to have common evolutionary ancestors, possibly a prokaryotic alga, like Prochloron. From this common ancestor the cyanobacteria and chloroplasts are thought to have developed along parallel lines of evolution. Photosynthetic bacteria, including cyanobacteria, have a typical prokaryotic membrane arrangement. The photosynthetic membranes are connected to the plasma membrane and are not within a seperate organelle. The membranes are not divided into stacked or unstacked regions. Photosynthesis carried out by cyanobacteria is very similar to that of higher plants involving two photosystems located in membrane protein complexes.

Figure 1.1 The Chloroplast and the Arrangement of the Membrane Spanning Proteins within the Thylakoids.

(a)

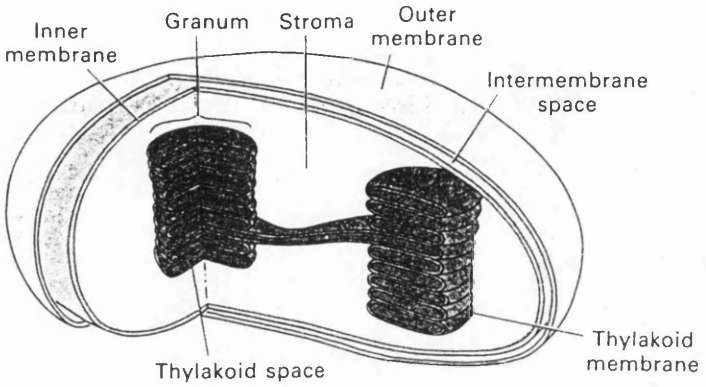

(b)

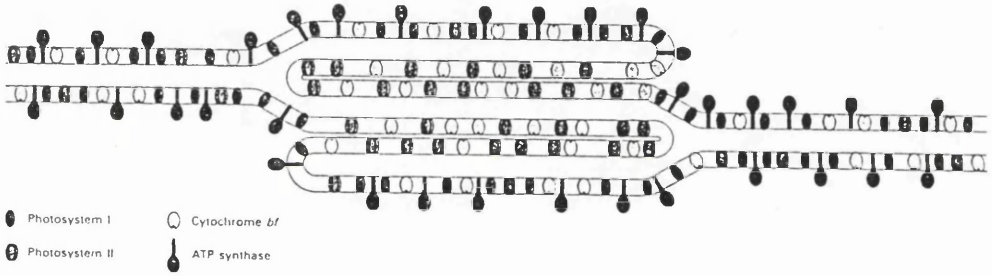

The chloroplast (a) is surrounded by a two membrane envelope, consisting of an inner and an outer plasmamembrane. These membranes have significant evolutionary implications. Chloroplasts are thought to have evolved from a symbiotic relationship between a green photosynthetic procaryote and a non photosynthetic eucaryote. The outer membrane is thought to be from the vacuole membrane of the host organism, whilst the inner membrane is thought to be from plasmamembrane of the symbiont. (Diagram from Wolfe (1972) Biology of the Cell). Chloroplast polypeptides coded for in the nucleus have to pass through both membranes and have at least two signal sequences to aid their passage. Within the chloroplast are two regions, an aqueous phase (the stroma - containing the enzymes involved in carbon fixation) and a membrane phase (the thylakoids). The light reactions occur in membrane bound protein complexes within the thylakoid membranes (b). Photosystem 2 complexes are located in the stacked regions (granal lamellae), whilst photosystem 1 and the ATP synthetase complexes are located in unstacked regions. (Diagram from Anderson & Andersson , 1982).

1.1.1 The Membrane Spanning complexes

Five membrane spanning protein complexes are involved in the light dependent reactions of photosynthesis (Fig. 2. a). Two photosystems, (labelled PS1 and PS2) with associated light harvesting chlorophyll complexes (shaded and labelled LHC2 in figure 2. a) and a cytochrome b6/f complex form the photosynthetic electron transport chain. This series of protein complexes generates a proton gradient across the photosynthetic membrane by "pumping" protons into the lumenal space. The oxidation of water molecules provides electrons for electron transport reactions. Oxygen and protons are released on the lumenal side of the thylakoid membrane. Figure 2. a shows the electron transfer events of the membrane bound protein complexes. Charge separation in photosystem 2 results in the reduction of the plastoquinone pool. Plastoquinone molecules (labelled PQ and PQH_2 in Figure 2.a) become protonated on the stromal side of the membrane and deprotonated on the lumenal side. The combined effect of the cytochrome b_6/f complex and photosystem 1 oxidises the plastoquinone pool. The sixth membrane spanning complex, the ATP synthetase, (labelled CF_o and CF_1) can utilise the proton gradient to generate ATP from ADP and phosphate. This process has the characteristics required by the chemiosmotic theory, first described to explain mitochondrial ATP production (Mitchell , 1961).

1.1.2 Lateral Heterogeneity of the Protein Complexes

The thylakoid membranes contained within chloroplasts of higher plants were discovered to have two distinct regions on examination using electron microscopy. Thylakoid membranes of higher plants were seen to have stacks of membranes termed grana or appressed regions and unstacked or stromal regions (Fig. 1. b). This difference in membrane arrangement has been linked to maintaining an even distribution of excitation energy between the two photosystems, but still remains a controversial topic. Experiments by Boardman & Anderson (1964) and Akerlund et al (1976) indicated that this membrane arrangement was linked with an uneven distribution of the proteins of photosynthetic electron transport. The light harvesting complexes LHC2 and PS2-A complexes have been shown to be preferentially located in the appressed regions of the thylakoid membranes and in exposed regions of the membrane stacks. The PS1 and ATPase complexes are found only in the unstacked stromal regions. The cytochrome b/f complexes can be found in both regions. Some PS2 complexes with reduced light harvesting chlorophyll can be found in the unappressed regions and these are known as B-units.

The stacking of thylakoid membranes is brought about by overcoming the repulsive electrical charges of adjacent membrane surfaces. Membrane surfaces are negatively charged and it is thought that cations,

particularly divalent cations, can to a certain extent neutralise this negative charge and allow stacking to occur. Phosphorylation and dephosphorylation of the mobile light harvesting chlorophyll complexes has been linked with this phenomenon. This process ensures that there is an equal distribution of excitation energy between the two photosystems, in all qualities of light. When the membranes are illuminated by light favouring PS2 excitation, phosphorylation of the LHC2 complex occurs. This is brought about by a membrane bound protein kinase, controlled by the redox state of the plastoquinone pool (Staehelin & Arntzen , 1983). The phosphorylated LHC2 complexes dissociate from PS2 and migrate to the unappressed thylakoid regions, decreasing the turnover of PS2. The PS2 enriched membrane surfaces have a lower net negative charge and tight membrane stacking occurs. PS1 is then able to oxidise the plastoquinone pool. The kinase is deactivated when the pool of plastoquinone is over oxidised. The mobile light harvesting complexes are then dephosphorylated by a membrane bound phosphatase. The LHC2 complexes can then reassociate with the photosystem II A-units.

It has been suggested that membrane stacking is necessary for efficient regulation of energy distribution. This theory however has several associated problems. Firstly cyanobacteria and red algae show excitation energy distribution but there is no membrane

Figure 2. Electron Transfer Events of the Light Reactions of Photosynthesis.

The Z scheme is a plot of electron transfer events, from water to $NADP^+$, using the midpoint redox potential of each component. This scheme has been widely used to explain the light reactions of photosynthesis. Diagram (a) shows the electron events within each membrane spanning protein complex. Solid lines indicate electron flow and dashed lines indicate proton flow. (Diagram from Anderson & Andersson , 1982). A proton gradient is formed, and protons from the lumenal space are used by the ATP synthetase to generate ATP.

The electron transfer events that occur in PS2 are shown in detail in diagram (b). The solid lines indicate the kinetics of electron transfer at room temperature. The dashed lines are recombination reactions, which give rise to fluorescence. The components are : P680, the reaction centre chlorophyll; Ph, pheophytin; Q_A^-, the primary semiquinone electron acceptor; Q_B^-, the secondary electron acceptor; Tyr Z, tyrosine which donates electrons removed from the manganese complex to the P680 chlorophyll. (Diagram from Rutherford , 1989).

(a)

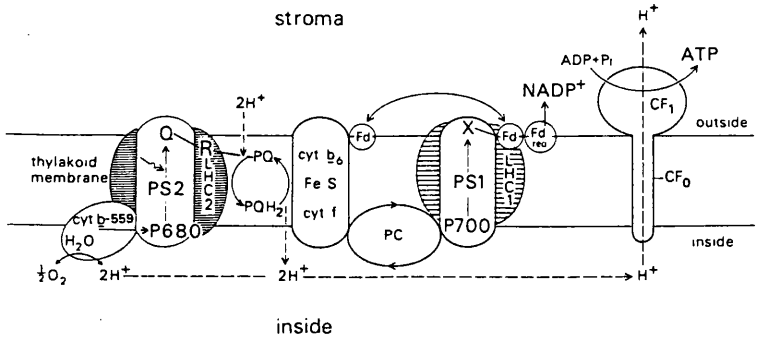
stroma
inside
thylakoid membrane
PS2
PS1
P680
P700
Q
PQ
PQH2
cyt b6
Fe S
cyt f
PC
Fd
X
Fd red
NADP+
ADP+Pi
ATP
CF1
CF0
outside
inside
cyt b-559
H2O
½O2
2H+
H+

(b)

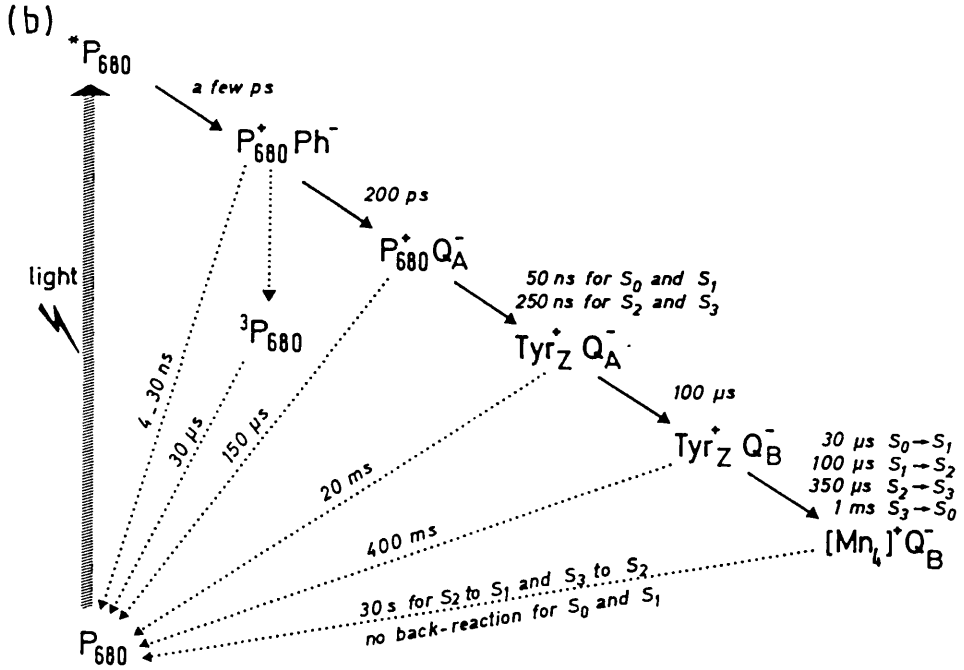
*P680
a few ps
P680+ Ph-
200 ps
P680+ QA-
50 ns for S0 and S1
250 ns for S2 and S3
TyrZ+ QA-
100 µs
TyrZ+ QB-
30 µs S0→S1
100 µs S1→S2
350 µs S2→S3
1 ms S3→S0
[Mn4]+ QB-
light
3P680
4 - 30 ns
30 µs
150 µs
20 ms
400 ms
30 s for S2 to S1 and S3 to S2
no back-reaction for S0 and S1
P680

stacking or lateral heterogeneity of protein complexes. Phosphorylation of polypeptides and light harvesting complexes still occurs, regulating the amount of excitation energy received by each photosystem. The other problem is how the LHC2 complexes migrate rapidly between the stacked and unappressed regions. The changes in energy distribution occur in milliseconds, faster than the protein complexes can migrate. The reasons for membrane stacking and lateral heterogeneity are still unclear.

1.1.3 Photosynthetic Electron Transport

The purpose of photosynthetic electron transport is to provide enough reducing potential to reduce $NADP^+$, used in the Calvin cycle for carbon fixation, and to produce a proton gradient for ATP production. The "Z" scheme has been a useful model to describe the process of photosynthetic electron transport (Fig. 2.).

The electron transport chain of events begins when the light harvesting chlorophylls of one or both photosystems become excited by light energy. This excitation energy captured by the accessory chlorophylls is transferred through other chlorophyll molecules to a reaction centre chlorophyll. A light induced charge separation occurs when an electron from the excited chlorophyll molecule "jumps" to the primary electron acceptor (initially by quantum tunnelling). There is a series of components involved in the transport of

electrons away from the reaction centre, stabilising charge separation and leading to the reduction of $NADP^+$ and/or proton pumping. The events following charge separation in photosystem 2 are summarised in figure 2.b. The transfer of electrons from excited P680 to Q_B shown as solid lines. Recombination of electrons with oxidised P680 are indicated by dashed lines.

1.2 Reaction Centre Polypeptides

The purple photosynthetic bacteria are not able to use water molecules as an electron donor. Instead they use organic acids and sulphur compounds, particularly H_2S as an electron source. Three polypeptides (Light L, Medium M and Heavy H) form the reaction centre (Okamura et al, 1982). Some purple bacteria (e.g. Rhodopseudomonas viridis) have a fourth polypeptide containing four cytochrome haems. These cytochromes are reduced by H_2S and succinate. The L and M subunits bind the reaction centre components. The amino acid sequences of the L and M sub units (Williams et al, 1983) were found to have homology with each other, both having five membrane spanning regions. Homologies were seen between L and M and the amino acid sequences of the D1 and D2 polypeptides of photosystem II (Zurawski et al, 1982). In particular L shows homology with D1 (Youvan et al 1984),(Williams et al, 1984) & (Michel , 1986) and M shows homology with D2 (Deisenhofer et al 1985) & (Michel & Deisenhofer , 1986). Each of these

polypeptides are proposed to have five hydrophobic membrane spanning regions, which are involved in binding the reaction centre complex.

Crystals of the purple bacterial reaction centre were obtained, and after crystallographic analyses the arrangement of the reaction centre components were determined. The similarities between the bacterial and higher plant PS2 reaction centre, particularly in conserved regions involved in reaction centre co-factor binding, was taken as strong evidence that the purple bacterial reaction centre is the ancestor of the PS2 reaction centre of higher plants (Michel & Deisenhofer , 1988) and (Feher et al, 1989).

Further evidence that D1 and D2 are the polypeptides which bind the reaction centre components in higher plants was provided by the isolation of a complex consisting of D1, D2, a 4.8kDa polypeptide and the 4 and 9 kDa cytochrome b_{559} polypeptides (Nanba & Satoh , 1987). The reaction centre complex consists of 4 chlorophyll a molecules, 1 B-carotene, 1 haem iron and probably 1 non haem iron. This complex was shown to be photochemically active by demonstration of photoreduction of pheophytin.

1.3 Photosystem II

Photosystem II is involved in the splitting of water into protons and dioxygen on the lumenal side of the membrane. A protein complex, called the oxygen evolving

complex (OEC), associated with photosystem II is involved in the catalysis of the water splitting reaction. The reaction centre chlorophyll (a monomer or a dimer) is located between D1 and D2 towards the lumenal side of the membrane. It is bound by an amino acid sequence containing histidine residues that are conserved in the L and M subunits of the purple bacterial reaction centre. The absorption of light of 680nm results in a charge separation across the membrane and the oxidation of P680 chlorophyll. The primary electron acceptor is a pheophytin molecule, which when reduced can pass an electron to the quinone electron acceptors (Fig. 2. b). Iron-quinone electron acceptors are located on the stromal side of the thylakoid membranes, and conserved histidines in this region are involved as ligands to the non haem iron. The charge separation is stabilized by the migration of the electron from Q_A to Q_B, resulting in the two electron reduction of plastoquinone to plastoquinol (PQH_2). The water splitting process provides electrons to reduce the oxidised P680 reaction centre chlorophyll. The structure and function of photosystem II and the numerous associated polypeptides will be discussed in detail in later sections.

1.4 <u>The Oxygen Evolving Complex (OEC)</u>

Water oxidation is known to occur at or near the lumenal surface of the thylakoid membrane, consistent with the location of the bound manganese associated with

the process. The four manganese ions involved in water splitting are located in a binding site formed by intrinsic polypeptides. Candidates for polypeptides involved in forming the manganese binding site include the D1, D2, 47 and 43 kDa polypeptides. Other lower molecular weight polypeptides may also be involved. The extrinsic 33 kDa polypeptide may have a role in stabilizing the manganese complex and may also provide some ligands to the complex (Hunziker et al, 1987). The C termini of the D1 and D2 polypeptides are highly conserved in all oxygen evolving organisms and are rich in histidine, aspartate and glutamate. As these regions are largely missing in the L and M subunits of the purple bacteria, which have no oxygen evolving complex, it has been suggested that these amino acids may play a role in providing ligands to the manganese complex. The cytochrome binding polypeptide of some purple bacteria (e.g. Rhodopseudomonas viridis) contains four cytochrome haems of different redox potential and these provide the electrons to reduce the bacterial reaction centre chlorophyll. Although this polypeptide binds in the same region as the OEC of higher plants it is not an evolutionary precursor of the oxygen evolving complex.

The OEC of photosystem II catalyses the light driven oxidation of water to oxygen. This is a four electron oxidation of the manganese cluster, which is produced by successive reduction of the $P680^{+}$ chlorophyll. The

Figure 3. The S state cycle of Oxygen Evolution

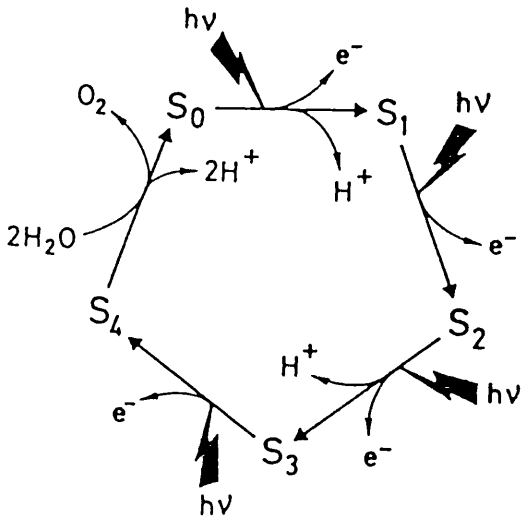

The S state cycle proposed by Kok et al in 1970 is a model used to describe the accumulation of four positive charges necessary for water oxidation. The model is based on the yield of oxygen following a sequence of single saturating laser flashes. Oxygen yield has a four flash periodicity after 4 hours dark adaptation. Under normal conditions of illumination there is a random distribution of each S state. The S_4 state is an undetected transient state, rapidly forming the S_0 state concomitant with the release of oxygen. Therefore at any one time during illumination there will be a 25 % population of the S_1, S_2, S_3 and S_0 state. In the dark the S_2 and S_3 states decay rapidly to the dark stable S_1 state. The S_0 state is oxidised more slowly to the S_1 state in the dark. After 4 hours a 100 % population of the S_1 state is achieved (Vermaas W.F.J. et al, 1984). A possible scheme for proton release is shown. This 0:1:0:2:1 pattern of proton release however is not detected. It has been suggested that proton release is dependent on the protonation state of the surrounding polypeptides (Junge , 1989). hv: saturating laser flash, e^-: electron. (Diagram from Rutherford , 1989).

manganese cluster is able to store the oxidising potential produced after each charge separation, in the form of a cycle of five intermediates. An S state cycle of oxygen evolution was proposed after studying the 4 saturating laser flash periodicity of oxygen evolution (Kok et al, 1970) (Fig. 3.).

Very little is known about the oxidation states and structure of the manganese ions in each S state. EPR and X-ray absorption spectroscopy are particularly useful techniques for the study of this problem.

It is not clear what is the minimum number of components for oxygen evolution. A highly purified oxygen evolving core complex has been isolated, consisting only of D1, D2, a 4.8 kDa polypeptide, the 43 and 47 kDa chlorophyll binding polypeptides, the extrinsic 33 kDa polypeptide, the 4 and 9 kDa cytochrome b_{559} associated polypeptides (Ghanotakis et al, 1987).

1.5 The Tyrosine Radicals Z and D of PS2

Two tyrosine molecules termed Z and D are now known to be involved in the process of oxygen evolution. When oxidised both of these molecules have a typical epr signal at g = 2.0046. Signal II was the first epr signal to be associated with electron transfer in PSII (Commoner et al, 1956) & (Kohl et al, 1969) and can be detected in both chloroplast membranes and PS2 preparations.

Electron transfer from the manganese cluster to the oxidised chlorophyll proceeds through an intermediate

charge carrier known as Z. The oxidised form Z^+ gives rise to the characteristic epr signal II with very fast decay kinetics (Warden , 1976) and (Babcock , 1987). When the manganese cluster is destroyed or uncoupled from Z, its oxidised form gives rise to a similar signal with slower reduction kinetics called signal II_{fast} (Babcock & Sauer , 1975).

The other tyrosine molecule on the donor side of PS2 with the same characteristic signal II is a component D^+. This signal has much slower decay kinetics and is consequently called signal II_{slow} (Babcock & Sauer 1973). This component does not change oxidation state during oxygen evolution in the light and is not involved in the transfer of electrons from the oxygen evolving complex to $P680^+$. The role of D is thought to be one of stabilisation and deactivation of the manganese complex in the dark.

It was originally suggested that D^+ was a plastoquinone radical (Weaver , 1962) and later suggested to be a plastoquinone cation radical (Ghanotakis et al, 1983) and (O'Malley et al, 1984). The growth of a mutant of Anabaena variabilis, unable to synthesise methionine, in a medium containing deuterated methionine indicated that the species giving rise to the epr signal had not been deuterated (Barry & Babcock, 1987). This raised doubts that signal II was due to a plastoquinone. Synechocystis 6803 was grown on a medium

containing deuterated tyrosine and this gave rise to an epr spectrum indicative of deuterated D^+ (Barry & Babcock, 1987 & 1988). Site directed mutagenesis of the tyrosine 160 residue of the D2 polypeptide converting the tyrosine into phenyalanine lead to the loss of the D^+ epr signal (Vermaas et al, 1988) and (Debus et al, 1988). It has been concluded that D^+ is Tyr-160 of D2 and by symmetry that Z^+ is Tyr-161 of the D1 polypeptide.

1.6 The Electron Acceptor Side of Photosystem II

Two quinone electron acceptors are thought to be located in Q_A and Q_B binding sites located on the stromal side of the D1 and D2 polypeptides (Trebst , 1987) and (Michel & Deisenhofer , 1988) (Fig. 2. b). The Q_A and Q_B binding sites are proposed to be either side of the non haem iron atom, which is thought to be ligated to both D1 and D2. The quinone binding region of higher plant PS2 is thought to be structurally different from that of the purple bacteria. There is a requirement for bicarbonate for a maximum rate of electron transport to Q_B (Govindjee & Van Rensen , 1978). The reduction of the quinone electron acceptors results in the production of a semiquinone epr signal (arising from Q_A^- Fe interaction) (Nugent et al, 1981, and 1982), (Evans M.C.W. et al, 1982) and (Rutherford & Zimmermann , 1984). Two forms of the iron semiquinone epr signal have been observed. In untreated PS2 membranes a typical "g = 1.9" epr signal is observed during or

after illumination, which decays in the dark (Rutherford & Zimmermann , 1984). In the presence of formate or at low pH, a "g = 1.8" epr signal is formed instead of the "g = 1.9" form (Nugent et al, 1981). This indicates that formate or low pH causes the displacement of bicarbonate. The non-haem iron is also able to act as an electron acceptor when oxidised to Fe^{3+} from the Fe^{2+} form (Petrouleas & Diner , 1986), (Nugent & Evans , 1980) & (Wraight , 1985). A "g = 6" epr signal from the oxidised iron can be observed after conditions of illumination which encourage electron transport to Q_B. Bicarbonate is thought to play a central role in electron transfer, binding at or close to the non-haem iron and is thought to provide the correct characteristics for the Q_B binding site. (Nugent et al, 1988)

1.6.1 The Acceptor side of OGP PS2

The electron acceptor side of oxygen evolving core complexes is known to be modified during treatment with OGP detergent (Ghanotakis & Yocum , 1986). DCMU does not inhibit oxygen evolution of OGP PS2 as efficiently as it does PS2 membranes.

1.6.2 The Affect of Trypsin on the Acceptor side of PS2

Trypsin has been used to modify the electron acceptor side of PS2 (Regitz & Ohad , 1976). The enzyme probably cuts the D1 polypeptide at arg 238 and the D2 polypeptide at arg 234. This treatment renders the

PS2 membranes insensitive to DCMU /triazine type inhibitors (Trebst et al, 1988). The presence of these type of inhibitors and to a certain extent the presence of bound plastoquinone inhibits the effect of trypsin. It has been postulated that the region of D1 around arg 238 is involved in forming the Q_B binding site, and the conformation of this region is altered in the presence of plastoquinone or DCMU /triazine inhibitors preventing the accessibility of the site to trypsin. Calcium chloride also prevents susceptibility to trypsin attack on DCMU /triazine inhibitor binding and p-BQ mediated electron transport (Renger et al, 1986 and 1988).

1.7 The Polypeptide Composition of PS2

1.7.1 Polypeptides Associated with Oxygen Evolution

The chloroplast and nuclear encoded polypeptides are listed in figure 4. Three nuclear encoded extrinsic polypeptides have been shown to play an important role in the water splitting process. Optimal oxygen evolving activity has been shown to be dependent on the presence of two extrinsic polypeptides of mass 17 and 23 kDa (Murata & Miyao , 1985), which can be removed from "inside out" thylakoids and PS2 membranes by treatment with salt (Akerlund et al, 1982; Miyao & Murata , 1983; Ghanotakis et al, 1984) (Fig. 5. b). These polypeptide depleted membranes show low rates of oxygen evolution without the addition of excess calcium and chloride ions (Ghanotakis et al, 1984; Miyao & Murata

Figure14. The Polypeptides of Photosystem 2

Gene	Polypeptide	(mol. mass)
Chloroplast Encoded Polypeptides		
psb A	D1 polypeptide	(32 kDa)
psb B	Light harvesting	(47 kDa)
psb C	Light harvesting	(43 kDa)
psb D	D2 polypeptide	(34 kDa)
psb E	Cytochrome b_{559}	(9 kDa)
psb F	Cytochrome b_{559}	(4 kDa)
psb G	poss NADPH dehydrogenase	(24 kDa)
psb H	Phosphoprotein	(9 kDa)
psb I	RC polypeptide	(4.8 kDa)
psb J	Hypothetical polypeptide predicted from orf 53.	-
psb K	-	(2.0 kDa)
psb L	"orf 38"	(3.2 kDa)
psb N	"orf 34" (Ikeuchi et al, in press)	-
Nuclear Encoded Extrinsic Polypeptides		
Chloride concentrator		(17 kDa)
Calcium concentrator		(23 kDa)
Manganese stabiliser "MSP"		(33 kDa)
Polypeptide removed by Tris wash		(10 kDa)
Nuclear Encoded Intrinsic Polypeptides		
LHC2 (composed of several polypeptides of around 24 kDa)		

Photosystem 2 consists of both chloroplast and nuclear encoded polypeptides. The components of the PS2 reaction centre core are coded for in the chloroplast. The genes coding for the extrinsic polypeptides involved in oxygen evolution and the light harvesting polypeptides are coded for in the nucleus. This suggests that these polypeptides have either evolved after the evolution of the symbiotic relationship or the genes coding for these polypeptides have been moved from the symbiont to the host nucleus.

Figure 1-5. Extrinsic Polypeptides Removed by Different Ionic Washes

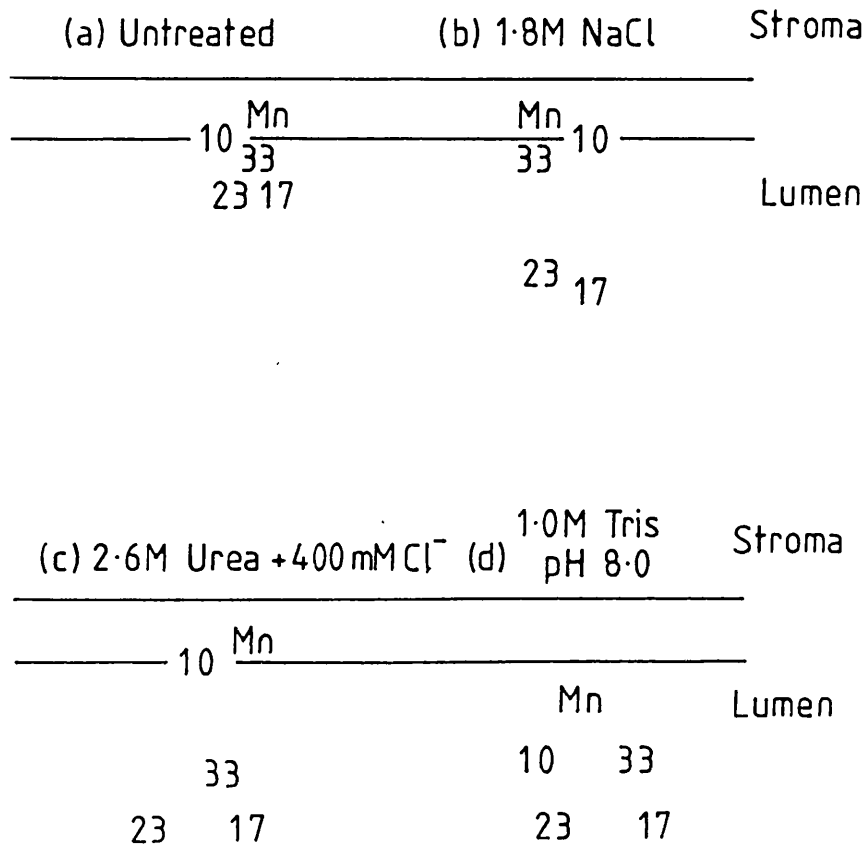

Extrinsic polypeptides of molecular mass 10, 17, 23 and 33 kDa, plus a cluster of 4 manganese ions per PS2 complex are present in untreated PS2 membranes (a). These can be removed from PS2 membranes using washes of differing ionic strengths. A 1.8 M NaCl wash removes the 17 and 23 kDa polypeptides only (b). The 33 kDa polypeptide can be removed separately after this treatment by washing with 2.6 M urea, or along with the 17 and 23 kDa polypeptides when performed on untreated PS2 (c). The same effect is achieved using 2.0 M divalent cations. Manganese ions remain bound to the PS2 membranes during these procedures if at least 400 mM chloride is maintained. All four extrinsic polypeptides are removed and the manganese cluster is destroyed when PS2 membranes are treated with 1.0 M Tris pH 8.0 (d).

, 1985; Imaoka et al, 1984). This effect has been linked with these polypeptides acting as calcium and chloride concentrators, or with non physiological amounts of calcium and chloride ions replacing the polypeptide functions.

The 33 kDa polypeptide stabilizes the manganese cluster in its site (Ono & Inoue ., 1983; Kuwabara et al, 1985). It has been reported that the manganese cluster remains intact and attached to its binding site, under suitable conditions, after the removal of the 33 kDa polypeptide (Ono & Inoue, 1983 ; Miyao & Murata, 1984) (Fig. 5. c). Very low rates of oxygen evolution have been reported after the removal of the 33 kDa polypeptide (Miyao et al, 1987), although this may be due to small amounts of the 33 kDa polypeptide remaining attached (Hunziker & Dismukes, 1987). A 10 kDa extrinsic polypeptide is removed with the other extrinsic polypeptides, and the manganese cluster is destroyed when the PS2 membranes are treated with 1.0 M Tris pH 8.0 (Fig. 5. d).

1.7.2 Low Molecular Weight Polypeptides of PS2

Until recently only a few low molecular weight polypeptides, including the 9 kDa large sub unit of cytochrome b_{559} (psb E), were identified. Several low molecular mass polypeptides (less than 10kDa) have now been reported, but their physiological functions are not yet known. PS2 membrane fragments have been reported to

contain at least nine low molecular weight polypeptides of between 3.9 kDa and 11 kDa, all of which occur in thylakoid membranes (Ikeuchi & Inoue , 1988). Oxygen evolving core complexes have been reported to contain a 9 kDa phosphoprotein (psb H), polypeptides of mass 5.0 kDa, 4.8 kDa (psb I) and 4.1 kDa, plus the 9.4 kDa (psb E) and 4.4 kDa (psb F) sub units of cytochrome b_{559} (Ikeuchi et al, 1989).

There are strong similarities between the low molecular weight polypeptides of cyanobacterial and higher plant PS2 membranes. A 9 kDa polypeptide however, that is found in cyanobacterial PS2 membranes, has no homlogous polypeptide in higher plant PS2 membranes (Stewart et al, 1985a & 1985b). This polypeptide is removed from cyanobacterial PS2 membranes when glycerol is not present and when the membranes are treated with 0.8 M alkaline Tris, 1.0 M NaCl, $CaCl_2$ or $MgCl_2$. Loss of this polypeptide has been shown to be correlated with the loss of oxygen evolving activity (Stewart et al 1985b). The loss of oxygen evolution on removal of the 9 kDa polypeptide is reversed by the re-addition and re-binding of the polypeptide but oxygen evolution is not restored by the addition of excess calcium and chloride ions. Cyanobacterial PS2 membranes contain no polypeptides homologous with the 17 and 23 kDa polypeptides of higher plants, but there is no evidence to suggest that the 9 kDa polypeptide has a similar

function.

1.8 The Manganese Complex of PS2

1.8.1 Location and Structure of the Manganese Ions

The fact that 4 manganese ions are involved in photosynthetic oxygen evolution is mostly agreed upon. These manganese ions are not equivalent, and have been shown to be released in pairs (Kuwabara & Murata , 1983), (Packham & Barber , 1984) with one pair more tightly bound than the other. Manganese (II) ions rebind in pairs to Tris washed PS2 membranes (Tamura & Cheniae , 1987).

The four manganese ions of the OEC are clustered on PS2 intrinsic polypeptides as discussed above, as a pair of dimers (Hansson . & Andreasson ., 1982) or as a tetramer (Dismukes & Siderer , 1981). Extended X - ray absorption fine structure (EXAFS) spectrometry has provided a certain amount of information about the ligand environment around the manganese. It has shown that nitrogen and oxygen atoms form the ligands to the manganese cluster (Yachandra et al, 1986). Histidine residues have been suggested to be involved in providing the nitrogen ligands to the manganese cluster (Tamura et al, 1989), whilst the oxygen ligands are probably provided by tyrosine and carboxyl side chains of the acidic amino acids.

EXAFS indicates that a manganese atom is approximately 2.7 A away from its nearest Mn atom and

possibly 3.3 A away from the other two (Yachandra et al, 1986). The EXAFS data for the S states transitions from the S_0 state to the S_3 state are similar. This suggests that only minor structural changes occur during these transitions (Sauer et al, 1988). The small changes probably reflect redox state changes of the manganese complex. Various conclusions can be drawn from the X-ray absorption data for the different S states. (1) The oxidation state of the manganese complex increases from S_0 to S_1 and from S_1 to S_2, with the loss of 1 electron, or at most 2 electrons in each step. The S_1 and S_2 states contain predominantly Mn (III) and Mn (IV) oxidation states. (2) The S_1 state resembles Mn (III) whilst the S_2 state more closely resembles Mn (IV) indicating an oxidation of Mn (III) to Mn (IV) during the S_1 to S_2 transition. (3) The EXAFS for the S_3 state is very similar to the S_2 state and this suggests there is no redox change or structural change from S_2 to S_3. This also rules out the cubane -like to adamantane -like tetranuclear structural shift suggested by Brudvig G.W. & Crabtree . 1986.

The reaction centre complex consisting of only D1 /D2 and the cytochrome associated polypeptides contains the high affinity manganese binding sites and is able to photo-oxidise Mn^{2+} or DPC (Tamura et al, 1989). D1 and D2 are probably the main manganese binding polypeptides, but the 43 and 47 kDa polypeptides may also be involved

in providing some ligands. The 33 kDa extrinsic polypeptide may bind to part of the functional manganese complex (Abramowicz & Dismukes , 1984), since its removal inhibits oxygen evolution. 23 glutamate or aspartate, 8 histidine and 7 tyrosine residues are exposed on the lumenal side of the D1 and D2 polypeptides. If a two fold symmetry for the binding of the manganese complex between D1 and D2 is applied as for the other components of the reaction centre, it is possible to suggest several regions of each polypeptide that could be involved in manganese binding.

Only two epr signals have been discovered which arise from the manganese cluster involved water splitting. These are the S_2 state multiline epr signal (Dismukes & Siderer 1980 & 1981) and (Brudvig et al, 1983) and the g = 4.1 epr signal (Casey & Sauer , 1984) & (Zimmermann & Rutherford ,1984). Both of these signals represent different forms of the S_2 state of the manganese cluster of the oxygen evolving complex. The S_2 state multiline epr signal occurs either as a "19 line" or a "16 line" spectrum after freeze thawing cycles (Dismukes , 1986). These spectra provide strong evidence that a 2-4 manganese ion cluster exists with the complex splittings arising from the interactions of the nuclear spins on the manganese atoms (Hannson & Andreasson , 1982) and (Dismukes et al, 1982). The 16 line form of the epr

signal is characteristic of dimanganese (III, IV) complexes. The 19 line form has not been satisfactorily modelled although trinuclear or tetranuclear manganese complexes are probable candidates (Dismukes ., 1986). Many structures for the manganese cluster have been proposed. For example a core of Mn_4O_5Cl arranged as a compressed right regular pyramid of 4 managanese atoms, with three u_3-oxo ligands and one u_3-chloro ligand has been suggested for the structure of the manganese cluster in the S_2 state (Dismukes , 1988). A catalytic binuclear cluster formed from a dimeric Mn (III,IV) core has also been suggested, with di- u-oxo bridges between the two manganese ions (Sauer . et al, 1988).

1.8.2. The LF1 Mutant of Scenedesmus obliquus

The low fluorescent mutant, LF1, of the green alga Scenedesmus obliquus is unable to carry out photosynthetic water splitting reactions (Metz C et al, 1980). The activity of the reaction centre of the mutant however, appears to be normal. The LF1 mutant appears to be affected primarily in its ability to bind manganese. There is less than half the usual manganese content per reaction centre in thylakoid membranes isolated from the mutant compared to the wild type (Metz . & Bishop , 1980). The wild type thylakoid membranes were reported to have 4.3 +/- 0.7 manganese atoms per reaction centre whilst the LF1 mutant had only 1.6 +/- 0.2 manganese atoms per reaction centre. Gel

electrophoresis to compare the polypeptide composition of the wild type and LF1 mutant revealed the presence of a 36 kDa polypeptide in the mutant membranes instead of the 34 kDa polypeptide of the wild type. These polypeptides were present in PS2 core preparations of the mutant and wild type respectively (Metz , & Seibert , 1984). Both of these polypeptides were labelled by azido[^{14}C]atrazine, (an analog of atrazine) which binds to the herbicide binding site of D1 (Metz , et al, 1986). Antibodies specific to D1 also label both the 34 kDa and 36 kDa polypeptides (Rutherford et al, 1988). Both of these proteins are equivalent to the D1 polypeptide found in the reaction centre complex of higher plants. It was therefore suggested that the 36 kDa polypeptide of the LF1 mutant is an unprocessed version of the 34 kDa, D1 polypeptide of the wild type. It has been suggested that the gene for a processing enzyme rather than the gene coding for the D1 polypeptide had been mutated (Metz & Bishop , 1980). In vivo pulse chase labelling and in vitro protein synthesis supported this hypothesis (Reisfeld A. et al, 1982) and (Minami & Watanabe , 1985). The D1 proteins produced by in vitro translation of the mRNA from wild type and the LF1 mutant cells have an identical molecular mass to the D1 from LF1 thylakoids. The D1 polypeptide from wild type thylakoids is 1.5 - 2.0 kDa smaller due to C terminal processing. The mutation associated with LF1

must therefore be a mutation in a nuclear encoded processing enzyme (Diner et al, 1988) and (Taylor et al, 1988). The precursor form of the D1 polypeptide is incorporated into the PS2 complex but not processed. After digestion with papain or the endoproteinase Lys-C, the peptide profiles of the D1 polypeptide from the wild type and LF1 mutant indicated that the extra 1.5 - 2.0 kDa segment associated with the LF1 mutant is located at or near the carboxyl terminus (Taylor et al, 1988). This part of the polypeptide would be on the lumenal side of the thylakoid membrane. The unprocessed portion of the D1 polypeptide of the LF1 mutant would also be on the lumenal side of the membrane, preventing binding of manganese ions either by steric hindrance or by alteration of affinity of the manganese binding site. This provides evidence that D1 is involved in manganese binding as well as having a role on the acceptor side of PS2.

1.8.3. The Mechanism of Water Oxidation

To try to understand the structure and functioning of the manganese complex, synthetic models of how the manganese complex is thought to be arranged in different S states have been produced (Christou & Vincent, G., 1987). These results suggest a "double pivot" mechanism for water splitting, where the manganese complex binds two water molecules at "wing tip" type configurations, which then become deprotonated and the oxygen atoms form

bridges between the two manganese atoms. However this theory relies on the formation of a cubane structure, which has been ruled out by EXAFS study.

The EXAFS data discussed above suggests that no oxidation state or structural change occurs in the manganese cluster on S_3 state formation. Therefore some other component must be oxidised. A two electron oxidation of water has been suggested to occur at this point (Rutherford , 1989), but this would involve reduction of the manganese cluster. Histidine residues have been incorporated into the model (Rutherford , 1989) as charge storage components (Fig. 6. a). Other models for manganese oxidation rely on UV absorption changes measured at 320 nm after successive saturating laser flashes. There is much disparity over which S state transitions show changes in UV absorption corresponding to manganese oxidation. This is probably due to the contribution of Q_B^- to UV absorption. UV absorption measurements made from S_0 to S_0 with successive saturating laser flashes gave a 0: +1: 0: −1 pattern for manganese oxidation (Lavergne , 1986). These results relied on oxidation of the manganese complex from S_0 to S_1 and S_2 to S_3 that were invisible in the UV region studied. More recently a pattern of manganese oxidation of +1: +1: +1: −3 for the same S state transitions was proposed (Saygin, & Witt , 1987) (Dekker et al, 1984) & (Renger & Hanssum

Figure 1.6. Current Speculative Models for the Redox States of the Manganese Complex During Water Splitting

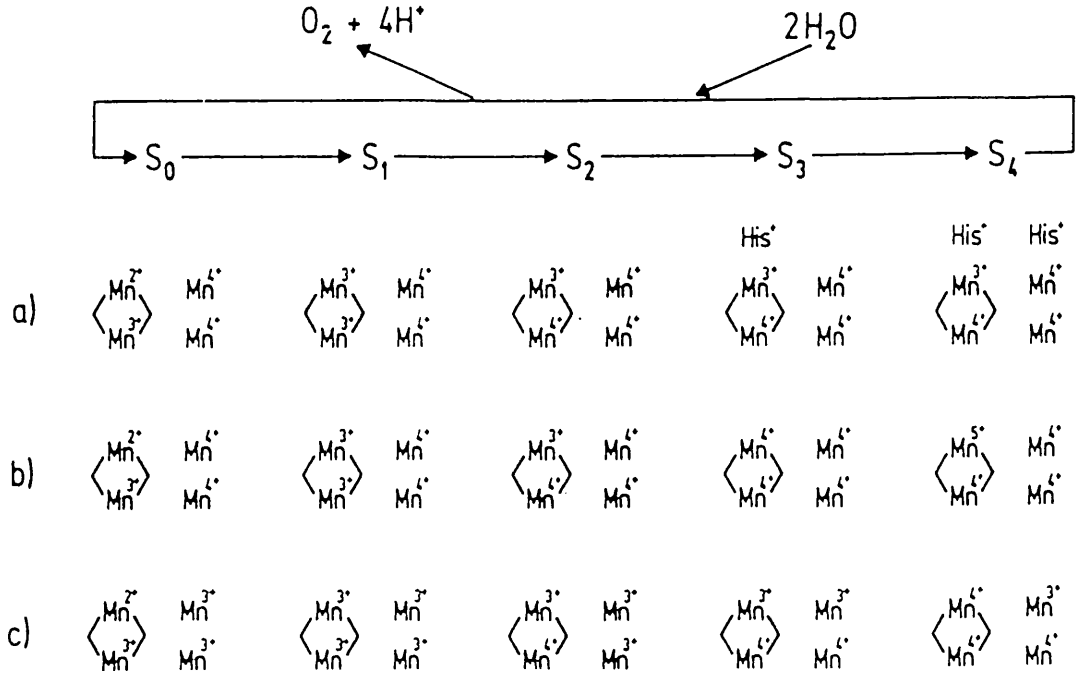

There are various speculative models outlining the redox states of the manganese complex in each S state during water splitting. The above models are based on results obtained from EPR, UV spectroscopy, X ray absorption and EXAFS studies. It is widely accepted that one electron oxidation of the manganese complex occurs on each of the steps from the S_0 state to the S_2 state. The S_2 state is accepted to be a distribution of Mn^{3+} and Mn^{4+} ions (for a recent review see Sauer , 1988). Model (a) involves the oxidation of a histidine residue on the formation of both the S_3 state and the S_4 state. Oxidation of the manganese complex does not occur in these transitions. The manganese complex is suggested to lose two electrons when water is oxidised, going from the S_4 state to the S_0 state. Model (b) suggests that manganese ions are oxidised on each S state transition, and model (c) is similar, but starting from a lower valence state. (Diagram from Rutherford , 1989).

, 1988). These results therefore suggest that the oxidation of the manganese on each S state advance is the same. There is some doubt about the S_0 state to S_1 state transition.

One of the main questions addressed by researchers, is when and where do the water molecules bind? Experiments using $H_2{}^{17}O$ in exchange for normal water have provided a certain amount of evidence. It was discovered that $H_2{}^{17}O$ induces line broadening in the S_2 state multiline epr signal (Hansson et al, 1986). Line broadening is induced by the ^{17}O nucleus ($I = {}^5/_2$) showing that oxygen ligands from water are bound to the manganese cluster when it gives rise to the S_2 state multiline epr signal. These experiments did not rule out the possibility of water binding in the S_0 or S_1 state.

When H_2O was replaced by ^2H_2O in oxygen evolving PS2 preparations an increased splitting of the fine structure of the S_2 state multiline epr signal was observed. This effect was interpreted as being due to proton binding, probably as water, at or near the manganese cluster. The effect of deuterated water at 200 K and 283 K support the theory that protons (probably as water) bind only when the S_2 state is formed at 283 K when the system is fluid rather than frozen at 200 K (Beck, 1986) & (Nugent, 1987).

Further evidence of the binding of the two water molecules to the manganese cluster in the S_2 state was

provided by the use of small molecules which act as substrate analogues, such as ammonia and hydroxylamine. Ammonia was found to alter the characteristics of the S_2 state multiline epr signal when formed at room temperature (Beck et al, 1986). The multiline epr signal was not affected by ammonia when the S_2 state was formed at 200K (Beck et al, 1986) and (. Nugent, 1987). This indicated that the ligand exchange only occured at room temperature following S_2 state formation. This idea was taken further and two distinct binding sites for NH_3 were proposed (Beck W.F. & Brudvig ., 1988). Type 1 binding of ammonia causes alterations in the hyperfine coupling of the S_2 state epr signal. Type 2 binding increases the proportion of the S_2 state that exhibits the g = 4.1 signal. The type 2 binding was found to be inversely dependent on the chloride concentration. The g = 4.1 signal formation has been linked with chloride depletion, and has been suggested to be a non functional form of the S_2 state (Ono et al, 1986). Sandusky & Yocum ,1984 & 1986 showed that hydroxylamine inhibits oxygen evolution by competing with chloride ions, whilst ammonia binds independently of chloride ions. Type 1 binding occurs only on formation of the S_2 state at room temperature, whilst type 2 binding occurs in the dark in the S_1 state. Chloride displacement is brought about by hydroxylamines, whilst NH_3 binds to a different site without chloride displacement.

1.8.4 The Proton Yield During the S state Cycle.

PS2 membranes that have been kept in the dark for 4 hours to obtain a 100% population of the S_1 state show a pattern of proton release of 0:1:2:1 when subjected to a series of rapid single saturating laser flashes (< 3 ms) (Saphon & Crofts , 1977), (Wille & Lavergne , 1982) and (Forster & Junge , 1985). The fact that protons are not removed during the S_1 to S_2 state transition means that a net positive charge is formed that is not neutralised until the two proton removal during the S_3 to S_4 state transition. Both the S_2 state and the S_3 state therefore have a positive charge of +1. This means that the electron removal from the manganese complex via Z is slowed because of coulombic attraction of the electron by the net positive charge. Recently it has been suggested that protons are extruded from the proteins of photosystem II, and their release is not linked to the S state cycle of oxygen evolution (Lubbers & Junge , 1989).

1.9 The Function of Calcium Ions

1.9.1 Calcium ions in biological processes

The role of calcium as an intracellular regulator has been studied in many biological processes. The biological ligands are complex, and often more than one binding site is involved. The bond between a ligand and a calcium ion is called a coordinate bond and requires the donation of pairs of electrons. Atoms such as N and O are

particularly common as biological ligands since they contain lone pairs of electrons in their outermost orbitals. Calcium ions have the electronic configuration of argon with empty 3d, 4s and 4p orbitals which are able to accept these lone pairs of electrons.

TABLE 1

Element	Atomic number	Electron configuration	Unhydrated ionic radius (Angstroms)
Mg	12	[Ne] $3s^2$	0.65
Ca	20	[Ar] $4s^2$	0.94
Sr	38	[Kr] $5s^2$	1.10

The number of ligands which bind a metal ion is called the coordination number. Calcium usually has a coordination number of six, but often a coordination number greater than six, up to ten, can occur due to the large size of calcium ions. Typical calcium chelators are shown in Fig. 7. These are all rich in the acidic amino acid residues asparatate and glutamate.

The role of calcium is widespread in many biological processes. The properties of calcium which are particularly important are: (1) Calcium carries a 2^+ charge and is able to balance the overall charge during removal or gain of electrons and/or protons. (2) Calcium ions are also able to act as a "gating system", by providing the correct ligand at the right time during biological reactions.

The larger size of calcium ions compared to

Carboxylic groups are important in forming ligands to calcium ions. The acidic side chains of the amino acids glutamate and aspartate are present in all kinds of biological metal ion binding sites. They are no doubt important in providing some of the ligands for the calcium binding sites of photosystem II. Asparagine and glutamine residues may also be present in a sequence of amino acids representing a calcium binding site. These amide residues would have to be hydrolysed to the acidic residues to become functional.

EGTA is the most widely used chelator of calcium, the four carboxyl groups providing ligands to the calcium ions. EDTA also has calcium binding capabilities but is more widely used to chelate larger ions such as manganese. Citrate has three carboxyl groups that are able to chelate calcium ions. Due to its small size citrate molecules can get close to calcium binding sites. This may partly explain why low pH citrate washing is effective at depleting at least one calcium ion from PS2 membranes.

Figure1.7. Examples of Calcium Chelators

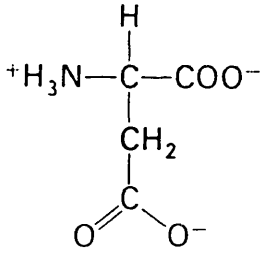

Aspartate
(Asp)

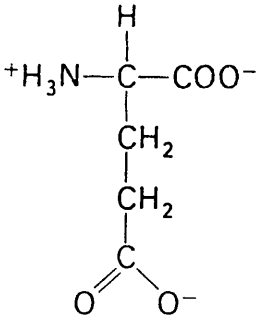

Glutamate
(Glu)

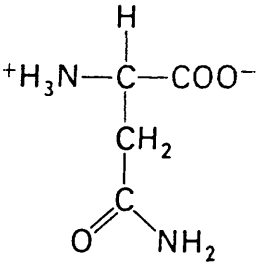

Asparagine
(Asn)

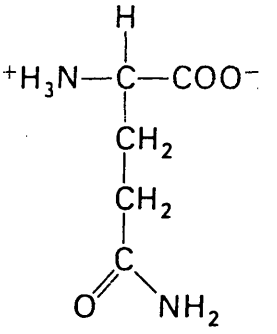

Glutamine
(Gln)

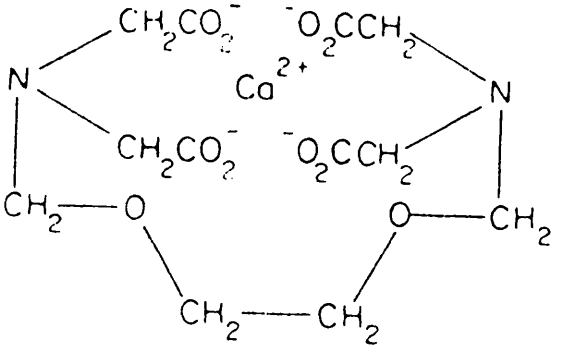

EGTA
(ethanedioxybisthylamine
tetraacetate)

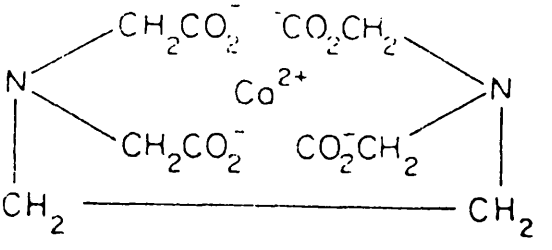

EDTA
(ethylenediamine
tetraacetate)

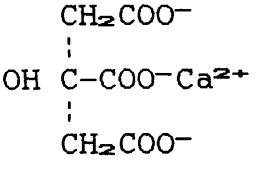

Citrate

magnesium ions gives the ion greater flexibility and although many calcium binding sites will bind magnesium ions they preferentially bind calcium ions. Calcium binding sites will also bind strontium ions and other metal ions of a similar size and configuration. This will be discussed further in a later section.

The best characterised calcium binding polypeptides are a group of proteins called calmodulins. Troponin C, involved in muscle contraction was the first to be characterised. The calmodulins all have similar properties containing 2-4 calcium binding sites of which magnesium may compete for two sites. They are of small molecular weight (10,000 to 20,000 kDa) and negatively charged at physiological pH, with a high proportion of acidic amino acid residues.

The oxygen atoms of the carboxylic acid side chains form the ligands for calcium ions. One or both of the oxygen atoms can coordinate to the calcium ions, with several amino acids involved. Water molecules are also probably involved in filling some of the ligand sites.

1.9.2 Calcium in Photosynthetic Water Splitting.

Various measurements of the number of calcium ions per D1/D2 reaction centre complex have been made (Shen et al, 1988a) & (Ono & Inoue , 1989). These seem to suggest that there are at least two calcium binding sites per spinach D1/D2 reaction centre complex. It is not known how many sites are involved in water

splitting. Using atomic absorption spectroscopy the number of calcium ions in spinach PS2 membranes has been shown to be approximately 2 per 200 chlorophylls (i.e. per D1/D2 reaction centre). When treated at low pH with citrate, this is reduced to 1 (Ono . & Inoue , 1988). The calcium content of salt washed spinach and rice PS2 membranes has also been compared to untreated PS2 membranes using the same technique (Cammarata & Cheniae , 1987). The number of calcium ions per 200 chlorophylls has been shown to be approximately equal to 2 in both salt washed and control membranes. These workers have also shown that salt washing in the light does not reduce the number of calcium ions significantly. The importance of the cycling of the S states by light to enhance calcium removal has been reported (Boussac et al 1988b). This data suggests that the different S states have different affinities for calcium binding.

More recently a chlorophyll b-deficient mutant of rice has been isolated which contains only one tightly bound calcium per D1/D2 complex (Shen et al, 1988b). This mutant is still competent in oxygen evolution and shows high rates of oxygen evolution comparable with the wild type. These results seem to suggest that one high affinity calcium binding site is involved in water oxidation, and other low affinity binding sites may also have some function.

1.9.3 Removal of Calcium ions from PSII

Various methods for the removal of calcium ions are known. There are three methods that are widely used and well documented:

(1) High concentration salt wash in the dark, (Ghanotakis . et al 1986 & 1987) and (Miyao & Murata , 1983).

(2) High concentration salt wash in the light + PPBQ, (Boussac & Rutherford , 1988a,b,c).

(3) Low pH citrate wash in the dark, (Ono & Inoue , 1988).

Readdition of calcium restores oxygen evolution after 17 and 23 kDa polypeptide removal and after calcium depletion. Several studies have been performed to determine the point of inhibition in the process of oxygen evolution. The fast reduction kinetics of the tyrosine molecule Z^+ have been shown to be reversibly inhibited by depletion of the 17 and 23 kDa polypeptides in the absence of calcium (Dekker et al, 1984). Cole and Sauer , (1987) observed that the rate of Z^+ reduction was slower in salt washed PS2 membranes. They interpreted this as an inhibition of electron donation from the S states to Z^+. Luminescence experiments showed that calcium was essential for the S_3Z^+ to S_0 transition (Boussac et al, 1985). This was supported by Ono & Inoue , (1986) who discovered that half of the NaCl washed PS2 membranes were inhibited after the formation of the S_3 state. Although it has been suggested that the

S_1 to S_2 state is inhibited by calcium depletion, this does not seem to be the case (Boussac & Rutherford , 1988b). There are many discrepancies as to the site of inhibition of calcium depletion, but it is likely that these can be explained according to the different protocols of calcium depletion used by various research groups. The presence of light and calcium chelators during and after the salt wash are important factors in calcium depletion (Boussac . & Rutherford, 1988a). Different degrees of calcium depletion are almost certainly due to the presence of high (Km = 50-100 uM) and low (Km = 1-2 mM) affinity calcium binding sites (Boussac et al 1985b) and (Cammarata & Cheniae , 1987).

1.9.4 <u>The Affinities of the Calcium Binding Site In Relation to the Redox State of the Manganese Cluster.</u>

Boussac A. & Rutherford A.W. (1988a) used saturating laser flashes to poise the OEC of PS2 membranes in the 4 S states (S_1,S_2,S_3 and S_0). Calcium was then removed from the PS2 membranes by high concentration salt washing. The degree of inhibition was then investigated. They have shown that the different S states influence the affinity of the calcium binding site. The S_3 state was found to have the lowest affinity for calcium, whilst the S_1 state had the highest affinity. The S_0 and S_2 states had an intermediate affinity approximately equal to each other. The depletion of calcium from PS2 in the different S

states indicated two different sites of inhibition of oxygen evolution. When calcium ions were removed in the S_1, S_2 or S_3 states, oxygen evolution was blocked at the S_3 to S_0 transition. It was still possible to advance from the S_1 state to the S_2 state and then to the S_3 state. When calcium ions were removed from PS2 in the S_0 state, the advance of the S state cycle was completely inhibited, and no other S states could be formed by single saturating laser flashes or continuous illumination until calcium was reconstituted.

1.9.5. <u>The Removal of Calcium by Low pH Citrate Washing inhibits the S_2 to S_3 Transition.</u>

A low pH citrate wash developed by Ono and Inoue (1988) selectively removed one calcium ions from PS2 membranes and inhibits oxygen evolution. Extrinsic polypeptides of molecular mass 17, 23 and 33 kDa remain attached to the PS2 membranes. The rate of oxygen evolution can be restored to normal by the readdition of calcium ions. This reconstitution of oxygen evolution is sensitive to EDTA, until the membranes have been incubated with calcium for 15 - 30 minutes. This indicates that firm religation of calcium was not immediate.

It has been suggested that the inhibition of the S state cycle by low pH citrate washing occurs in a different manner to other methods of calcium depletion (Ono & Inoue , 1989). The measurements of peak

temperatures of thermoluminescence B- and Q- bands (arising from $S_2Q_B^-$ and $S_2Q_A^-$ charge recombinations) were elevated to higher temperatures after low pH citrate treatment, largely reversed by the readdition of calcium. The amplitude of the modified B- band generated on the first flash was not altered by a second flash. These results were interpreted as the formation of an abnormal S_2 state after the extraction of the one calcium ion by low pH citrate washing. The S_2 to S_3 transition was suggested to be inhibited by this treatment.

1.9.6 Proposed Calcium Binding Sites of PS2.

1.9.6.1 The D1 Polypeptide

Two regions on the D1 polypeptide have been proposed as calcium binding sites, one of low affinity and the other of high affinity (Dismukes , 1988) (Fig. 8.).

An unusual sequence between Asn 296 and Asn 303 of the D1 polypeptide bears a strong resemblance to the calcium binding sites of all the other five proteins shown in Fig. 8. The assumption that this region is a calcium binding site has been made on the basis of comparison to other calcium binding sites of calcium binding proteins, determined by crystallographic techniques. The proposal that there is a high affinity calcium binding site on the D1 polypeptide relies on the hydrolysis of the amide residues to the functional carboxylate residue in the presence of Lewis acid metals, and at the acidic pH of the lumen of the thylakoid

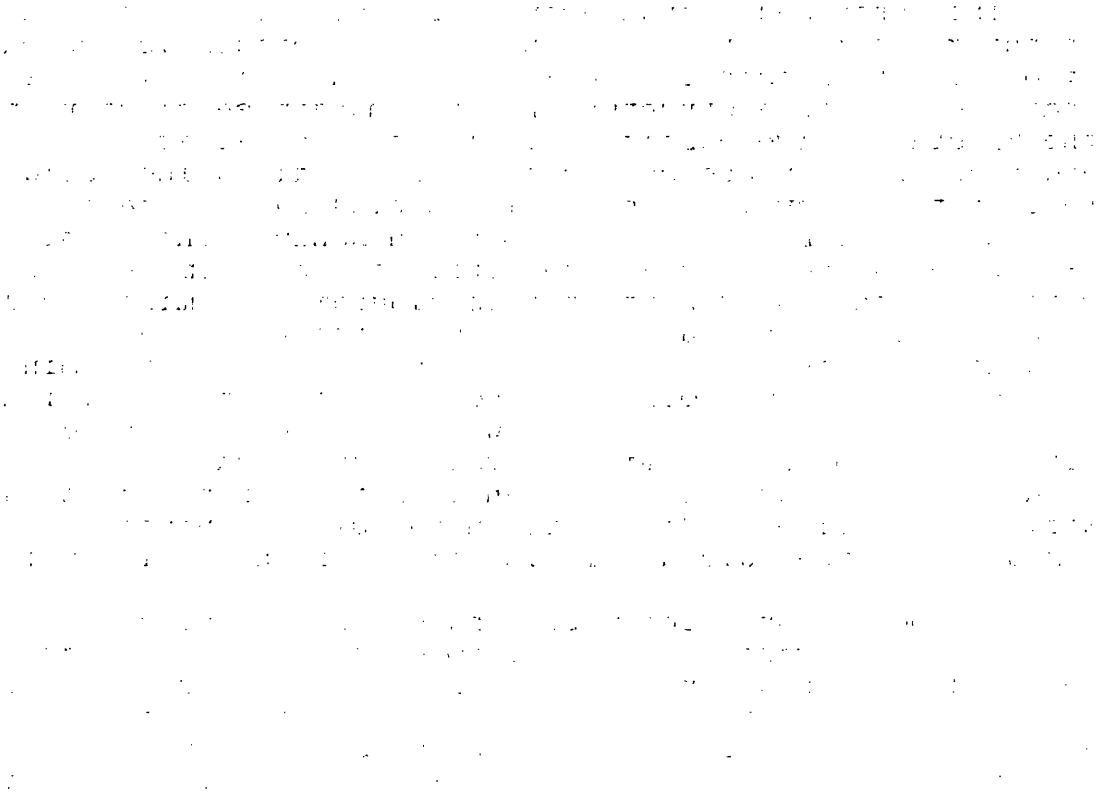

The proposed arrangement of the five membrane spanning regions of the D1 and D2 polypeptides is shown opposite. A possible manganese binding site is also indicated, with a structure for the manganese cluster in the S_2 state. Two possible calcium binding sites of low and high affinity are suggested. The acidic amino acids thought to be involved in metal ion binding are shaded. A region of the D1 polypeptide between Asn296 and Asn303 has been proposed as a high affinity calcium binding site. In the lower part of this diagram the amino acid sequence of EF-hand calcium binding sites from galactose binding protein (GBP), calmodulin, carp parvalbumin, troponin C and vitamin D dependent intestinal calcium binding protein (ICaBP) are shown. These calcium binding sites have been determined crystallographically or by sequence homology. The sequence of the proposed high affinity calcium binding site on the D1 polypeptide is compared to the calcium binding sites of the calmodulin type proteins.

The model for calcium binding on the D1 polypeptide relies on the hydrolysis of the amide asparagine residues to acidic aspartate residues. This would occur in the acidic lumen in the presence of transition metal ions acting as Lewis acids. The hydrolysis of asparagine to the functional aspartate amino acid in the acidic lumen may ensure that the correct ion is bound only when the polypeptide has been inserted into the membrane. This may have implications for the insertion of the D1 polypeptide into the thylakoid membrane. (Diagram from Dismukes ., 1988)

Figure 8. A Comparison of a Region of Amino Acids on the Fifth membrane Spanning Helix of the D1 Polypeptide to the Amino Acid Sequence of Calcium Binding Sites Found in Calmodulin Type Proteins

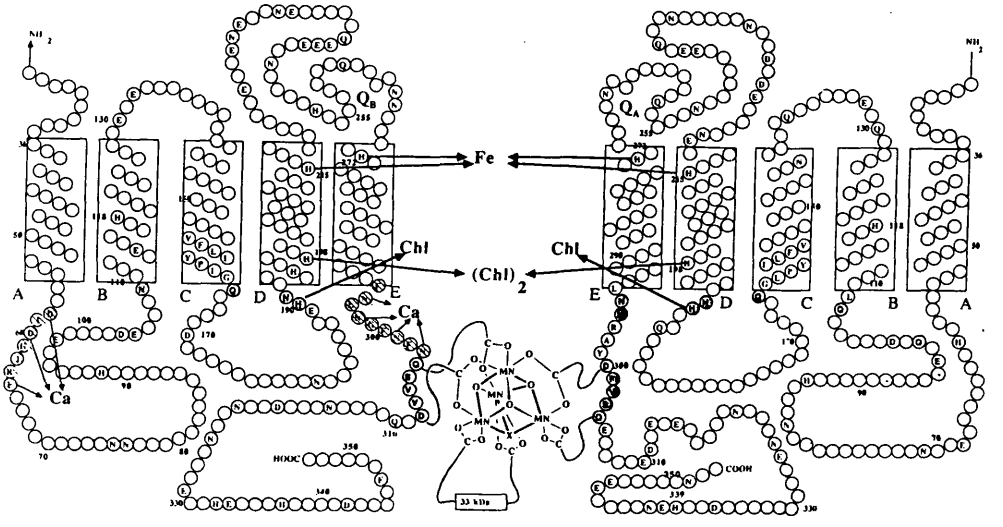

		1 •	2	3 •	4	—	5 •	6	7 •	
PS II D1	296	Asn	Leu	Asn	Gly	Phe	Asn	Phe	Asn	303
GBP										
Site	134	Asp	Leu	Asn	Lys		Asp	Gly	Gln	140
Parvalbumin										
Loop CD	51	Asp	Gln	Asp	Lys		Ser	Gly	Phe	57
Loop EF	90	Asp	Ser	Asp	Gly		Asp	Gly	Lys	96
Troponin C										
Loop I	30	Asp	Ala	Asp	Gly		Gly	Gly	Asp	36
Loop II	66	Asp	Glu	Asp	Gly		Ser	Gly	Thr	72
Loop III	106	Asp	Lys	Asn	Ala		Asp	Gly	Phe	112
Loop IV	142	Asp	Lys	Asn	Asn		Asp	Gly	Arg	148
ICaBP										
Loops III-IV	54	Asp	Lys	Asn	Gly		Asp	Gly	Glu	60
Calmodulin										
Loop I	20	Asp	Lys	Asp	Gly		Asn	Gly	Thr	26
Loop II	56	Asp	Ala	Asp	Gly		Asn	Gly	Thr	62
Loop III	93	Asp	Lys	Asp	Gly		Asn	Gly	Tyr	99
Loop IV	129	Asn	Ile	Asp	Gly		Asp	Gly	Glu	135

membrane. Four asparagines are located in conserved positions, which would co-ordinate to calcium via the carboxylate side chains. This leaves two undetermined co ordination sites. There are many possibilities, including chloride, water, other carboxylate groups provided by extrinsic polypeptides, or another part of the D1 or D2 polypeptides. This proposed calcium binding site would be very close to a proposed manganese binding site formed by the histidine residues of D1 and D2 and therefore implies a direct role for calcium in the structural regulation of the manganese site. The other proposed calcium binding site on D1 (Asp 58 to Glu 64), contains only three carboxylate side chains in suitable positions for calcium binding. This may therefore act as a lower affinity calcium binding site.

1.9.6.2 Calcium Binding Polypeptides Identified by Their Ability to Bind ^{45}Ca when Immobilised on Nitrocellulose.

Polypeptides which bind radioactive calcium (^{45}Ca) when immobilised on nitrocellulose following SDS - polyacrylamide gel electrophoresis have been detected (Webber & Gray , 1989). Two of these polypeptides which bound calcium were shown to be the 26 and 24 kDa polypeptide components of the LHC2. The 24 kDa polypeptide was characterised by N - terminal sequencing and shown to be the product of a type II cab gene. Davis and Gross (1975) showed that an isolated LHCII complex can bind calcium very specifically. A

Figure1.9. The Proposed Calcium and Chloride Binding Sites of the 33 kDa Extrinsic Polypeptide

The 33 kDa extrinsic polypeptide is thought to have a high affinity EF hand type calcium binding site. This would be similar to that of carp muscle parvalbumin shown opposite (a). The region suggested to form this structure is indicated in (b) opposite. The acidic and amide amino acids thought to be involved in calcium binding are indicated in blue. The basic amino acids, lysine and arginine are indicated in pink. The bend of the EF hand is most likely to be formed by glycine (indicated in green). Glycine has no side chains to prevent folding, and therefore a bend can occur most easily at this point. Two possible chloride binding sites are shown. These are in the sequence region from Glu103 - Asp106 and Glu187 - Asn191. Chloride binding sites are thought to consist of a basic lysine residue (which would form the ligand to the chloride) surrounded by acidic amino acid residues.

The Test Sequence for an EF Hand Calcium Binding Site is shown below (Gray , 1989).

K - - K - - K * - * - * G * I * K - - K K - - K

* = Oxygen containing acidic amino acid residues
G = Glycine forming the bend of the EF Hand
K = Lysine

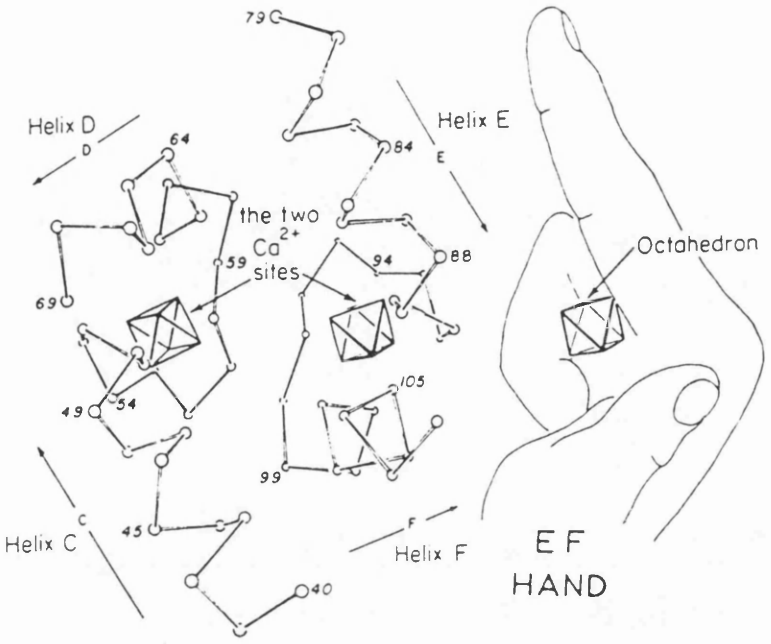

Fig. 9. (a) The Structure of the Two EF hand Calcium Binding sites of Parvalbumin from Carp Muscle (Diagram from Krestinger 1976, Annual review of Biochemistry).

Fig. 9. (b) A Summary of the Sequence Studies of Spinach 33 kDa Extrinsic Polypeptide (Oh-oka . et al, 1986).

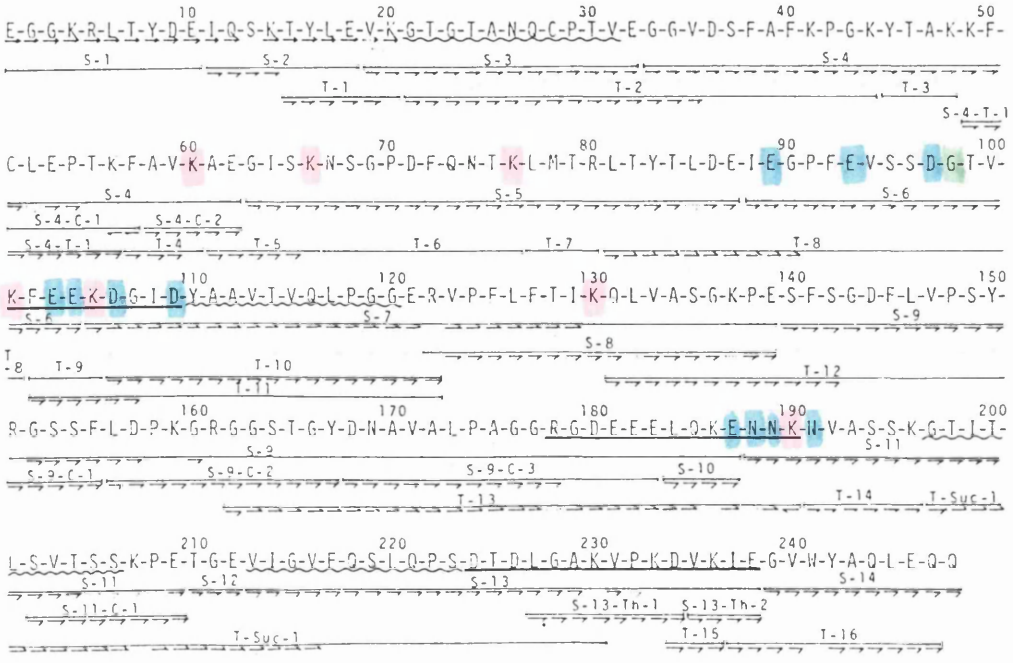

polypeptide of approximate molecular mass 33 kDa was also shown to bind calcium weakly. These experiments however did not identify this polypeptide, and it is possible that it could be the extrinsic 33 kDa polypeptide or the D1 or D2 intrinsic polypeptide (Webber & Gray ., 1989).

1.9.6.3 Is the 33 kDa Extrinic Polypeptide a Calcium Binding Polypeptide?

The 33 kDa polypeptide is thought to have an EF hand type calcium binding site (Fig. 9.). A region of the 33 kDa extrinsic polypeptide of 27 amino acid sequences has been compared to amino acid sequences of EF hand type binding sites, found in calcium binding polypeptides such as calmodulin and bovine intestinal calcium binding proteins (Colman & Govindjee, 1987). This region of the 33 kDa polypeptide has all the structural requirements necessary for the formation of a calcium binding EF hand (Wales et al, 1989).

1.9.7 The Calcium Requirement for Oxygen Evolution by Cyanobacteria.

The pool of calcium associated with thylakoids from the cyanobacteria Anacystis nidulans can be reduced by half simply by washing in a HEPES/ glycerol buffer (England & Evans ., 1985). This treatment reduces oxygen evolution to a low rate. PS2 preparations can also be depleted of calcium. Readdition of calcium in the presence of magnesium gives a stimulation of oxygen

evolution with sigmoid kinetics. From a Hill plot an n = 2 value for the number of calcium binding sites was obtained (Evans et al, 1988). The binding of magnesium shows no cooperativity with calcium binding. The 33 kDa polypeptide has been implicated in the sigmoid binding of calcium since when this polypeptide is removed there is a loss of the sigmoid kinetics of calcium binding, replaced by a simple binding curve. Antagonists of calmodulin are known to inhibit PS2 both from higher plants and from cyanobacteria (England & Evans , 1983). Evans et al, 1988 have shown that calcium restoration of oxygen evolution is inhibited by the addition of an antibody to guinea pig calmodulin. This antibody shows immunoreactivity with a polypeptide of molecular mass 60 - 62 kDa, which could be the D1/D2 polypeptide dimer. These results suggest that a calmodulin type calcium binding site may be formed by regions from both the D1 and the D2 polypeptide.

1.10 The Effect of pH on Photosynthetic Water Oxidation

It has been known for some time that photosynthetic water splitting is sensitive to small changes in pH. Oxygen evolution is inhibited by both acidic and alkaline pHs in PS2 enriched membrane fragments. Acidic pH however, inhibits oxygen evolution in intact thylakoids. This inhibition may therefore affect more than one component of PS2. Alkaline pH does not inhibit oxygen evolution in intact thylakoids unless a suitable

ionophore is present to equilibrate the pH between the solution and lumenal space (Cohn et al, 1975; Reimer & Trebst, 1975; Briantais et al, 1977). Since the oxygen evolving components are situated on the inner surface of the membrane it can be concluded that specifically electron donation is inhibited by high pH.

Both reversible and irreversible effect of alkaline pH have been described (Cole et al, 1986). In these experiments it was found that a reversible inhibition occured up to pH 8.0, and an irreversible inhibition occured above pH 8.0. The irreversible inhibition has been linked with the loss of the 17, 23 and 33kDa extrinsic polypeptides and the eventual loss of the manganese cluster (Chapman et al, 1989). The reversible inhibition has been suggested to be caused by the displacement of an ionizable group on the proteins associated with the water splitting site. It is suggested that this may be a displacement of chloride from an anion binding site by hydroxide (Cole et al, 1986). At pH 8.0 and above there is a loss of the multiline S_2 epr signal which is reversed upon returning to physiological pH, providing the 33kDa polypeptide remains attached and the manganese cluster is intact. The steady state level of signal II induced by continuous illumination is also increased.

There are several reports of the S_1 state of the manganese cluster becoming destabilised to S_0 after a

short period in the dark at pH 8.3 (Plitjer et al, 1986 & De Groot et al, 1985). Recently a report on the nanosecond reduction kinetics of Chl a^+ at different pHs has suggested that at pH 8.3 there is an increased percentage of misses during the water splitting cycle, (Meyer et al, 1989). This data does not exclude an increased population of S_0 at pH 8.3 in the dark. The first flash reduction kinetics are not altered in the dark between pH 7.0 and 9.0, indicating that the alkaline inhibition does not occur in the dark. It is thought that only the higher S states are sensitve to the alkaline pH.

The chloride and calcium requirements have been investigated as a function of pH (Homann . ., 1988). Chloride ions are expected to interact with positvely charged, protonated groups (Homann . .., 1987) which should be more abundant at low pH, while calcium ions bind to negatively charged carboxylate groups which proton binding would neutralise. At pH 5 the apparent Km for Cl^- binding is well below 1 mM even in the absence of the 17 and 23 kDa polypeptides. A pK_a < 5 estimated for the chloride binding components, which is not altered by the presence or absence of the 17 and 23 kDa polypeptides, must be assigned to groups close to the oxygen evolving manganese cluster (Homann . 1988). Chloride ions probably play a structural role as well as an active role in the water splitting reaction.

In the research for this thesis I have investigated the role of several components of the oxygen evolving complex and monitored the effects of calcium depletion from PS2 preparations.

CHAPTER 2

MATERIALS AND METHODS

2.1 Preparation of PS2 membranes from Thylakoids of Higher Plants

Chloroplast thylakoids were isolated either from greenhouse grown pea (Pisum sativum L c.v. Feltham First) or market spinach (Spinacia oleracea) using the method of Ford and Evans (1983) by homogenisation in 330 mM sorbitol, 20 mM Mes (pH 6.5, adjusted with Tris base), 0.2 mM $MgCl_2$ (grinding medium), with approximately 1 mM ascorbate added to each grind. The homogenised leaf material was filtered through nine layers of muslin, then centrifuged at 3000 xg for 5 minutes at 4 °C. The pellet was resuspended in 5 mM $MgCl_2$ to osmotically lyse the intact chloroplasts. An equal volume of the grinding medium was added to buffer the solution followed by centrifugation for 20 minutes. A membrane fraction rich in PS2 was prepared essentially according to the method of Berthold et al (1981) with modifications as described by Ford & Evans (1983) by resuspending the thylakoid pellet to approximately 4 mg Chl. ml^{-1} in 25 mM Mes (to pH 6.3 with Tris base), 15mM NaCl, 5mM $MgCl_2$ (resuspending medium). Incubation on ice, in the dark for 90 minutes was followed by the addition of Triton X-100 to a final concentration of 5% and 2 mg Chl.ml^{-1}. This was then incubated for a further 25 minutes incubation in the dark. Centrifugation at 40,000

xg for 25 minutes gave a pellet which was washed with 25 mM Mes (pH 6.3/NaOH), 20 mM NaCl, 1 mM EGTA and then centrifuged again as above. The pellet was resuspended in resuspending medium containing 20 % glycerol v/v and stored at 77 K.

2.2 Preparation of Oxygen Evolving Core Complexes

Oxygen evolving PS2 core complexes were isolated using n- octyl B-D glucopyranoside (OGP) essentially as described by Ghanotakis et al (1987) with modifications for calcium depletion. PS2 membranes with high rates of oxygen evolution were resuspended to a concentration of 2.5 mg Chl. ml^{-1} in 0.4 M sucrose, 25 mM Mes /NaOH pH 6.0, 10 mM NaCl. This was mixed thoroughly with an equal volume of 1.0 M sucrose, 25 mM Mes /NaOH pH6.0, 0.8 M NaCl and 70 mM OGP and incubated on ice in the dark for 10 minutes. The suspension was then diluted threefold with a solution of 1.0 M sucrose, 25 mM Mes /NaOH pH 6.0, 0.4 M NaCl, 1 mM EGTA, mixed and incubated on ice in the dark for a further 5 minutes. The preparation was centrifuged for 90 minutes at 40,000 xg until a pellet of light harvesting chlorophyll was formed. The supernatant was dialysed twice for 30 minutes in the dark at 4 ^{o}C against 25 mM Mes /NaOH pH6.0, 20 mM NaCl, 1 mM EGTA, and then diluted twofold with 25 mM Mes /NaOH pH 6.3, 30 mM NaCl and 5 mM $MgCl_2$. After this procedure the sucrose had been removed and it was possible to form a pellet of oxygen evolving core complexes by centrifugation at

40,000 xg. The pellet formed was resuspended in 25 mM Mes /NaOH pH 6.3, 30 mM NaCl, 5 mM $MgCl_2$ and 20% glycerol. Oxygen evolving core complexes were very sensistive to light and were therefore always handled in the dark. To maintain bound calcium, 5 mM $CaCl_2$ was added to each preparation medium in replacement for 1 mM EGTA. Due to the hygroscopic nature of the OGP detergent, the concentration suitable for core preparation varies considerably from batch to batch. It was therefore essential to determine the concentration of OGP necessary to remove light harvesting chlorophyll polypeptides and maintain a high rate of oxygen evolution. The other variable in the preparation of oxygen evolving core complexes is the use of different preparations of PS2 membranes. It was therefore necessary to do a test of suitable detergent concentration for core preparation for each different batch of PS2 membranes. The tests were carried out on a small scale with concentrations of OGP ranging from 60 - 100 mM. The rates of oxygen evolution from each concentration of detergent were assayed. The extent of light harvesting chlorophyll removal was determined for each concentration using SDS / polyacrylamide gel electrophoresis. The concentration of detergent which gave greatest removal of light harvesting chlorophyll and the highest rate of oxygen evolution was used in a scaled-up preparation.

2.3 Preparation of PS2 Reaction Centre Complexes

Photosystem II reaction centre complexes were isolated using the method of Nanba & Satoh (1987) with modifications according to Barber et al (1987). PS2 membrane fragments were incubated in 1.0 M Tris (pH 8.8 with HCl) for 1 hour at 0 °C in room light to remove the 17, 23 and 33 kDa extrinsic polypeptides. Centrifugation at 40,000 xg for 30 minutes at 4 °C produced a pellet which was resuspended in 50 mM Tris/HCl pH 7.2. The membrane fragments were then digested at a concentration of 1 mg Chl $.ml^{-1}$ using the detergent Triton X-100 at 4 % in 50 mM Tris/HCl pH 8.8, 1 mM ortho -phenanthroline for 1 hour, stirred on ice in the dark. After centrifugation at 40,000 xg for 60 minutes the supernatant was loaded onto a Fractogel TSK DEAE - 650(S) column, previously equilibrated with 50 mM Tris/HCl pH 8.8, 0.2 % TX-100, 30 mM NaCl, 1 mM ortho-phenanthroline, in subdued light at 4 °C. The column was thoroughly washed (using the same buffer) to remove light harvesting chlorophyll. The purified reaction centre was eluted from the column using an increasing stepwise 30 mM NaCl gradient (30 - 150 mM). The reaction centre fractions were concentrated using PEG precipitation as described by McTavish N. et al, 1988. 0.325 g of PEG (Sigma: mol wt = 3,350) per ml was added slowly to the reaction centre fraction and dispersed carefully with a soft paintbrush. This was incubated for 90 minutes and then centrifuged

at 40,000 xg for 15 minutes. The pellet was resuspended in the Tris buffer described above and then centrifuged at 1,100 xg for 90 s. The purity and activity of the reaction centre was assayed using SDS / polyacrylamide gel electrophoresis and epr measurement of spin-polarised triplet respectively. The optical absorption spectrum of the reaction centre complex was measured using a Philips PU 8740 spectrophotometer. This also gave some indication of the purity of the preparations as detailed later.

The D1 / D2 reaction centre complexes are very unstable and need to be kept on ice in complete darkness. Above 0 °C the reaction centres decay rapidly. These preparations are also sensitive to illumination, with rapid loss of activity. This results in a blue shift in the red peak and loss of the triplet epr signal. In order to prepare more stable reaction centres the DEAE column was eluted with the same Tris buffer, but containing 4 mM B-D-maltoside instead of TX-100 (Gounaris et al, 1988).

2.4 Preparation of PS2 membranes from the Green Alga Scenedesmus obliquus

The wild type of Scenedesmus obliquus and various mutants were grown photosynthetically, heterotrophically and mixotrophically (Bishop ., 1971) & (Bishop , 1972).

The growth medium for Scenedesmus obliquus was as follows. 1mM KNO_3, 10uM $MgSO_4$, 5mM NaCl, 5 uM $ZnSO_4$, 10uM

$CaCl_2$, 100 uM Na_2HPO_4, 5 uM $MnCl_2$, 10 uM $FeSO_4$ and 2.0g yeast extract /litre. To grow the cells mixotrophically or heterotrophically 300 mM glucose was included in the medium. The suspension of cells was incubated in an orbital shaker maintained at 30 °C. The cells were grown under illumination for autotrophic and mixotrophic growth.

The length of time allowed for growth depended on whether it was the wild type or the LF1 mutant. Once the cells had grown to a dark green colour (after approximately 7 days), the cells were harvested.

Harvesting was carried out by centrifuging the cell suspension at 3000 xg for 5 minutes. The supernatant was discarded and the cells were then washed three times with resuspending medium, centrifuging as before. The pellet of washed cells was resuspended in a solution of 20% glycerol, 10 mM Hepes /NaOH, 5 mM PO_4^{3-}, 5 mM $MgCl_2$, pH 7.5 that was 40 % of the pellet volume.

Cells were disrupted using a bead beater cooled by an ice/water jacket, giving a number of 1 minute bead beats with 0.5 mm glass beads, in the solution described above until the cells were broken releasing the chloroplasts. The ratio of beads to cell suspension was approximately 1.5 : 1.0. Cell breakage was determined by microscope examination. Thylakoids were collected by centrifugation at 18,000 rpm for 30 mins (Metz & Seibert 1984). A Triton X-100 digestion was carried

out on the membranes at 2 mg Chl.ml^{-1}, using a 5% solution of Triton X-100 in 25 mM $MgCl_2$, 75 mM NaCl and 100 mM Mes / NaOH pH 6.3, for 25 minutes on ice in the dark after mixing thoroughly. After this time the suspension was centrifuged at 40,000 xg for 30 minutes. The pellet of PS2 membranes formed was stored at 77 K in the dark in 20% glycerol, 20 mM Mes /NaOH, 5 mM $MgCl_2$, 15 mM NaCl pH 6.3.

2.5 Removal of the Extrinsic Polypeptides Involved in Oxygen Evolution

Before any treatments the PS2 membrane fragments were washed in resuspending medium and centrifuged at 40,000 xg for 30 minutes twice or until no chlorophyll was observed in the supernatant.

PS2 membranes completely devoid of oxygen evolution were prepared by removal of the 10, 17, 23, 33 kDa extrinsic and the manganese complex from PS2 enriched membrane fragments. The membranes were initially washed in 50 mM Tris/HCl pH 7.2 and then centrifuged for 30 minutes at 40,000 xg. The pellet was resuspended in a small volume of the same buffer before washing in 1.0 M Tris /HCl (pH 8.8) at a concentration of 1 mg Chl /ml in room light for 1 hour at 4 °C. Centrifugation at 40,000 xg was followed by resuspending the pellet formed in pH 6.3 resuspending medium, 20% glycerol as described above.

A high concentration of urea removes only the 17, 23 and 33 kDa extrinsic polypeptides. (Miyao & Murata ,

1984). The PS2 membranes were resuspended to 1 mg Chl /ml in 2.6 M urea, 200 mM NaCl, 25 mM Mes /NaOH pH 6.5, 20 % glycerol and stirred in the dark at 4 °C for 30 minutes. This was followed by centrifugation at 40,000 xg for 30 minutes. The pellet was washed and resuspended in 200 mM NaCl, 25 mM Mes /NaOH pH 6.5, 20% glycerol before storing at 77 K. The high concentration of NaCl (200 mM) was maintained throughout any further treatments of these membrane fragments, as this was necessary to keep the manganese cluster intact within the manganese binding site.

Another method used to remove the 17, 23 and 33 kDa polypeptides and maintain an intact manganese cluster was a 2.0 M divalent cation wash (Ono & Inoue, 1983). Divalent salts used included $CaCl_2$, $MgCl_2$ and $SrCl_2$. Clean PS2 membranes were resuspended in 25 mM Mes /NaOH, 2.0 M divalent cation (as above) pH 6.3 to 1.0 mgChl /ml and stirred on ice in the dark. This was followed by centrifugation at 40,000 xg. The pellet formed was resuspended in resuspending medium 20% glycerol as above. A 200 mM NaCl concentration was maintained in all buffers during all treatments to keep the manganese cluster intact.

To remove the 17 and 23 kDa polypeptides from PS2 membranes a 1.0 M NaCl wash was carried out as in Miyao & Murata, 1983 with modifications as in Boussac & Rutherford, 1988a. Clean preparations of PS2 membranes

were resuspended to 1.0 mg Chl /ml in 25 mM Mes /NaOH, 1.0 M NaCl, 5 mM $MgCl_2$, pH 6.3 and stirred on ice in the dark for between 5 and 20 minutes. The pellet formed after centrifugation as above was washed in the 1.0 M salt buffer and centrifuged as above, before resuspending in resuspending medium, 20% glycerol.

2.6. Calcium Ion Removal

Washes were developed to bring about maximum calcium depletion from the calcium binding sites involved in oxygen evolution. This was monitored using a Clark type oxygen electrode, and epr techniques as described later in this section.

2.6.1 Removal of Calcium at pH 6.3 in the Light

A salt concentration higher than 1.0 M was known to enhance the removal of calcium ions (Boussac A. et al, 1985). PS2 membrane fragments were washed in 20 mM Mes/NaOH pH 6.5, 40 mM NaCl, 1 mM EGTA and then centrifuged at 40,000 xg for 30 minutes. The pellet was resuspended to 1 mg chlorophyll /ml in 1.8 - 2.0 M NaCl, 25 mM Mes/NaOH pH 6.5, 1 mM EGTA and stirred on ice for 30 minutes in room light with 50 uM PPBQ (an artificial electron acceptor) added to the incubation buffer. This was to ensure that the S states were advanced during this treatment. The S_1 state has the highest affinity for calcium binding, therefore it was important to form the other S states (Boussac & Rutherford , 1988b). The suspension was centrifuged at 40,000 xg for 30 minutes,

and the pellet was washed and resuspended in the same buffer and centrifuged as before. A further wash and centrifugation in resuspending medium removed the high concentration of salt and EGTA. Finally the pellet was resuspended in resuspending medium containing 20 % glycerol and stored at 77 K. Sucrose was omitted from this procedure to prevent possible calcium contamination (Boussac et al, 1985), and to allow faster reconstitution with calcium and other divalent cations (Boussac & Rutherford ..., 1988a). 5 mM $MgCl_2$ was present in all assays to prevent any non specific effects of divalent cations on oxygen evolution and 40 mM NaCl was added to prevent chloride depletion.

2.6.2 Removal of Calcium at pH 8.3 in the Dark

A novel method for the removal of calcium in the S_0 state was devised. The S_0 state is suggested to have a lower affinity for calcium ions than the S_1 state (Boussac & Rutherford ., 1988b). Therefore if the S_0 state is formed at pH 8.3 in the dark (DeGroot et al, 1986), calcium ions should be more easily removed. The calcium ions were removed from PS2 membranes by high concentration salt washing at pH 8.3 in the dark. PS2 membranes were washed with 20 mM Mes/NaOH pH 6.3, 40 mM NaCl, 100 uM EGTA and centrifuged at 40,000 xg for 20 minutes. The membranes were then washed in 5 mM Tricine /HCl, 30 mM NaCl, 5 mM $MgCl_2$, pH 8.3 centrifuged again and resuspended in a small volume of 10 mM Tricine

/HCl, 40 mM NaCl, pH 8.3. The PS2 membranes were placed in the dark on ice for 15 minutes. The membrane suspension was diluted with 2.2 M NaCl, 25 mM Tricine /HCl, 1 mM EGTA pH 8.3 (to give a final concentration of 2.0 M NaCl and 1 mg Chl/ml) and stirred on ice for 20 minutes in the dark. After this time the pH was adjusted to pH 6.3 with a strong stock solution of Mes buffer (approx pH 3.0) in the dark followed by centrifugation at 40,000 xg. The preparations were then washed with 25 mM Mes /NaOH, 40 mM NaCl, 100 uM EGTA, pH 6.3 centrifuged at 40,000 xg for 20 minutes and resuspended in 25 mM Mes / NaOH, 5 mM $MgCl_2$, 20 mM NaCl, 20 % glycerol.

As a control the effect of pH 8.3 on PS2 membranes (with particular reference to the multiline and D^+) was monitored by carrying out exactly the same protocol as described for salt washing at pH 8.3, without incorporating the 2.0 M salt wash at pH 8.3. The PS2 membranes were washed as above and resuspended in 25 mM Tricine /HCl, 40 mM NaCl, pH 8.3 for 30 minutes in the dark on ice. The pH was adjusted as above followed by centrifugation. The PS2 membranes were then washed in resuspending medium with 40 mM NaCl, centrifuged as above and resuspended in resuspending medium with 20% glycerol and 40 mM NaCl.

2.6.3 Removal of Calcium at pH 3.0 in the Dark by Citrate Treatment

A low pH citrate wash as described by (Ono T.-A. & Inoue Y., 1988) was used to remove one calcium ion per D1 / D2 $cytb_{559}$ from PS2 membranes, without the loss of extrinsic polypeptides. Resuspending medium at pH 6.5 was removed by initially washing the PS2 membranes with 400 mM sucrose, 20 mM NaCl at pH 6.5 and centrifuging at 40,000 xg. PS2 membranes were resuspended in 400 mM sucrose, 20 mM NaCl, 10 mM citrate pH 3.0 to 2.0 mg Chl/ml and stirred on ice in the dark for 5 minutes. The PS2 membranes were then diluted x5 with 400 mM sucrose, 40 mM Mes /NaOH, 20 mM NaCl, pH 6.5 and centrifuged at 40,000 xg for 25 minutes. The pellet was resuspended in glycerol buffer as described above.

2.7 Reconstitution of Calcium Depleted Photosystem II Membranes

Photosystem II membranes depleted of calcium as described above were reconstituted with calcium, strontium and vanadyl ions. The depleted PS2 membranes were diluted to approximately 1 mg Chl /ml in 25 mM Mes /NaOH, 5 mM $MgCl_2$. Reconstitution was achieved by the addition of 20 mM calcium chloride or 20 mM strontium chloride or by the addition of micromolar concentrations of vanadyl sulphate hydrate (both sample and solutions gassed thoroughly with oxygen free nitrogen in this case). It was necessary to remove oxygen from samples to

be reconstituted with vanadyl ions since the vanadyl ions are unstable and readily oxidised to vanadium (V) at physiological pH. In the case of vanadyl reconstitution 40 mM NaCl was added to provide the chloride associated with the other two divalent cations. The suspension of PS2 membranes was then stirred at 4 °C in room light for 20 minutes with 50 uM PPBQ added. This was then centrifuged at 40,000 xg for 25 minutes. The pellet formed was resuspended in room light in the above solution with 50 uM PPBQ and the appropriate divalent cation added. EPR samples were prepared in room light. The presence of light was again important, allowing S state cycling and efficient binding of the divalent cation.

2.8 Measurement of the Rate of Oxygen Evolution

Oxygen evolution was measured using a Clark type oxygen electrode. The oxygen electrode was maintained at a constant temperature by the use of a water jacket and a water bath maintained at 18 °C. The sample in the oxygen electrode was illuminated using a 1000 W photographic lamp, with 2 serum bottles filled with water in between the lamp and electrode to prevent heating effects. The assay buffer was 25 mM Mes /NaOH, 30 - 40 mM NaCl, 5 mM $MgCl_2$ at pH 6.3 unless stated otherwise. Other additions are described in the text. Measurements were made in at least triplicate, to maintain an error no greater than 5%.

2.9 SDS/Polyacrylamide Gel Electrophoresis

Gel electrophoresis was carried out essentially as described by Chua & Bennoun (1975), Chua , (1979) and by Laemmli (1970). Slab gels of various uniform acrylamide concentrations were used (see gel photos for details).

Slab Gels - (non gradient)

Separating Gel: 12.5 - 18 % acrylamide, 0.334 - 0.48 % methylene bis acrylamide, 375 mM Tris /HCl pH 8.8, 0.4 % SDS, made up to volume with double distilled water.

Stacking Gel: 6% acrylamide, 0.16% methlene bis acrylamide, 125mM Tris /HCl pH6.8, made up to volume with double distilled water.

The polymerisation of the gels was brought about by the addition of 100 ul ammonium persulphate solution (0.2 g / 2.0 mls) and 20 ul of TEMED.

Running Buffer: 375 mM Tris, 2.0 M Glycine, 0.1% SDS.

The mobility of polypeptides with and without 6.0 M urea was compared. Non urea gradient gels 16 - 22 % gave good resolution of PS2 polypeptides. However non urea gels were not suitable for observing polypeptides of 3 - 5 kDa as a band of lipids obscured this region. To study the low molecular weight polypeptides gradient gels of 16 - 22 % acrylamide containing 6.0 M urea and 600 mM Tris pH 8.8 (with the same higher concentration of 600 mM Tris in the running buffer) were used. The urea gradient gels helped to prevent the lipid bands from obscuring the low

molecular weight polypeptides by retarding the mobilty of the polypeptides with respect to the lipid band associated with PS2.

A Pharmacia Phast gel system was also used for polypeptide analysis using 8 - 25 % acrylamide gradient gels, with solid gel running buffer. The polypeptide composition was analysed using a laser analyser.

Gel Sample Preparation - Samples of polypeptides were solubilised in 4% SDS, 5% mercaptoethanol, 90 mM Tris pH 6.8, bromophenol blue. Solubilisation was carried out at room temperature for at least 1 hour. It is not possible to heat membrane proteins to enhance the solubilisation, since the polypeptides aggregate when heated. 6.0 M urea was added to the solubilising buffer for samples to be loaded onto urea gels. Markers were from Sigma (molecular weights as on gels) and were solubilised in the above buffer with or without urea as necessary.

A technique for studying the calcium binding polypeptides of calmodulin (Gitelman S.E. & Witman G.G., (1980) was used to investigate PS2 preparations. Non urea slab gels of uniform 18% acrylamide concentration were prepared as described above. Gels were prepared in pairs, one with 1 mM EGTA and the other with 1 mM $CaCl_2$. Samples of PS2 preparations for these gels either had 1 mM EGTA or 1 mM $CaCl_2$ added to them before solubilisation. The gels were run at the same time under exactly the same conditions. The mobility of each polypeptide with respect

to the position of the markers was investigated.

2.10 Generation of the S_2 State Multiline EPR signal

A uniform S_1 state was achieved by 4 hour dark adaptation of PS2 preparations on ice (Vermaas W.F.J. et al, 1984). The S_2 state was produced by transferring the epr sample of the PS2 preparation (already frozen at 77 K in the dark) to an alcohol bath maintained at 200 K by the addition of solid carbon dioxide. The sample was then illuminated with a 1000 W photographic lamp for 8 minutes, turning the sample around after 4 minutes. With the light still switched on, the epr sample was removed from the alcohol bath, wiped to remove the alcohol and then placed in liquid nitrogen at 77 K. Another method for the generation of the S_2 state multiline epr signal was known as freezing under illumination. This was performed by adding 100 uM 3 (di-chloro phenyl) 1,1 dimethyl urea (DCMU) to the 4 hour dark adapted PS2 preparation (not frozen) and illuminating the sample for 1 minute, with a 1000 W photographic lamp. DCMU restricts the PS2 reaction centre to one stable turnover. The sample was rotated for even illumination whilst it was kept cool just above the surface of the liquid nitrogen. After 1 minute had elapsed the sample was slowly lowered into the liquid nitrogen and frozen with the lamp still switched on. The amplitudes of the S_2 state multiline epr signal generated by this method were compared with and without the addition of DCMU.

2.11.1 Measurement of the D^+ signal II (slow) epr signal

The time course of the amplitude of the D^+ epr signal was observed during 4 hour dark adaptation after illumination. Samples of equal chlorophyll concentration from the same batch of PS2 were placed in the dark, and frozen in liquid nitrogen (77 K) in duplicate at specific time intervals during the 4 hour dark adaptation. The size of the D^+ epr signal in each sample was measured in the dark.

2.11.2 Depletion of the D^+ Epr Signal (Signal II slow)

Depletion of the D^+ epr signal was carried out as described by (Nugent et al, 1987).

PS2 preparations were dark adapted for 4 hours on ice to obtain a uniform S_1 state. The samples were then illuminated for 5 minutes at 77K using a 1000 W photographic lamp and placed in the dark at 77 K for 7 days. After this period of dark, the sample was again illuminated, but at 200 K for 8 minutes, turning the sample around after 4 minutes, then returned to 77 K and left in the dark for a further 7 days at 77 K. After this treatment to deplete D^+ the amplitude of D^+ and the S_2 state multiline epr signal were compared before and after thawing. The epr samples for thawing were removed from the liquid nitrogen in the dark and warmed for a few seconds in the air. The sample was then plunged into water (approximately 10 - 15 °C) for rapid thawing in the dark (approx 15 seconds). The sample was either

immediately refrozen, or was placed on ice in the dark for a specific length of time. The exact time (in seconds) after removal from the liquid nitrogen until the sample was re frozen was noted. Each measurement was repeated in duplicate samples. The size of the two epr signals before and after thawing were compared, giving a final measurement of the D^+ amplitude changes.

2.12 Optical Spectroscopy

Optical spectra for preparations of PS2 were obtained by scanning the wavelengths of light from 350nm to 720 nm. This was carried out using a Philips PU 8740 spectrophotometer.

2.13 Electron Paramagnetic Resonance Spectroscopy (epr)

Epr spectroscopy was performed at cryogenic temperatures using a Jeol X-band spectrometer with 100 kHz field modulation and an Oxford instruments liquid helium cryostat. For sample observation between 4 - 25 K liquid helium was used, whilst for higher temperatures (77 - 200 K) liquid nitrogen was used. Samples of 0.3ml in 3mm diameter calibrated quartz tubes were used. Conditions for observation of epr signals such as power and temperature, etc, are given in each figure of epr spectra.

Low temperature epr spectroscopy has played an important role in this study of photosynthetic water splitting. This section will give a brief and simplified description of the technique.

Epr is used to detect species with unpaired electrons. There are several types of atoms or molecules in biology that contain unpaired electrons. Free radicals (molecules containing one unpaired electron), radicals with more than one unpaired electron, transition metal ions and triplet state entities (containing two strongly coupled paired electrons in a ground or excited state). This form of spectroscopy, like all spectroscopy techniques, measures a change in energy state of a sample due to the absorption of electromagnetic radiation (in this case microwaves). The absorption of microwaves stimulates the oscillation of a magnetic dipole, causing resonance. Resonance is only detected in a molecule containing a magnetic dipole, and in the presence of a static magnetic field. All electrons have a magnetic moment arising from the spinning of the electron about its axis, and this is known as a spin state. In an S = 1/2 system (i.e. with one unpaired electron) there are two energy levels with a very small energy difference, only split in an external magnetic field. The energy difference between the two states is linearly related to the magnetic field strength according to the equation $E = gBH_o$, where E is the energy span, H_o is the applied magnetic field, g is the g value and B the Bohr magneton.

A pair of electrons have small but opposite spin states and so the magnetic moments cancel each other out. Only unpaired electrons will have a magnetic moment

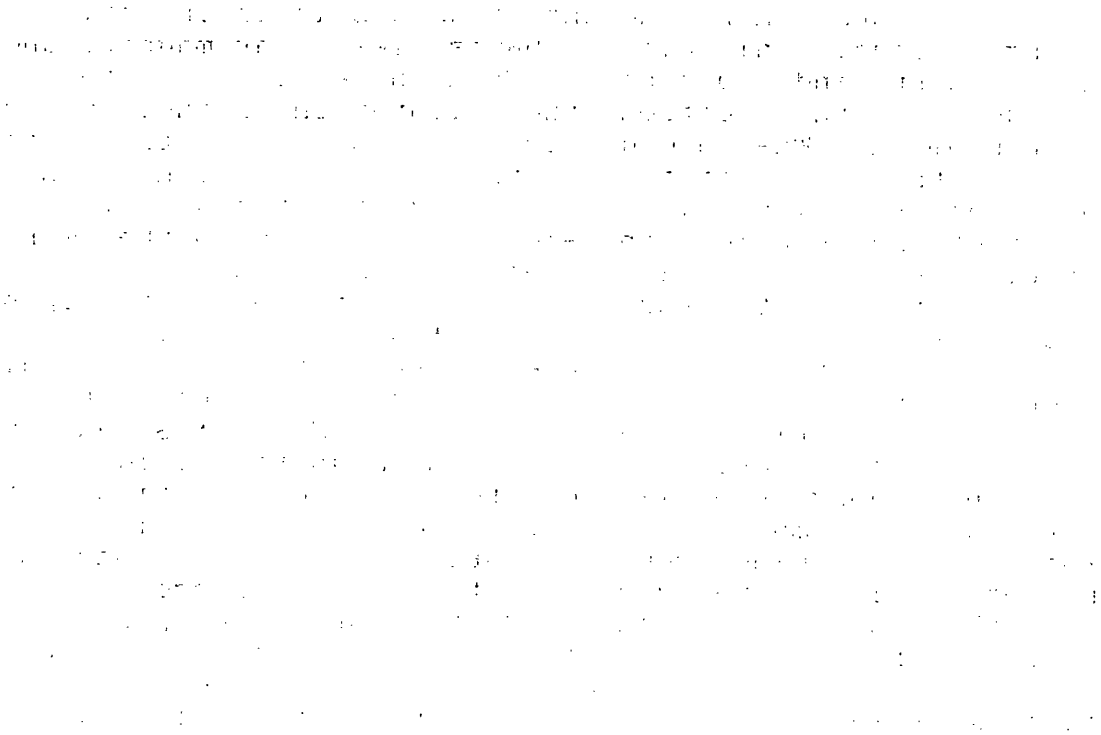

Fig.2.1. Electron spin and the Electron Energy Levels as a Function of Magnetic Strength.

Electrons can be thought of as a spinning,negatively charged cloud. This cloud behaves like a bar magnet, and has a north and south pole. When there is no external influence on the electrons the orientation of their poles is random (A). When a magnetic field is imposed the north and south poles of the electron clouds align either parallel or anti-parallel to the magnetic field (B). An input of energy allows the electrons to flip to the more stable arrangement. This is detected as resonance.

Electromagnetic radiation is used to change the spin state of a system. In a spin $^1/_2$ system (i.e. one unpaired electron) there are two spin states of equal energy. These are only split in the presence of an external magnetic field (C). The $S = {}^1/_2$ energy splitting is linearly related to the magnetic field.

In theory two methods for the observation of paramagnetic compounds could be used. (D) The microwave radiation frequency could be varied keeping a constant magnetic field (analogous to optical spectroscopy), or (E) the magnetic field could be varied keeping the microwave radiation constant. It is impractical to vary the microwave radiation and so epr techniques have a fixed microwave frequency. The magnetic field is scanned until the resonance point matches the magnetic field. (Diagram from Swartz et al, 1972).

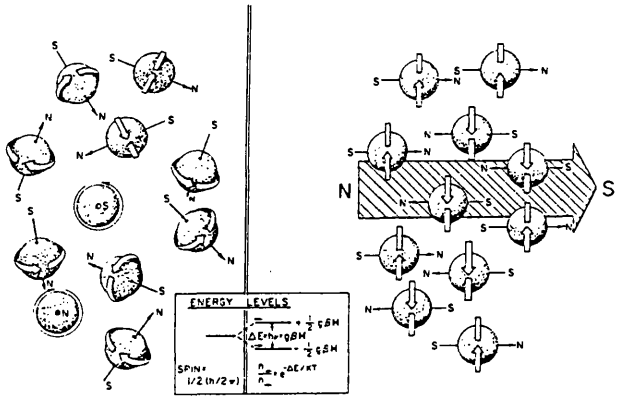
ENERGY LEVELS
N
S
A
B

Fig. 1

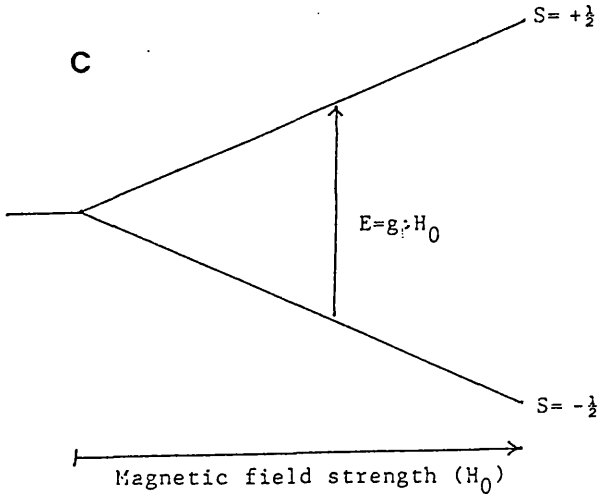
C
S= +½
E=g$_i$H$_0$
S= -½
Magnetic field strength (H$_0$)

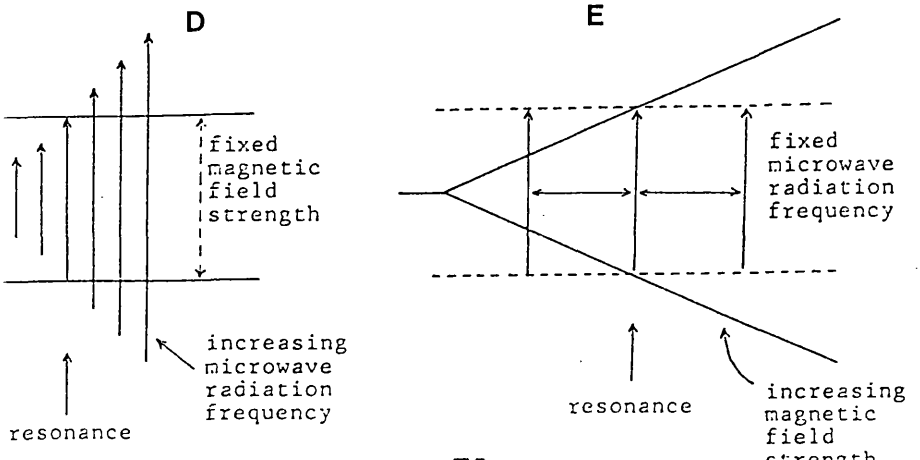
D
fixed magnetic field strength
increasing microwave radiation frequency
resonance
E
fixed microwave radiation frequency
resonance
increasing magnetic field strength

detectable by epr. In any population of unpaired electrons there will be a distribution of spin states in a given magnetic field. This distribution favours the more stable state, giving an unequal population of spin states. When there is an input of microwave energy, transitions from one state to the other can occur, giving a net absorption of electromagnetic energy, which is detected as resonance.

2.13.1 g - values

The g - value is characteristic of the molecule and of its environment in which the unpaired electron is located. It refers to the position in the magnetic field where resonance occurs and hence where the epr signal is found. The epr signal is detected by maintaining a constant microwave frequency and amplitude and then scanning a magnetic field until resonance occurs at a specific magnetic field strength, the g value. This value can be useful in the identification of an unknown epr signal.

2.13.2 Microwave Power Saturation

The difference between two energy levels is small, and any change in the population distribution can only occur when there is a net loss or gain in the total energy of the spin system. The spin system is in thermal contact with its surroundings, and energy therefore flows from the spin system to the lattice. Energy in the form of microwave power is removed from the spin system in the

Fig. 2-2. Energy Flow Between the Spin System and Spin Lattice.

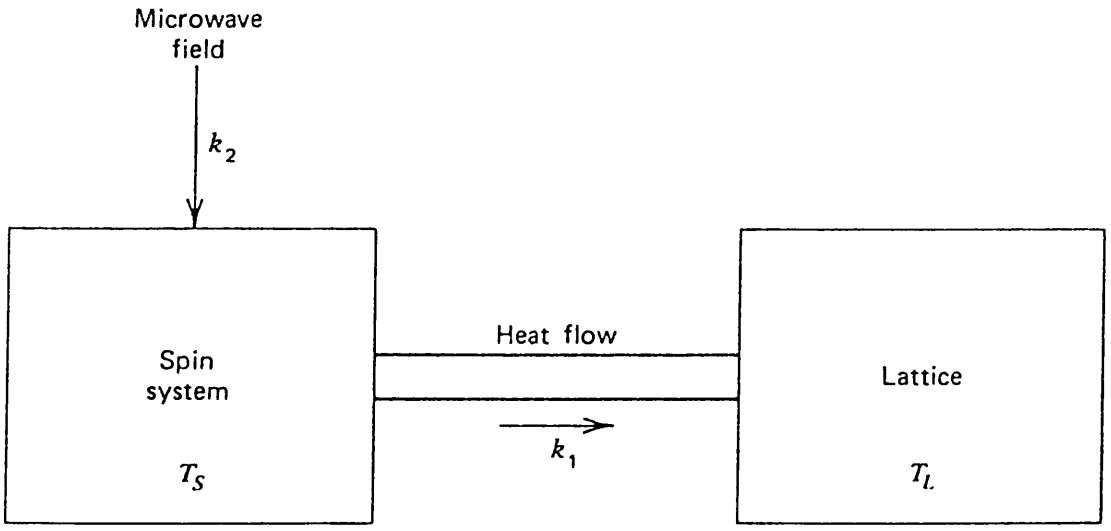

The energy flow through a spin system is represented in this diagram. Energy that is absorbed by the system (k_2) will be lost to the surrounding lattice according to the equation $dE/dt = k_1k(T_S - T_L)$ where T_L is the lattice temperature and T_S is the temperature of the spin system. k_1 and k_2 are rate constants describing the rate of heat flow. This phenomenon produces power saturation characteristics in an epr signal. Each epr signal has a characteristic $P^{1}/_{2}$ (the power when the signal is half saturated). The power saturation or rate of loss of energy to the lattice depends on the surrounding components and their redox state. (Diagram from Swart . et al, 1972).

same manner.

The rate of energy transfer from the spin system to the lattice is given by the equation $dE/dt = k_1k(T_s - T_L)$. Microwave energy will flow into the spin system at a rate characterised by k_2 (Fig. 2) and will be passed to the lattice at a rate (k_1). When K_2 is less than k_1 the energy can be efficiently released to the lattice. When K_2 and k_1 are equal or k_2 is greater than k_1 then the spin system cannot release the extra energy to the lattice quickly enough, leading to a phenomenon known as power saturation. Spin systems will therefore have power saturation characteristics according to the efficiency of the transfer of energy to the surrounding lattice.

2.13.3 Data Handling

Epr spectra were recorded on a PDP-11 mini-computer. At least three of each spectra were recorded, this was increased if the spectra were noisy. These were then averaged to improve the signal to noise ratio and transferred to a Tektronix 4051 micro-computer for further manipulation and plotting. Difference spectra were obtained by subtracting the spectrum of a dark adapted sample from the spectrum of an illuminated sample.

2.14 Vanadyl Ions as EPR Spin Probes

Proteins that have metal ions which are important in the enzyme function can be studied when the metal ion is replaced with a suitable spin probe. Vanadyl ions have

been used as spin probes of several different types of metal binding sites in several protein complexes (Boer et al, 1988; Fitzgerald & Chasteen, 1974; Cannon & Chasteen, 1975; DeKoch et al, 1974; Sakurai et al, 1987; Nieves et al, 1987). The oxycation VO^{2+} has spectroscopic and chemical properties which make it a useful spin probe ion. Vanadyl ions forms strong complexes with a variety of ligands and binds to a number of metalloproteins (Chasteen, 1981). The ion has a single unpaired electron in the 3d orbital, which gives rise to an epr signal observable at room temperature. It is a vanadium (IV) ion, and is the most stable oxycation of the first row transition metals. Vanadyl ions, however, are readily oxidised to vanadium (V) in the presence of oxygen at physiological pHs and samples have to be handled in a nitrogen atmosphere (Iannuzzi et al, 1975). Chelation of the ion stabilises the IV oxidation state, slowing the oxidation process. The ability of vanadyl ions to bind to diverse proteins and metal binding sites may arise in the flexibility of the coordination geometry of VO^{2+}. The complexes of oxovanadium (IV) typically have square pyramidal or bipyramidal structures, with the oxygen in an apical position (Chasteen et al, 1981) (Fig. 3).

VO^{2+} ions form various hydroxide species. $VO(OH)_2$ is formed as a precipitate at pH 6.5 and this is epr silent. If the buffer is gassed with nitrogen and VO^{2+} is added to give 1 or 2mM concentrations from a pH 3.0 stock

Fig.2-3. The Coordination Properties of the vanadyl Ion

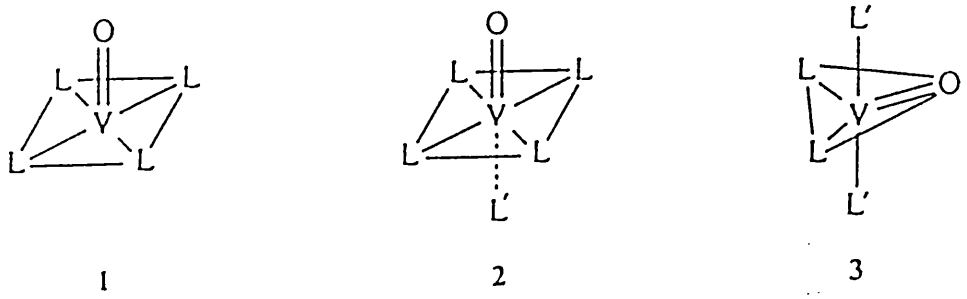

The vanadyl ion is a useful spectroscopic probe, and forms strong associations with many kinds of ligands. The vanadyl ion typically has (1) a square pyramidal structure, a bipyramidal structure (2) or a trigonal bipyrimidal structure (3). The oxygen atom occupies an apical position. This flexibility in co-ordination probably accounts for the fact that VO^{2+} ions can be bound to a diversity of proteins with different metal binding sites. The vanadyl ion is epr silent in solution at physiological pH providing no oxygen is present. When the ion forms a ligand to a protein it becomes epr active, displaying a typical 8 line epr spectrum. (Diagram from Chasteen, 1981).

solution, no precipitate is formed, and the resultant clear solution is epr silent. If the ion binds to a ligand of a protein or any type of chelator a characteristic epr signal is seen, which is very sensitive to its environment or binding site.

Of greatest significance to this study is the use of vanadyl ions to study the calcium binding sites of calmodulin (Nieves et al, 1987). At least two calcium binding sites of the calmodulin complex were found to bind vanadyl ions.

2.14.1 Reconstitution of PS2 preparations with Vanadyl ions

A 300 mM solution of vanadyl sulphate hydrate at pH 3.0 was prepared in distilled water gassed with oxygen free nitrogen. This stock solution was prepared fresh for each experiment. The vanadyl sulphate hydrate was from Aldrich and was 99% pure, with no details of contaminating calcium. PS2 prepartions to be reconstituted with vanadyl ions were first gassed with oxygen free nitrogen for at least 30 minutes, to ensure all dissolved oxygen was removed. Reconstitution for epr measurements was achieved with 25 - 100 uM vanadyl ions. Measurements of oxygen evolution with added vanadyl was with between 1 - 3 mM vanadyl.

CHAPTER 3

RESULTS AND DISCUSSION

3.1 The Preparation of Photosystem II from Thylakoids

Spinach thylakoid membranes were used to obtain various PS2 preparations. Gel 1 shows the polypeptide composition of these preparations. Thylakoid membranes contained a large number of polypeptides (lane A). Many polypeptides not associated with PS2 were almost completely removed by the 5% TX-100 treatment for 25 minutes. This resulted in an enrichment of the PS2 polypeptides (lane B). The polypeptides most easily recognised were: (1) the 24 kDa light harvesting chlorophyll polypeptides, (2) the 33 kDa extrinsic polypeptide, with the faintly staining D1 and D2 bands and (3) the 47 and 43 kDa chlorophyll binding polypeptides. Further purification from these PS2 membranes using the detergent OGP yielded oxygen evolving core complexes (OGP PS2) with less light harvesting chlorophyll (lane C). These had a similar polypeptide composition to the PS2 membranes, but lacked the 24 kDa light harvesting chlorophyll proteins and the 17 and 23 kDa extrinsic polypeptide. D1 /D2 cytochrome b_{559} reaction centre complexes were isolated from PS2 membranes (lane D). The most distinct band was at approximately 60 kDa, due to the D1 /D2 dimer.

Gel. 1. The polypeptide profile of thylakoids, PS2 membranes, OGP PS2 and PS2 reaction centres from spinach.

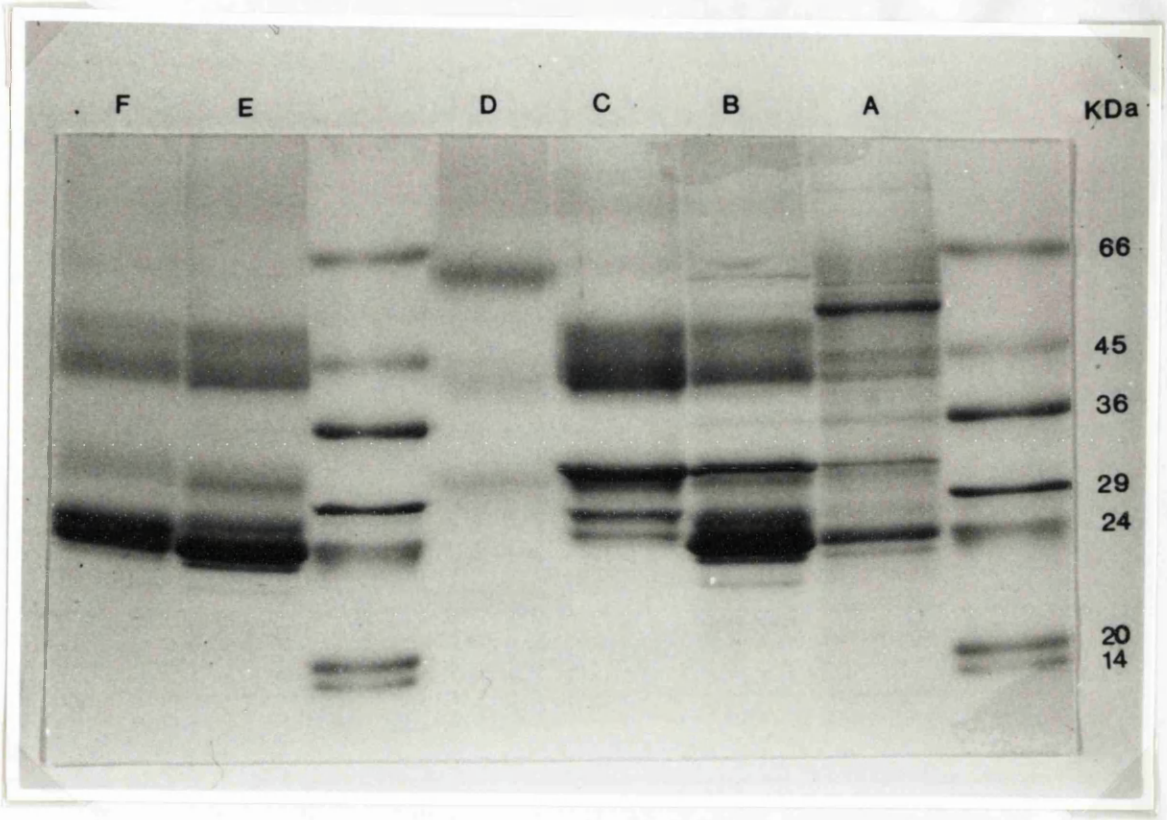

Polypeptide profiles as resolved by SDS polyacrylamide gel electrophoresis and Coomassie blue staining of thylakoids and PS2 preparations from spinach are shown. Lane A; thylakoids, containing many polypeptides from the 5 membrane spanning complexes. Lane B; PS2 membranes with a prominent band of light harvesting chlorophyll at approx 24 kDa. Lane C; OGP PS2, Photosystem II oxygen evolving core complexes made using the detergent OGP, with a prominent band at 33 kDa (the "33 kDa" extrinsic polypeptide), but lacking light harvesting chlorophyll. Lane D; PS2 reaction centre, containing a D1 /D2 dimer of approx 60 kDa. Lane E is the polypeptide profile of Tris washed PS2 membranes and lane F is Urea washed OGP PS2. The 33 kDa extrinsic polypeptide is absent in both types of PS2 after this treatment. Lanes 1 and 6 (the unlabelled lanes) are the molecular weight marker polypeptides. Electrophoresis was according to Chua and Bennoun, using an 18% acrylamide slab gel. A constant voltage 450 V was applied. The current was initially set at 10 mA until the polypeptides had passed at least half way into the stacking gel. The current was then increased to 40 mA and the gel was run to completion taking approximately 4 hours.

3.2 The Oxygen Evolving Core Complex

PS2 preparations lacking light harvesting chlorophyll proteins, but maintaining high rates of oxygen evolution were prepared using n- octyl B D-glucopyranoside (OGP). Gel 2 shows the removal of light harvesting chlorophyll to different degrees according to the concentration of detergent present. The concentration of the OGP was critical for maximum light harvesting chlorophyll removal and maintaining maximum oxygen evolution. Lane 7 of the gel corresponds to preparation of the core complexes using 35 mM OGP. The detergent concentration was increased by 2.5 mM consecutively as indicated. The detergent OGP worked by specifically solubilising the PS2 core complex. The membranes were removed as a pellet containing the light harvesting chlorophyll binding polypeptides. Higher concentrations of OGP solubilised the light harvesting polypeptides as well as the core complexes. In these samples the light harvesting chlorophyll remained in the supernatant along with the PS2 core complexes. The core complexes of Lane 7 (gel 2) showed the lowest level of light harvesting chlorophyll, with increasing rates of oxygen evolution per mg chlorophyll left to right, from lane 1 to lane 7.

Optical absorption measurements of the OGP PS2 compared to PS2 membranes also indicated that a large amount of light harvesting chlorophyll was removed during the OGP detergent treatment (Fig. 1.). Both untreated PS2

Gel. 2. The Preparation of Oxygen Evolving Core Complexes of PS2 using the detergent OGP.

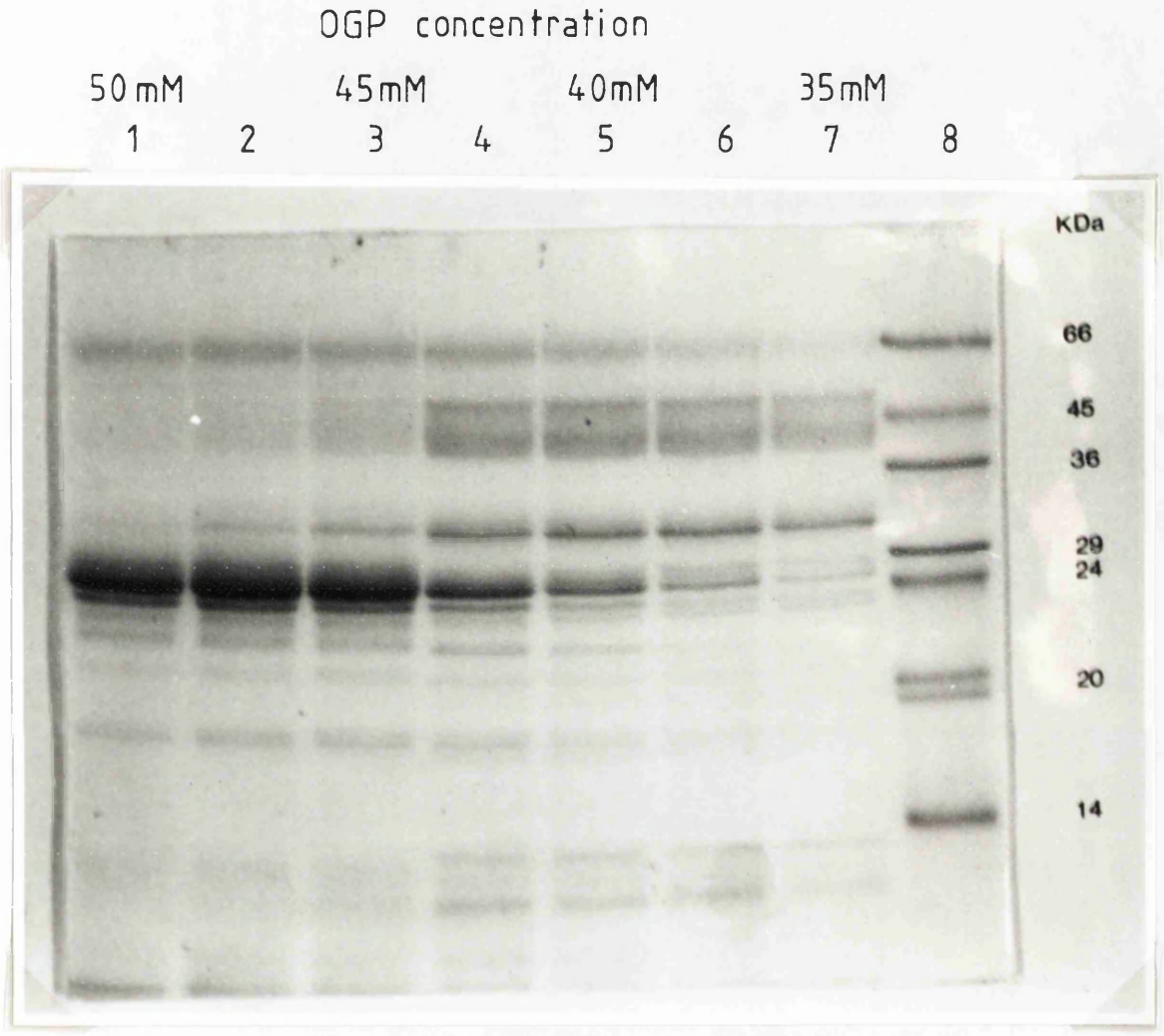

Polypeptide profiles of PS2 core complexes made using the detergent n octyl B- D glucopyranoside. Lanes 7 to 1 are oxygen evolving core complexes prepared with increasing concentrations of detergent. Lane 7 corresponds to 35 mM OGP, increasing by 2.5 mM in each lane up to 50 mM OGP in lane 1. The most efficient removal of light harvesting chlorophyll with high levels of oxygen evolution maintained is shown in lane 7 (i.e. 35 mM OGP). The purification of the oxygen evolving core complexes is indicated by the removal of the 24 kDa band of light harvesting chlorophyll, with an enhancement of the 33 kDa extrinsic polypeptide and the 47 and 43 kDa chlorophyll binding polypeptides. The molecular weight markers are shown in lane 8. The gel is an 18% acrylamide slab gel made and run according to Chua and Bennoun, with the current and voltage as for gel 1.

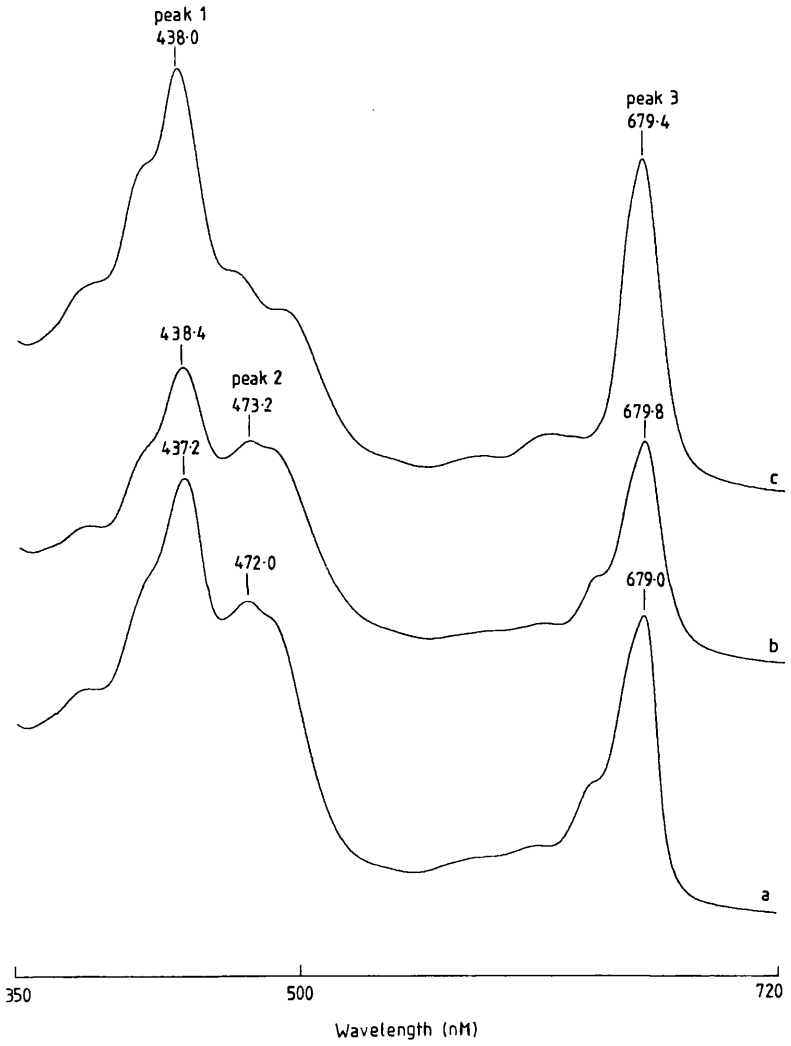

Fig. 3.1. Optical absorption spectra of different preparations of PS2. (a) Untreated PS2 membranes. (b) NaCl washed PS2 membranes. (c) OGP PS2 particles. The peak at approximately 473 nm (peak 2) is dramatically reduced with respect to the peak at approximately 438 nm (peak 1) in OGP PS2, indicating the removal of a large proportion of the light harvesting chlorophyll polypeptides by this treatment (see gel 2). NaCl washing did not alter the relative proportion of each peak compared to untreated PS2 membranes, as no pigment binding polypeptides are removed.

membranes and NaCl washed PS2 had a large peak at approximately 473 nm (Fig. 1 b,c), due to the absorption by light harvesting chlorophyll. This peak was largely absent in the optical absorbance spectrum of OGP PS2, whilst the peak at 438.0 nm was enhanced (fig. 1. a).

The 17 and 23 kDa extrinsic polypeptides were also removed by the OGP treatment. Therefore to obtain the maximum rate of oxygen evolution, mM concentrations of calcium and chloride were added. The rate of oxygen evolution (measured as u moles O_2 /mg Chl /h) was only slightly higher from OGP PS2 than that obtained from untreated PS2 membranes (see tables below).

3.3 The Reaction Centre D1 /D2 Cytochrome b_{559} Complex

PS2 membranes were solubilised with triton X-100 and applied to a DEAE column as given in the materials and methods.

Figure 2 shows the absorbtion spectra of fractions eluted from the DEAE column with increasing concentrations of NaCl. Peak 4 at about 450 nm arises from Chlorophyll a and was present in large quantities in fractions eluted between 60 and 90 mM NaCl (Fig. 2. b,c,d). The fraction eluted at 120 mM NaCl had the lowest amount of light harvesting chlorophyll and only a small peak in the region of 450 nm indicating that a large proportion of chlorophyll a had been removed (Fig. 2. a).

Fig. 3.2. Optical absorption spectra of the fractions eluted from a DEAE column with different concentrations of NaCl. (a) eluted at 120 mM NaCl, (b) eluted at 90 mM, (c) eluted at 60 mM, (d) eluted at 30 mM. The fraction eluted at 120 mM NaCl corresponds to the D1 /D2 cytochrome b_{559} reaction centre complex. This fraction has a very small peak at approximately 470 nm, compared to the other fractions eluted at lower concentrations of salt. This reflects the removal of light harvesting chlorophyll proteins including the 43 and 47 kDa chlorophyll binding polypeptides associated with PS2. Peak 1 at 418 nm arising from cytochrome b_{559} and pheophytin is enhanced in this fraction indicating a greater proportion of reaction centre components per chlorophyll a.

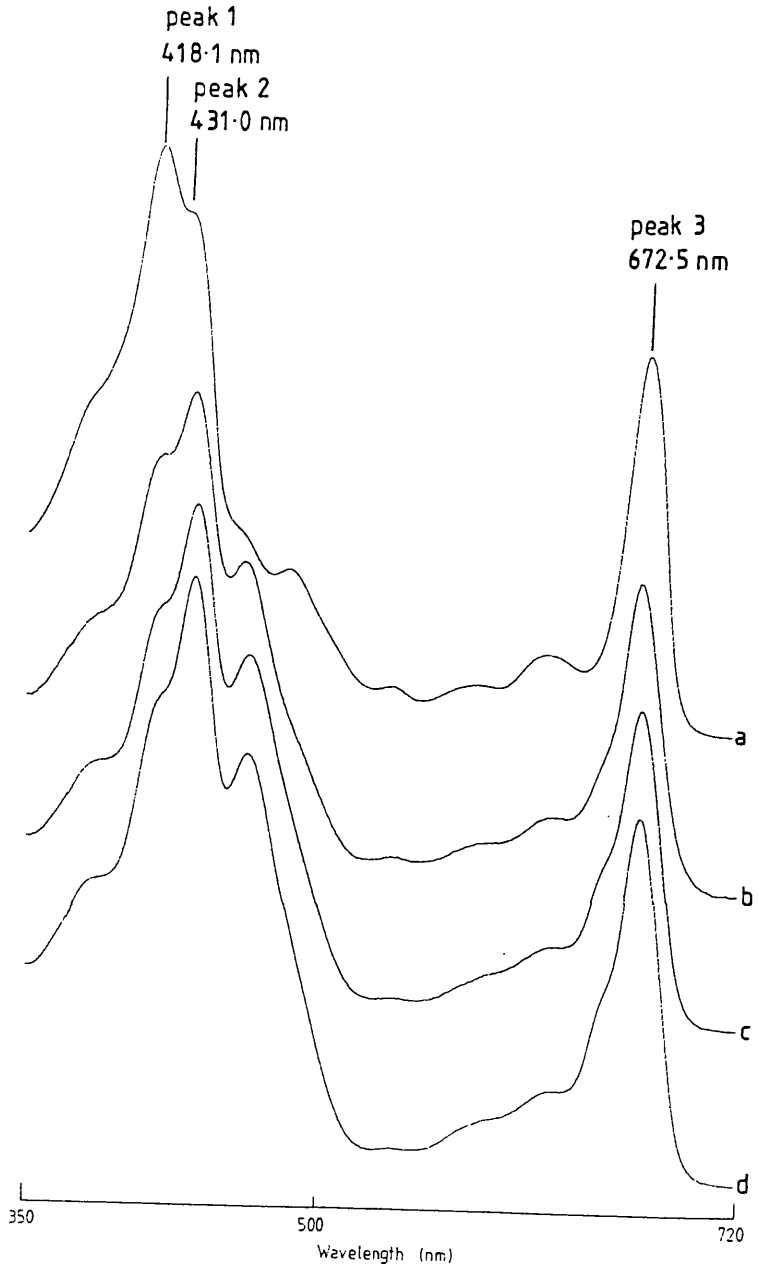
peak 1
418·1 nm
peak 2
431·0 nm
peak 3
672·5 nm
a
b
c
d
350
500
720
Wavelength (nm)

Peak 1 at approximately 420 nm arises from both the pheophytin and cytochrome b_{559} complex. This peak was larger and more sharply defined in the fraction eluted at 120 mM NaCl, indicating a higher purity of the D1/D2 reaction centre components (Fig. 2. a). The peak at approximately 672 nm, is the red peak of chlorophyll a. The photochemical activity of the reaction centre complexes was indicated by the position of peak 3. A highly active reaction centre preparation had a peak corresponding to peak 3 at 676 nM. The wavelength of this peak shifted towards 670 nM as the activity of the reaction centre was lost. The reaction centre complex was sensitive to light and when studied was handled at 4°C in the dark.

A spin polarised triplet epr signal was detected when reaction centre complexes eluted at 120 mM NaCl were examined by epr under continous illumination at 4.2 K (Fig. 3. a,b,c). The spin polarised triplet signal (Fig. 3. c) originates from a radical - pair recombination between the oxidised primary donor chlorophyl $P680^{+}$ and the reduced pheophytin acceptor I^{-} (Rutherford A.W. et al, 1981).

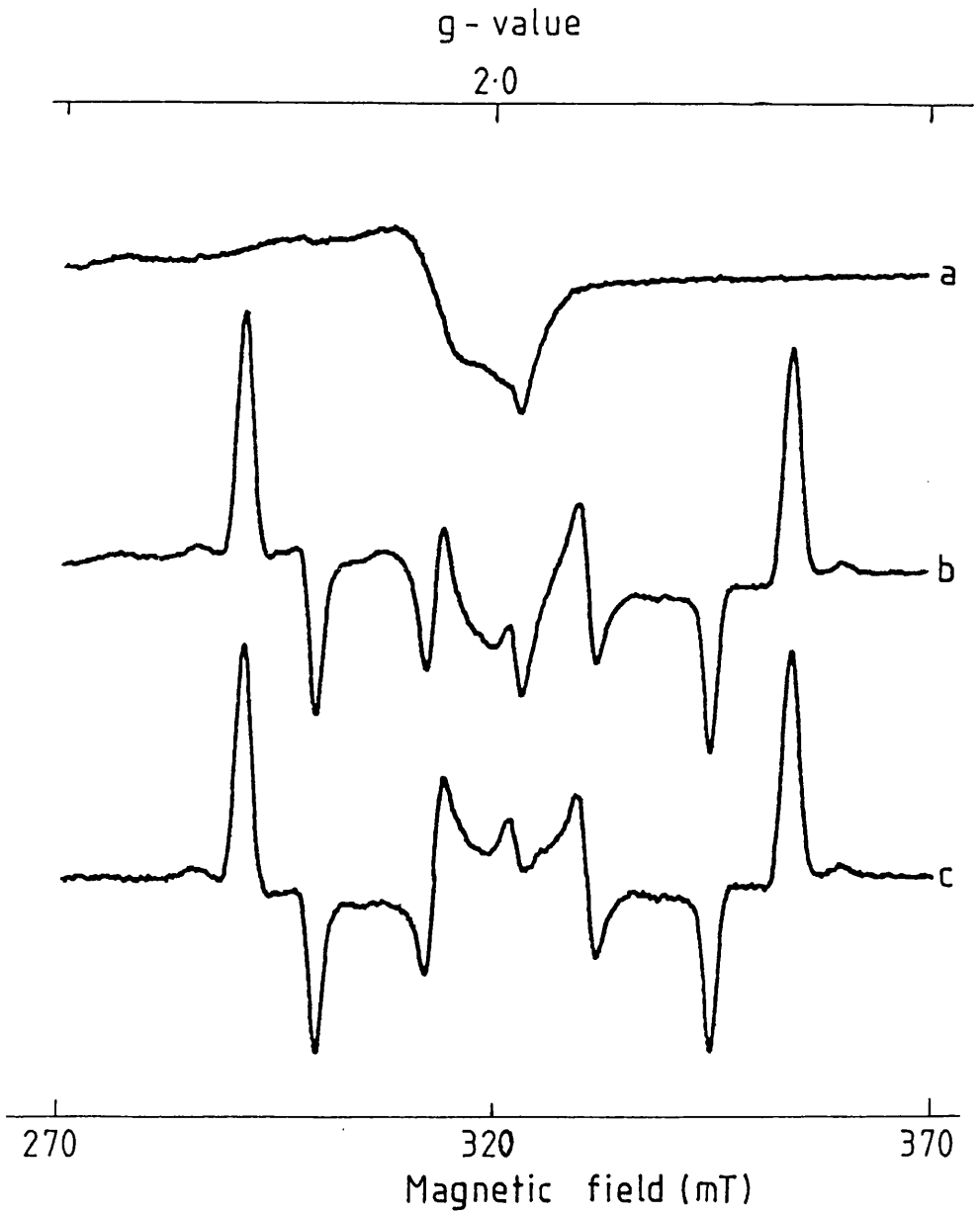

Fig. 3·3. The spin polarised triplet epr signal of spinach PS2 generated by continuous illumination at 4.2 K of the D1 /D2 cytochrome b$_{559}$ reaction centre complex. (a) The dark spectrum of the reaction centre complex. (b) The triplet epr signal generated by continuous illumination at 4.2 K. (c) Difference spectrum (b - a) showing the symmetrical spin polarised PS2 triplet. This signal arises from a radical pair recombination between the primary donor chlorophyll P680^{+} and the reduced pheophytin acceptor. Epr conditions: power, 25 uW; modulation width, 1 mT; temperature, 4.2 K.

3.4 The EPR Characteristics of the PS2 Preparations

Photosystem II preparations capable of oxygen evolution had a typical multiline epr signal (with either 16 or 19 lines) when poised in the S_2 state. This signal was induced after 4 hours dark adaptation at 4 °C either by (1) freezing the epr sample under illumination in the presence of the herbicide DCMU (Fig. 4.) or by (2) illuminating the dark adapted sample at 200 K. Both of these treatments allow single turnover of the reaction centre resulting in the S_1 to S_2 state change.

OGP PS2 was more stable when stored in the dark at 4 °C. (i.e. the particles retained oxygen evolution better than PS2 membranes). Some differences in the power saturation characteristics of the multiline epr signal in the untreated, pH 6.3 NaCl washed and OGP PS2 were observed. At non saturating powers, a straight line parallel with the X - axis is obtained. At high saturating powers a sloped straight line is formed. The intersection between these two straight lines corresponds to the power at half saturation ($P^{1}/_{2}$) read from the inverse log of the X - axis value. The untreated PS2 membranes were power saturated at a lower power than both NaCl washed and OGP PS2 (Fig. 5). This implies that the manganese cluster has undergone some minor alteration during the NaCl wash and the OGP detergent treatment that increased the transfer of energy to the surrounding lattice.. Comparisons of the size of the S_2 state

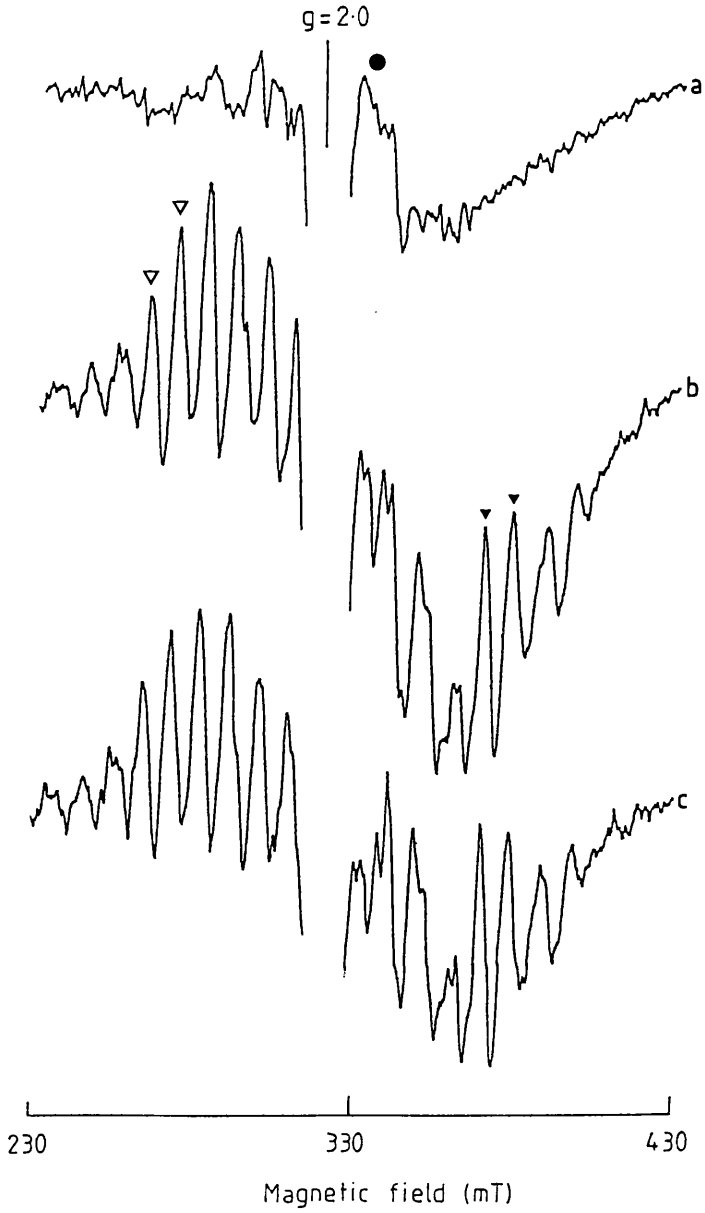

Fig.3·4. The S_2 state multiline epr signal. (a) PS2 membranes dark adapted for 4 hours (S_1 state) and then illuminated at 77 K. (b) PS2 membranes frozen under illumination after 4 hours dark adaptation. (c) Light minus dark difference spectrum of the above spectra, showing the 19 line form of S_2 state multiline epr signal. The signal is quite symmetrical apart from the 5^{th} and 6^{th} high field peaks (indicated ▼) which are particularly prominent. No multiline signal is detected after 77 K illumination, only the generation of the g = 1.9 iron semiquinone epr signal occurs (indicated ●). Chl concentration: 8 mg /ml. Epr conditions: power, 10 mW; temperature, 8.5 K; modulation amplitude, 1 mT.

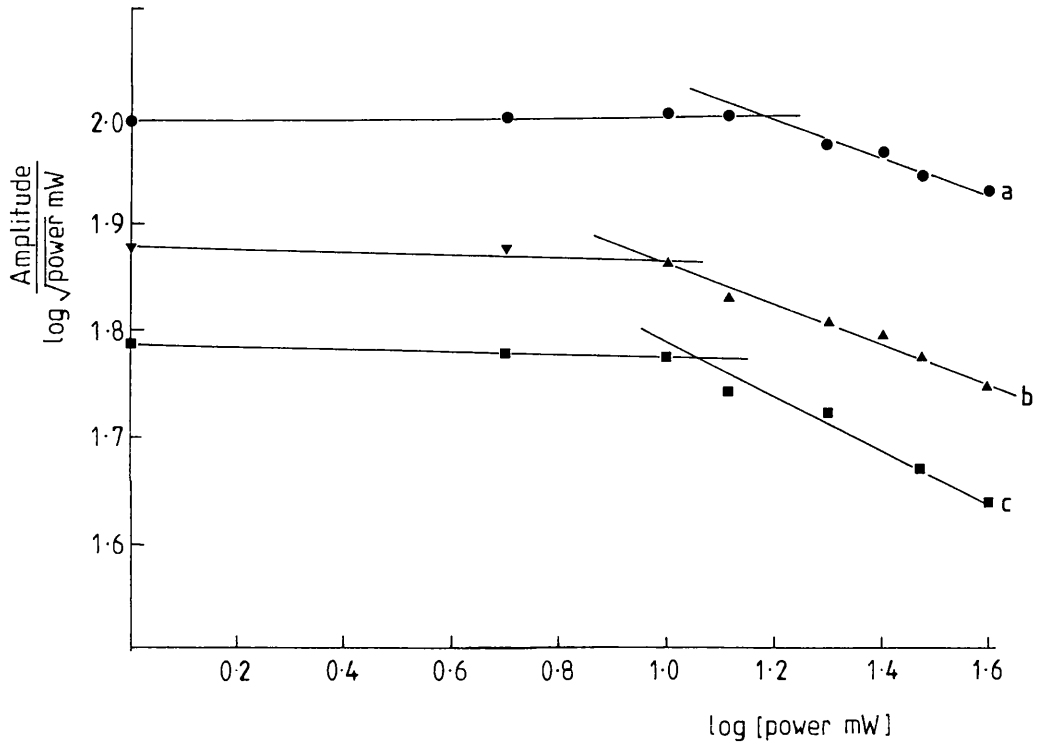

Fig.3·5. Measurement of power saturation of the S_2 state multiline epr signal. The 5th and 6th low field peaks (marked in fig 4. ▽) (a) Untreated PS2 dark adapted for 4 h and then illuminated at 200 K, power saturated at 15 mW. (b) pH 6.3 room light salt washed PS2, 4 h dark adapted then illuminated at 200 K, power saturated at 9.5 mW. (c) OGP PS2 , 4 h dark adapted and illuminated at 200 K, power saturated at 12.0 mW.

multiline epr signals revealed that the multiline signal from OGP PS2 was only slightly larger per mg Chl than the signal obtained from untreated PS2 membranes (Table 1).

Table 1 Comparison of Multiline Amplitude of Three Different Preparations of Oxygen Evolving PS2

Sample of PS2 (+20 mM $CaCl_2$)	Multiline Amplitude/mg chl (low field peaks were measured as indicated in Fig. 4b)
1) Untreated PS2	
a) 200 K ILL	67.0
b) FR ILL	62.0
c) FR ILL + DCMU	66.0
2) NaCl washed PS2	
a) 200 K ILL	52.0
b) FR ILL	30.0
c) FR ILL + DCMU	52.0
3) OGP PS2	
a) 200 K ILL	75.5
b) FR ILL	19.0
c) FR ILL + DCMU	75.0

The number of chlorophylls per D1/D2 was known to be approximately 40, whilst in untreated PS2 membranes there were approximately 200 Chl per D1/D2 (Dunahay T.G. et al, 1984). This suggests that the OGP PS2 was enriched

five times compared to untreated PS2 membranes. Manganese is enriched approximately four fold, with a corresponding increase in the size of Z^{+} (Ghanotakis , & Yocum , 1986). The measurements of oxygen evolution and multiline epr signal do not correspond to this increase in purity. This may be due to damage incurred during the detergent treatment. The result of this is that there is a reduced efficiency of charge separation and turnover of the S states in the light. This was investigated further.

In untreated PS2 membranes the iron semiquinone epr signal occured as the g = 1.9 form (Fig. 6. a,b). The g = 1.8 form of the iron semiquinone epr signal can be induced in untreated PS2 membranes by the depletion of bicarbonate on addition of formate (Fig. 7. a, g = 1.8 indicated ●) or acetate (Fig. 7. b). The transfer of electrons from Q_A to Q_B is blocked during these treatments and there is some loss of charge separation. This may account for the lower amount of the S_2 state multiline epr signal formed on 200 K illumination in the presence of acetate and formate (Fig. 7). The iron semiquinone epr signal of OGP PS2 was found to occur as the g = 1.8 form, not as the normal g = 1.9 form. The presence of the g = 1.8 iron quinone signal in OGP PS2 suggests that bicarbonate has been depleted during the treatment. The depletion of bicarbonate may be due to or may cause structural alterations of the acceptor side of the PS2. This depletion of bicarbonate and loss of charge

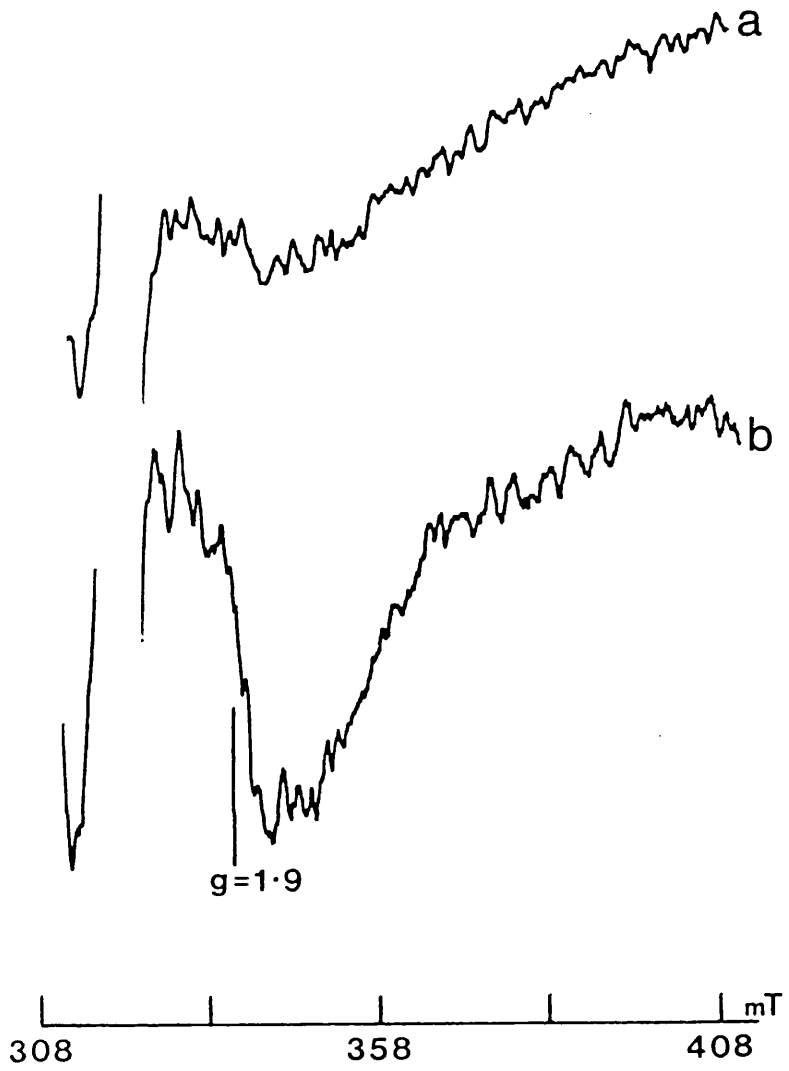

Fig. 3·6. Epr spectra of the g = 1.9 iron-semiquinone signal. (a) 77 K illuminated sample stored for 6 days at 77 K in the dark. (b) as in a), but after a further illumination at 77 K. Chl concentration: 4 mg/ml. Epr conditions: power, 10 mW; temperature, 5.5 K; modulation width, 1 mT. The g = 1.9 iron semiquinone epr signal decays after 77 K storage for 6 days in the dark, by recombination with D^+. The signal can then be induced again by further illumination at 77 K.

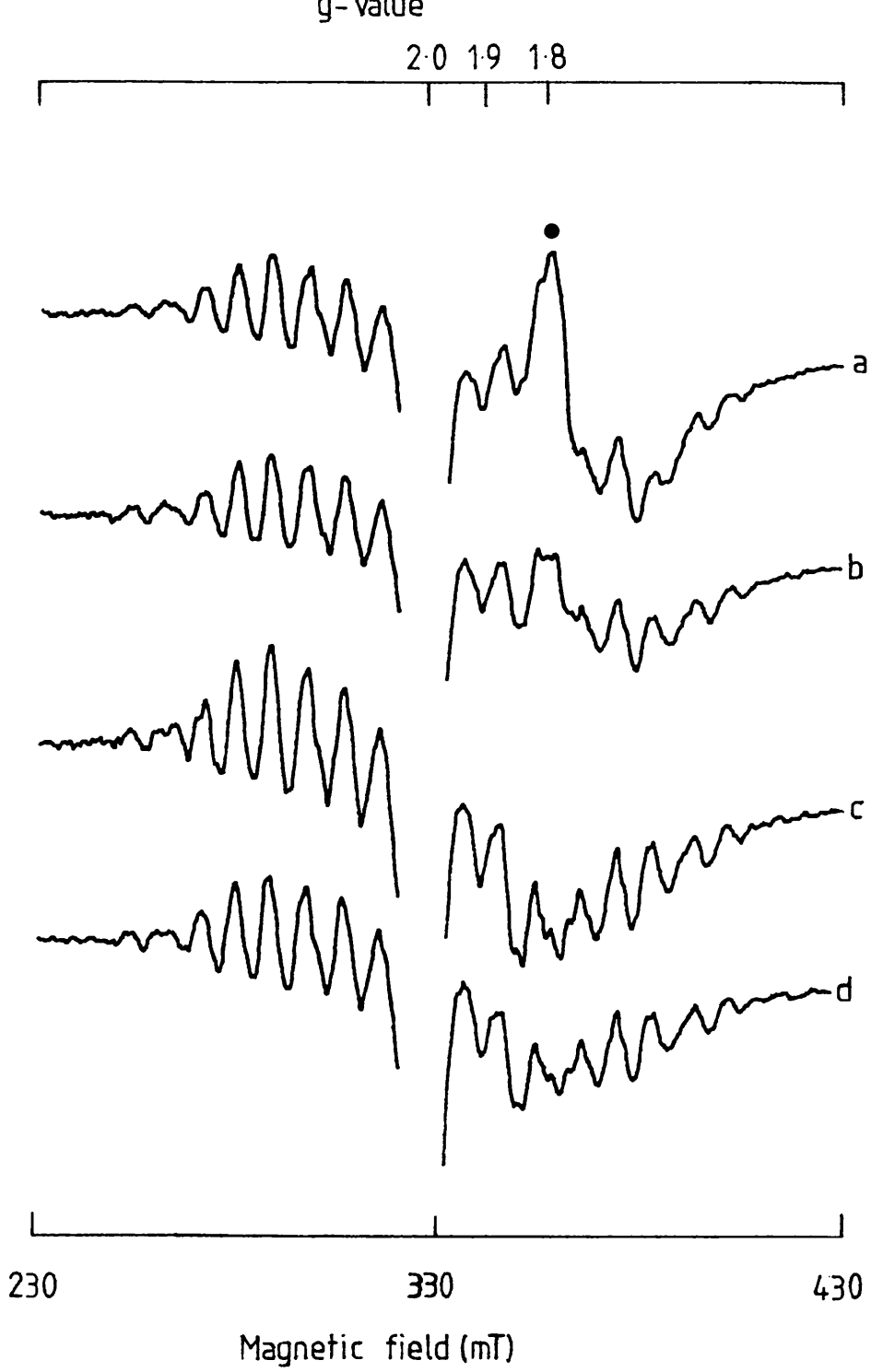

Fig.3·7. The effect of bicarbonate replacement on the iron semiquinone epr signal and the S_2 state multiline epr signal. (a) Sample of untreated PS2 with 100 mM formate after 200 K illumination. (b) as a, but 100 mM acetate added. (c) as a, but 100 mM glycollate added. (d) no additions. Chl concentration: 6 mg /ml; Epr conditions: power, 10mW; temperature 8.5 K; modulation amplitude, 1 mT.

separation partly explains the lower rate of oxygen evolution and smaller S_2 state multiline epr signal of OGP PS2 per chlorophyll than expected.

Cytochrome b_{559} occured in either a high or low mid point redox potential forms, both having characteristic epr signals. Untreated PS2 membranes possessed the high potential form of the cytochrome b_{559}, which can act as an electron donor at 77 K. PS2 treated with the detergent OGP showed only the low potential cytochrome b_{559}. This is further evidence that substantial modification of the PS2 had occured during the OGP detergent preparation.

In Summary:

Illumination at 77 K cyt b_{559}^{+} ---> P680 ---> Q^{-}

Illumination at 200 K S_1 state ---> S_2 state

P680 ---> Q^{-}

3.4.1 The Effect of Ammonium Chloride as a Substrate Analogue

Ammonium chloride acts as a substrate analogue to water. It has been used to investigate the site of water binding and the S state in which binding occurs. There are thought to be two types of binding (type 1 and 2) that can occur. When 100 mM NH_4Cl was added to PS2 preparations, only a small amount of the S_2 state multiline epr signal was formed when samples of NaCl washed PS2, or OGP PS2 were frozen under illumination in the presence of DCMU. The g = 4.1 epr signal was also formed (Fig. 8.). The formation of this signal was probably due to chloride co-factor displacement which occurs when there is type 2 binding of NH_4Cl (Sandusky & Yocum ., 1988).

Type 1 binding results in the modification of the hyperfine structure of the multiline S_2 state epr signal. The small amount of multiline formed did not show the alterations in width observed with type 1 binding of NH_4Cl (Beck & Brudvig ., 1986). This suggests that NH_4Cl was able to displace chloride ions more easily due to the absence of the 17 and 23 kDa polypeptides in NaCl washed or OGP PS2. This is possible if the two extrinsic polypeptides are involved in maintaining high affinity chloride binding site.

In untreated PS2 membranes it was possible to observe both type 1 and 2 binding, although rather

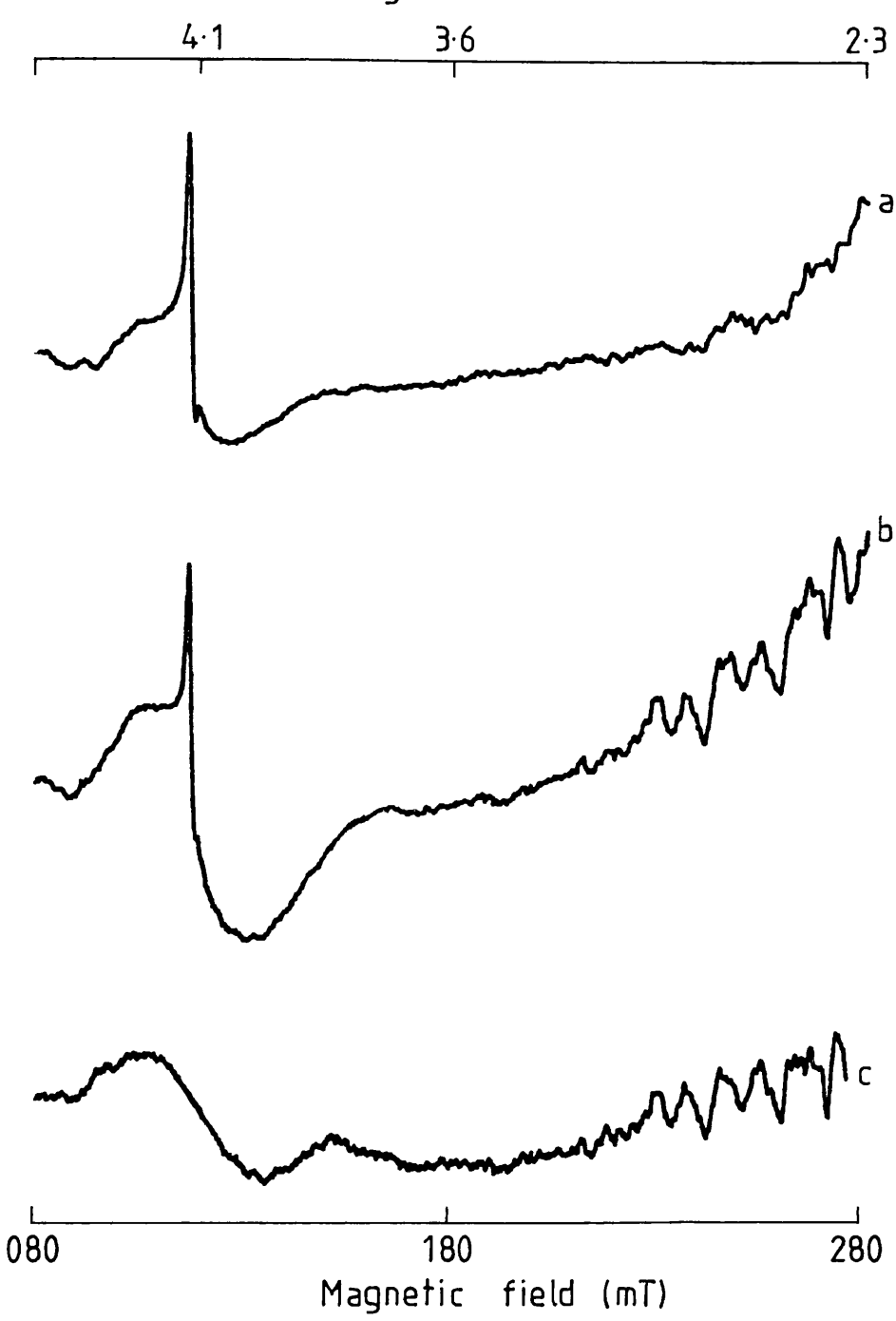

Fig. 3·8. The g = 4.1 epr signal from a modified S_2 state of the OEC. (a) 4 hour dark adapted NaCl washed PS2. (b) as in a) with 100 uM DCMU and 80 mM NH_4Cl added, then frozen under illumination. (c) difference spectrum, light minus dark. The g = 4.1 signal is thought to arise from a non functional conformation of the S_2 state of the OEC. This was only generated in the presence of NH_4Cl, either by freezing under continuous illumination or by 200 K illumination. Chl concentration: 5 mg /ml. Epr conditions: temperature, 8.5 K; power, 10 mW; modulation amplitude, 1 mT.

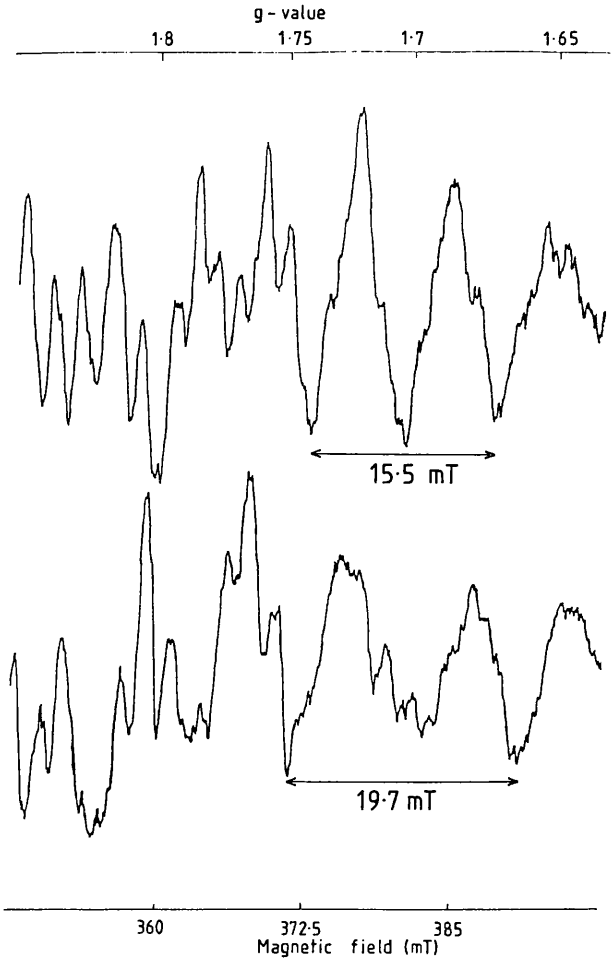

Fig. 3·9. Comparison of the high field S_2 state multiline epr signal with and without addition of NH_4Cl at pH 7.5. The S_2 state was formed by illumination at 10°C with 100 uM DCMU added after 4 h dark. (a) 80 mM NH_4Cl added. (b) Untreated PS2. Epr conditions: modulation amplitude, 0.4 mT; power, 1 mW; temperature 7.0 K.

inconsistently. Type 1 binding only occured when 100 mM NH_4Cl was added to a 4 h dark adapted PS2 sample at pH 7.5, and the sample of PS2 was frozen under illumination in the presence of DCMU (Fig. 9.). Type 1 binding of NH_4Cl resulted in a narrowing of the S_2 state multiline epr signal, most easily observed in the high field part of the spectrum (Fig. 9. a). When the sample of PS2 was illuminated at 200 K, an S_2 state multiline epr signal was formed with normal characteristics (Fig. 9. b). Type 1 binding did not occur readily, and more often the generation of the g = 4.1 epr signal replaced the formation of the multiline epr signal after freezing under illumination with DCMU (Fig. 8. b and c).

3.5 The Oxygen Evolving Complex of PS2

3.5.1 The Removal of the Extrinsic Polypeptides

Treatment with at least 1.0 M NaCl completely removed the 17 and 23 kDa extrinsic polypeptides (gel 5. lanes 3, 4,and 5). Removal of the polypeptides in the dark was complete within 5 minutes.

The 33 kDa polypeptides was then completely removed by treatment with 2.6 M urea (gel 5. lanes 1 an 2). The same polypeptides were removed by a single treatment with 2.0 M $CaCl_2$, $MgCl_2$ or $SrCl_2$ (not shown). The oxygen evolving capacity of these preparations was investigated. Only very low levels of oxygen evolution were detected

Gel. 5. The Removal of the Extrinsic Polypeptides Associated with the Water Oxidising Complex

The 17 and 23 kDa polypeptides were removed by a wash with 1.8 M NaCl, and the 33 kDa polypeptide was removed by a wash with 2.6 M urea. Lane 6 shows the molecular weight standards. Lane 5 is the polypeptide profile of untreated PS2 membranes. The 17, 23 and 33 kDa polypeptides are present. Lane 4 is the supernatant from the wash with 1.8 M NaCl, after dialysis and PEG concentration. The 17 and 23 kDa polypeptides are clearly visible. Fainter bands of polypeptides are thought to be contaminating polypeptides, but it is not possible to rule out the depletion of other low molecular weight polypeptides during this procedure. Lane 3 shows the polypeptide profile of the NaCl washed PS2 membranes. The bands at 17 and 23 kDa are absent. Lane 2 is the supernatant from the 2.6 M urea wash of the NaCl washed PS2 membranes, after dialysis and PEG concentration. The 33 kDa extrinsic polypeptide is present in large amounts with faint amounts of lower molecular weight polypeptides. These are thought to be contaminating polypeptides, but again the depletion of low molecular weight polypeptides cannot be ruled out. Lane 1 shows the polypeptide profile of the PS2 membranes after NaCl washing followed by urea washing. The 17, 23 and 33 kDa polypeptides are all absent. The gel was an 18% acrylamide slab gel according to Chua and Bennoun. Current and voltage as in gel 1.

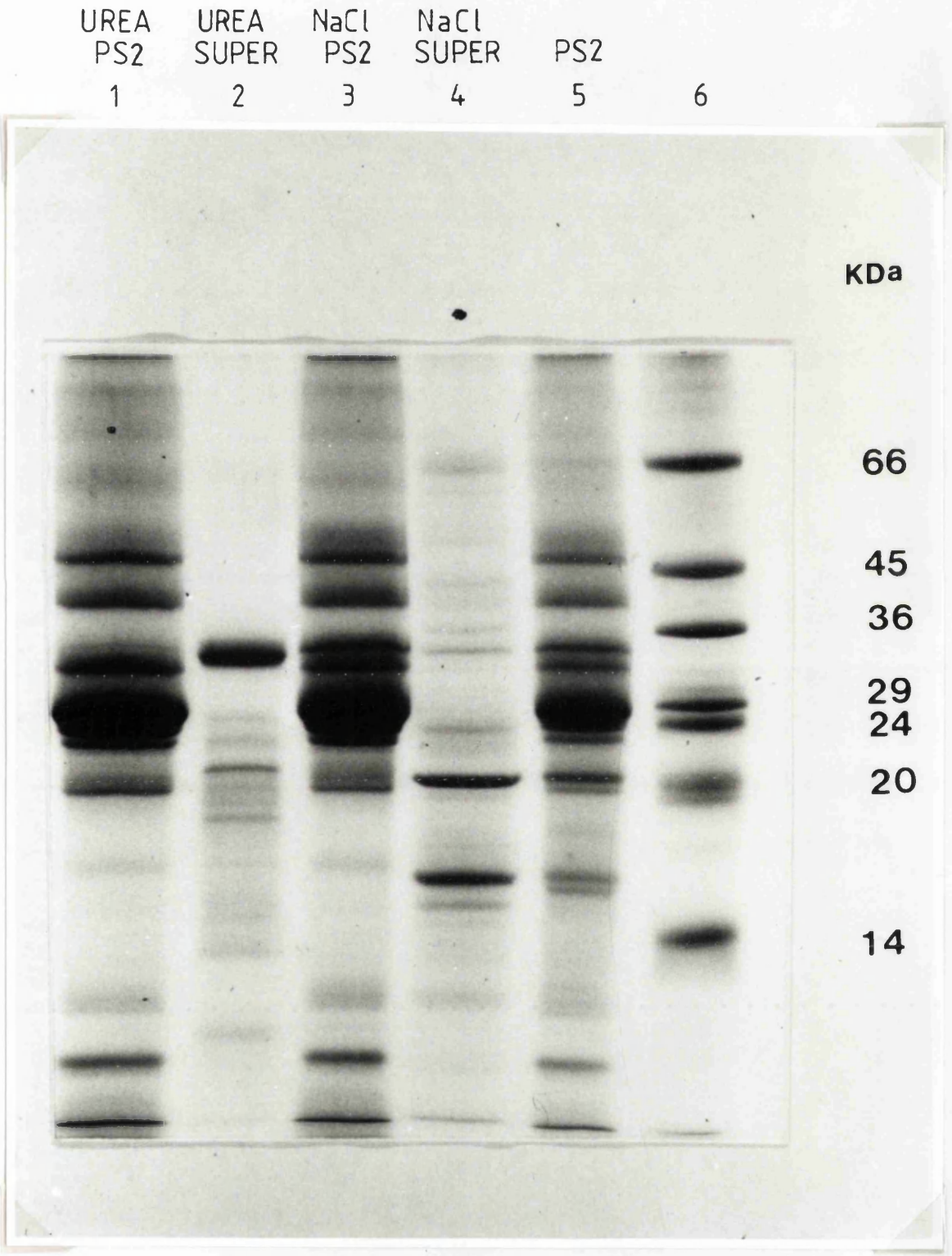
UREA PS2
UREA SUPER
NaCl PS2
NaCl SUPER
PS2
1
2
3
4
5
6
KDa
66
45
36
29
24
20
14

after these treatments (< 30 umoles O_2 /mg Chl /h) in the presence of a high chloride concentration (>400 mM). When high concentrations of chloride were not present no oxygen evolution was detected, and a broad epr signal corresponding to free Mn^{2+} (near g = 2.0) was present. These results indicate that manganese only remains attached to the PS2 complex after removal of the 33 kDa polypeptide in the presence of >400 mM chloride. After reconstitution with the 33 kDa polypeptide (in the presence of 400 mM Cl^-) an increase in oxygen evolution was detected. This suggests that the extrinsic 33 kDa polypeptide plays a role in stabilising the manganese complex, and that its presence is vital for oxygen evolution to occur.

PS2 membranes washed with 1.0 M Tris at pH 8.0 were depleted of all three extrinsic polypeptides with additional depletion of a 10 kDa polypeptide. The manganese cluster was destroyed with complete loss of oxygen evolution. The rate of oxygen evolution was not reconstituted by the addition of the 33 kDa polypeptide.

3.5.2 The Low Molecular Weight Polypeptides of PS2

In non - urea gels the low molecular weight regions are obscured by co - migrating bands of lipids (gel 4).

Several low molecular weight polypeptides between 3 and 11 kDa were detected in different PS2 preparations by gel electrophoresis (gel 3). These low molecular weight

Gel. 3. The Low Molecular Weight Polypeptides of Photosystem II.

The gel shown opposite is a 16 to 22 % polyacrylamide gradient gel containing 6.5 M urea (Laemmli), showing the low molecular weight polypeptides of different PS2 preparations. The polypeptide profiles are: lane 3, thylakoids; lane 4, PS2 membranes; lane 5, OGP PS2; and lane 6, PS2 reaction centres. It was necessary to load large amounts of each preparation in order to show the low molecular weight polypeptides. Many low molecular weight polypeptides are present in lanes 3, 4 and 5. The reaction centre preparation contains three low molecular weight polypeptides of 9, 4.8 and 4.0 kDa. Lane 1 shows the molecular weight standards (66, 45, 36, 29, 24, 14 kDa). Lanes 2 and 7 are the myoglobin low molecular weight standards (Sigma) (16.95, 14.40, 8.16, 6.21, 2.51 kDa). The voltage was as in gel 1 with 30 mA current, and the gel took approximately 17 hours to run to completion.

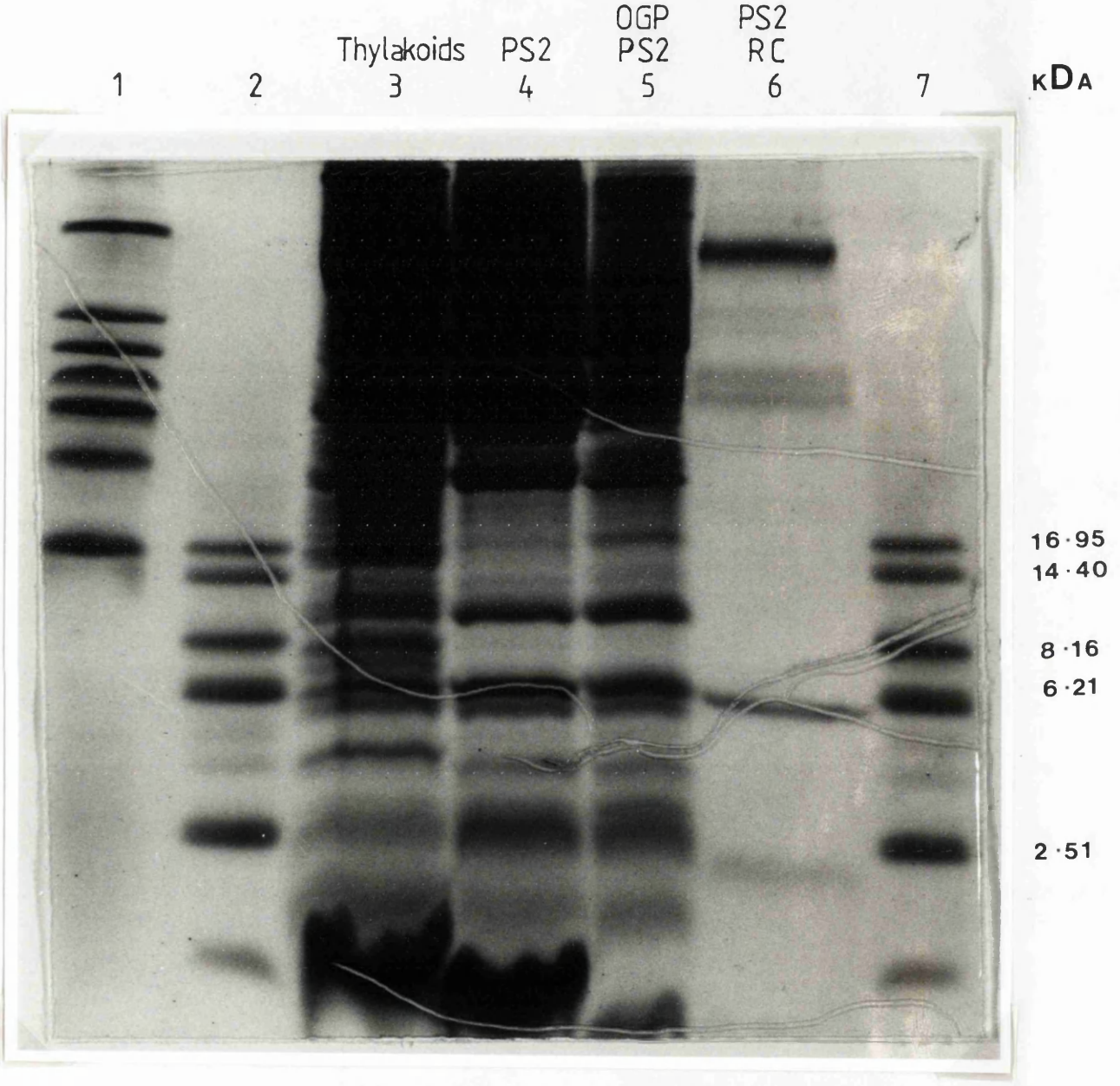
1
2
Thylakoids
3
PS2
4
OGP
PS2
5
PS2
RC
6
7
kDa
16·95
14·40
8·16
6·21
2·51

Gel. 4. A 16 - 22% Acrylamide (Non Urea) Gradient Gel of PS2 preparations and Extrinsic Polypeptides.

Lanes 2 to 6 show the polypeptide profiles of various PS2 preparations. In the absence of urea the low molecular weight region is obscured by the presence of lipids. The D1 / D2 reaction centre preparation and the OGP PS2 preparation contain less lipid. The addition of 6.5 M urea retards the migration of the polypeptides with respect to the lipids allowing them to be visualised (see gel 3). Citrate washed PS2 (lane 4) has the same polypeptide profile as the untreated PS2 membranes (lane 3). The three extrinsic polypeptides remain attached during the low pH citrate wash. Lane 7 is the supernatant of the 1.0 M Tris wash. The 23 kDa polypeptide appears to be absent in this supernatant, and also in the salt wash supernatant (lane 9). The 33 kDa and 17 kDa polypeptides are present in large quantities in lane 7, plus a polypeptide of between 36 to 45 kDa. This may be an aggregate of the 23 kDa polypeptide. It is also present in the salt wash supernatant (lane 9). A number of low molecular weight polypeptides are present in this supernatant. Lane 8 shows the effect of the 2.6 M urea wash on OGP PS2. The 33 kDa polypeptide is removed. There also appear to be a number of lower molecular weight polypeptides removed during this treatment. There are no lipids to obscure the low molecular regions of the wash supernatants. The current and voltage was as in gel 1. The mobility of the polypeptides was slower than for the slab gels, taking approximately 8 hours to run to completion.

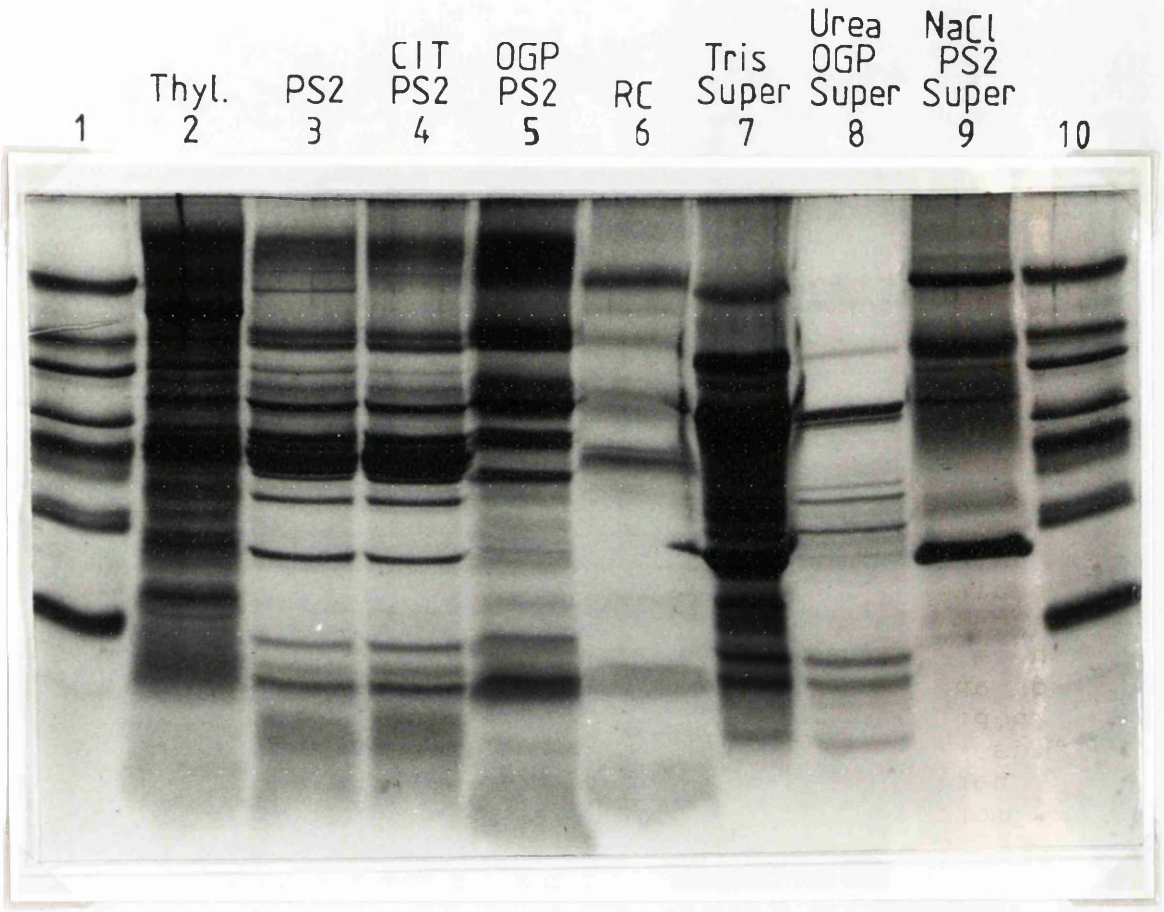
1
Thyl.
2
PS2
3
CIT
PS2
4
OGP
PS2
5
RC
6
Tris
Super
7
Urea
OGP
Super
8
NaCl
PS2
Super
9
10

polypeptides were only resolved successfully in 16 - 22% gradient gels with 6.5 M urea and high concentrations of Tris buffer. The high concentration of urea helped to retard the migration of the polypeptides in relation to the lipids, exposing the low molecular weight polypeptides for visualisation.

3.5.3 Calcium Depletion from PS2 Membranes

3.5.3.1 The Removal of Calcium by High Concentration Salt washing at pH 6.3

After salt washing in the dark a requirement for calcium ions to obtain maximum oxygen evolution was observed. After a 2.0 M NaCl wash, in the absence of calcium a lower rate of oxygen evolution was observed compared to the rate observed after a 1.0 M NaCl wash (Table 2. B & C). This suggests that a greater amount of calcium was removed by the higher concentration of salt. Calcium ions were however only partially depleted by 1.8 to 2.0 M salt washing.

If NaCl washing was performed in room light, with PPBQ added as an artificial electron acceptor, a rate of oxygen evolution was observed that was lower than the rates obtained from the above calcium depletion methods (Table 2. D). This is interpreted as a requirement for the cycling of the S states for more efficient calcium

removal. The S states other than the S_1 state are associated with a lower affinity for calcium. The artificial electron acceptor PPBQ increases the turnover of the S state cycle and allows the low affinity S_3 state to be formed (Boussac A. & Rutherford A.W., 1988a,b,c).

Table 2. Rate of Oxygen evolution by PS2 membranes treated with NaCl

Assay Conditions	Rate (umoles O_2/mgChl/h)	
A. Untreated PS2		
No Additions	560	
B. 1.0 M NaCl washed PS2 (dark)	% Ca^{2+} rate	
(1) No Additions	103	(38.0)
(2) 20 mM $CaCl_2$	270	(100.0)
C. 2.0 M NaCl washed PS2 (dark)		
(1) No Additions	75	(27.0)
(2) 20 mM $CaCl_2$	275	(100.0)
D. 2.0 M NaCl washed PS2 (room light)		
(1) No Additions	30	(11.5)
(2) 20 mM $CaCl_2$	260	(100.0)

(Other details as in materials and methods).

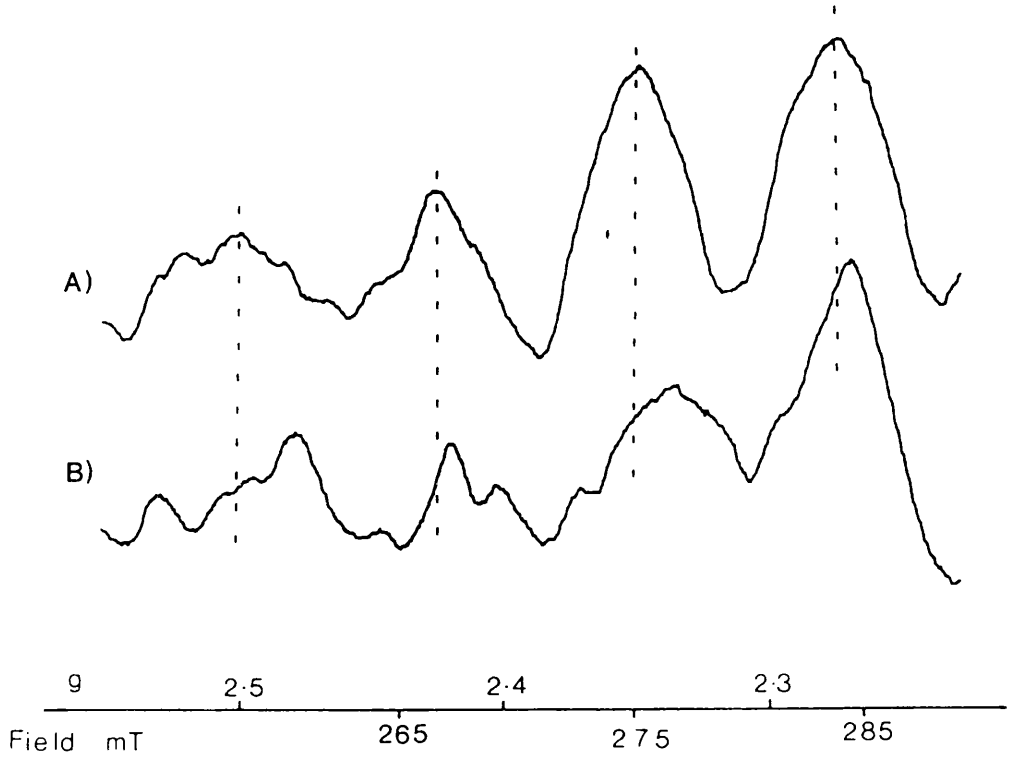

Fig.3·10. The effect of strontium ions on the low field region of the S_2 state multiline epr signal. (A)· pH 6.3 room light salt washed PS2 reconstituted with calcium ions. (B) pH 6.3 room light salt washed PS2 reconstituted with strontium ions, showing changes in the hyperfine splittings, caused by the magnetic nucleus of the strontium ion. Chl concentration: 8mg /ml; epr conditions: power, 10 mW; temperature, 8.5 K; modulation amplitude, 1 mT.

The turnover of the S states (in particular the generation of the S_3 state) is therefore important for efficient depletion of calcium. The rate of calcium reconstitution is also dependent on light, but light is not an absolute requirement (Boussac & Rutherford 1988c). Strontium reconstitution appears to be entirely dependent on light and the presence of PPBQ. Reconstitution with strontium can be detected as a modification of the S_2 state multiline epr signal (Fig. 10. a and b). This modification is only observed after a period of illumination (in the presence of PPBQ) before 4 hour dark adaptation. This modification is thought to be induced due to the larger sized strontium ion bound at the calcium binding site close to the manganese binding site. The strontium ion has a larger nucleus and therefore has a stronger magnetic field associated with it. This magnetic field interacts with the magnetic field of the manganese cluster in a different manner to that of the calcium ion and causes alterations in the hyperfine structure of the S_2 state multiline epr signal.

3.5.3.2 The Citrate Wash at pH 3.0

PS2 membranes washed with citrate at pH 3.0 in the dark showed very low rates of oxygen evolution without addition of calcium. The rate of oxygen evolution on reconstitution of calcium was stimulated to a rate similar to that of untreated PS2 (Table 3). Magnesium

ions were added in each assay to prevent non specific effects. The calcium analogues strontium and vanadyl partially reconstituted the rate of oxygen evolution. The stimulation of oxygen evolution by these two ions was a specific effect of only these divalent cations. Other divalent cations did not stimulate oxygen evolution, and did not prevent stimulation by these ions.

Table 3. Rates of Oxygen Evolution by pH 3.0 Citrate Washed PS2

Assay Conditions	Rate (umoles O_2/mg Chl/h)	
A. Untreated PS2		
No Additions	583	
B. Citrate washed PS2	% Ca^{2+} rate	
(1) No Additions	65	(12.0)
(2) 10mM $CaCl_2$	516	(100.0)
(3) 20mM $SrCl_2$	310	(60.0)
(4) 20mM VO^{2+}	260	(50.5)

Other details of assay in Materials and Methods

Gel electrophoresis of the citrate washed PS2 membranes indicated that some of the 17, 23 and 33 kDa extrinsic polypeptides remained attached to the membranes (gel 6). The supernatant from the citrate wash did contain the 17, 23 and 33 kDa extrinsic polypeptides (gel

Gel. 6. The Effect of the Low pH Citrate wash on the Polypeptide Profile of PS2 Membranes.

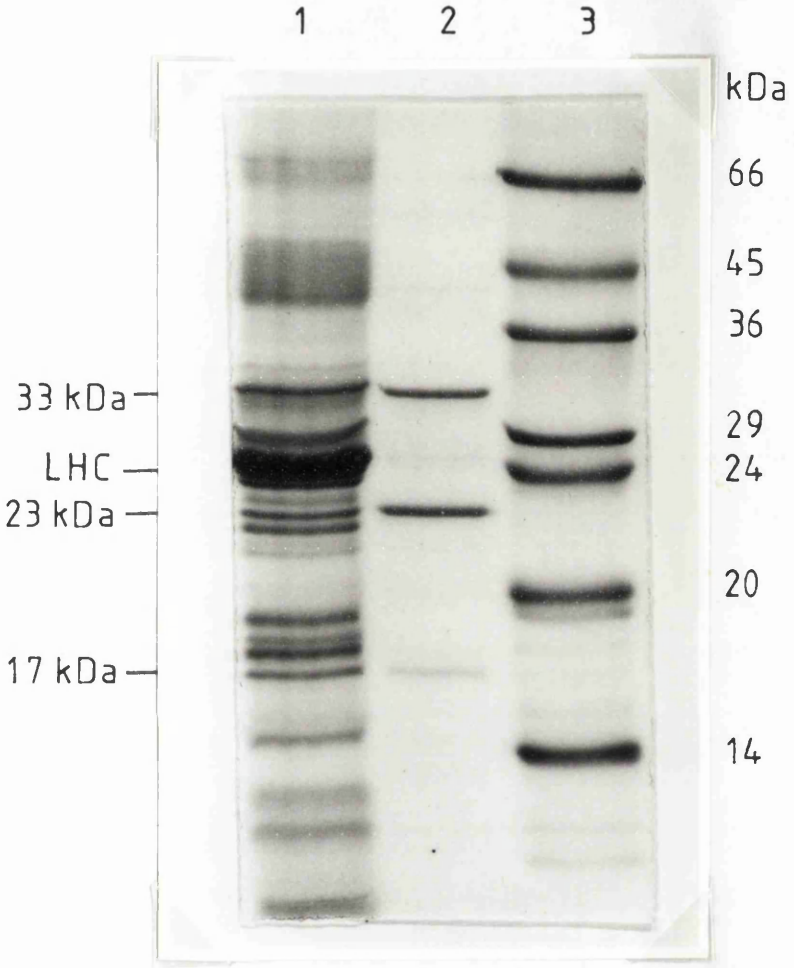

The gel shown is an 18% acrylamide slab gel showing the polypeptide profiles of the supernatant of the citrate wash (lane 2) and of citrate washed PS2 membranes (lane 1). The molecular weight standards are shown in lane 3. Polypeptides of mass 17, 23 and 33 kDa are present in the citrate supernatant, indicating some depletion of these polypeptides. The profile of the citrate washed PS2 membranes reveals that all three polypeptides are present. Only a proportion of the 17, 23 and 33 kDa extrinsic polypeptides are therefore removed during the citrate wash. This may account for the very efficient restoration of oxygen evolution upon the addition of calcium chloride. The gel was according to Chua N.H. and Bennoun P. with the current and voltage as in gel 1.

6. lane 2). This indicated that some depletion of all three extrinsic polypeptides had occured. Calcium addition restores the rate of oxygen evolution to almost 100 % of the untreated rate indicating that little damage to the manganese cluster had occured. The extrinsic polypeptides remaining attached in most centres after the citrate wash may account for this high rate of restoration.

3.5.4 The Extrinsic polypeptides of the LF1 mutant and Wild Type of Scenedesmus obliquus

The extrinsic polypeptides of both the LF1 mutant and the wild type Scenedesmus obliquus removed by 1.8 M NaCl and 2.6 M Urea washes and examined by gel electrophoresis are shown in gels 7 and 8. A polypeptide of approximately 30 kDa molecular mass equivalent to the 33 kDa extrinsic polypeptide of spinach is present in both the mutant and wild type in approximately equal amounts (gel 7. lanes 4 and 5). Both mutant and wild type have a 23 kDa polypeptide equivalent to the 23 kDa extrinsic polypeptide of spinach (gel 7. lanes 4 and 5 & gel 8. lanes 3 and 6). There appear to be several polypeptides in the region corresponding to the 17 kDa extrinsic polypeptide of spinach (gel 8. lanes 3 and 6). A large number of polypeptides (at least 13 polypeptides)

Gel. 7. The Polypeptide Profile of the LF1 mutant and Wild type of the green alga Scenedesmus obliquus

The gel shows the polypeptide profile of the PS2 membranes and the extrinsic polypeptides removed from the PS2 membranes of the LF1 mutant and wild type. Lane 1 shows the molecular weight standards (66, 45, 36, 29, 24, 20 and 14 kDa). Lane 2 is the polypeptide profile of the untreated PS2 membranes and lane 3 is after 1.0 M Tris pH 8.0 washing. Lanes 4 and 5 are the supernatants from the Tris wash of the same amount of chlorophyll from the LF1 mutant and wild type PS2 membranes respectively. Lane 6 is the Tris wash supernatant from spinach for comparison. Both the LF1 mutant and the wild type are depleted of a 30 kDa polypeptide after the Tris wash, equivalent to the extrinsic 33 kDa polypeptide of spinach. They were depleted of a polypeptide of 23 kDa molecular mass and some smaller polypeptides. The LF1 mutation does not appear to affect the amount of "33 kDa" extrinsic polypeptide per mg /Chl, and the occurence of the other extrinsic polypeptides is similar. This is investigated further in gel 8. The gel is an 18% acrylamide slab gel (Chua & Bennoun) (current and voltage as in gel 1).

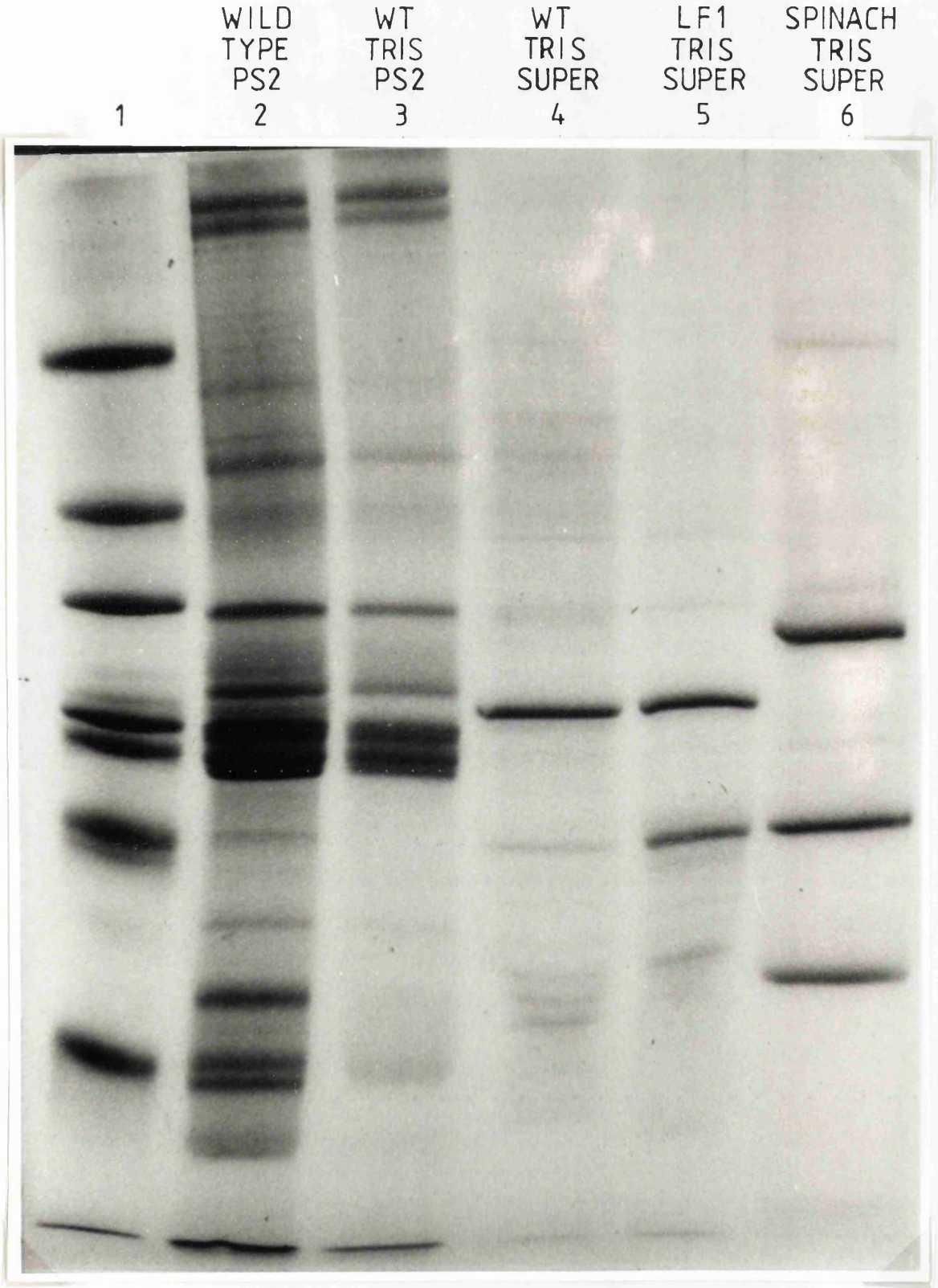
1
WILD TYPE PS2
2
WT TRIS PS2
3
WT TRIS SUPER
4
LF1 TRIS SUPER
5
SPINACH TRIS SUPER
6

Gel. 8. Polypeptides Removed by 1.8 M NaCl and 2.6 M Urea from the LF1 mutant and wild type of Scenedesmus obliquus.

Lane 1 shows the polypeptide profile of untreated wild type PS2. All extrinsic polypeptides are attached at this point. Lanes 2 to 5 show the removal of extrinsic polypeptides from the wild type, firstly by a salt wash (lanes 2 & 3) and secondly the removal of the "33 kDa" polypeptide by a 2.6 M urea wash (lanes 4 & 5). Lanes 6 and 7 are the supernatants from equivalent washes, but from the LF1 mutant and lane 8 is the polypeptide profile of urea treated LF1 PS2. A large number of polypeptides were removed by the salt wash from both the WT and LF1 mutant. There are three polypeptides in both cases between 14 and 20 kDa, which may be equivalent to the 17 kDa polypeptide. A 23 kDa polypeptide is present in the WT salt wash supernatant, but only faint in the LF1 mutant. The "33 kDa" polypeptide is present in both LF1 and WT urea wash supernatants. From the previous gel we know that the "33 kDa" polypeptide is present in similar amounts in the WT and LF1 mutant. Therefore the only diiference in polypeptides apart from the difference in the size of the unprocessed D1 polypeptide (Metz J.G. & Bishop N.I., 1980) appears to be the lower quantity of the 23 kDa polypeptide of the LF1 mutant. Lane 10 shows the molecular weight standards (66, 45, 36, 29, 24 and 14 kDa). Lane 9 shows the effect of pH 8.3 treatment of spinach PS2 membranes. The pH was not returned to pH 6.3 and the treatment was done in room light. All three extrinsic polypeptides (17, 23, and 33 kDa) are lost during this treatment. This was different from the pH 8.3 NaCl wash. During the pH 8.3 NaCl wash the 33 kDa extrinsic polypeptide remained attached. (current and voltage as in gel 1).

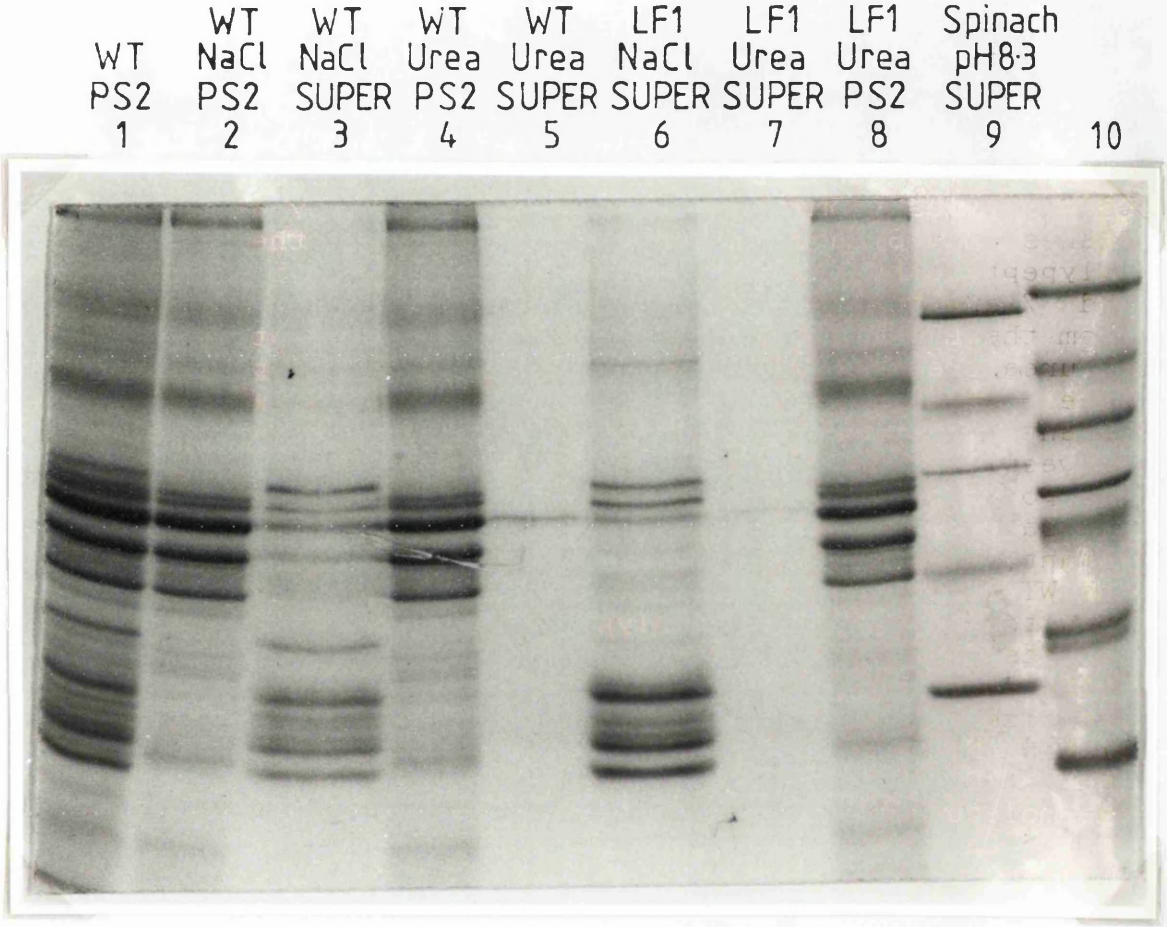
WT PS2 1
WT NaCl PS2 2
WT NaCl SUPER 3
WT Urea PS2 4
WT Urea SUPER 5
LF1 NaCl SUPER 6
LF1 Urea SUPER 7
LF1 Urea PS2 8
Spinach pH8·3 SUPER 9
10

with molecular mass between 14 and 36 kDa were removed from both the mutant and wild type during treatment with 1.8 M NaCl (gel 8. lanes 3 and 6). After these polypeptides had been removed, the "33 kDa" polypeptide could be obtained in a relatively uncontaminated fraction by 2.6 M urea treatment (gel 8. lanes 5 and 7). There was no detectable difference between the size or quantities of the extrinsic polypeptides from the mutant or wild type Scenedesmus obliquus. The LF1 mutation (a mutation of the gene coding for a processing enzyme of the D1 polypeptide) does not affect the occurence of the extrinsic polypeptides.

3.5.5 Calcium binding polypeptides of PS2 identified by their mobility in polyacrylamide gel electrophoresis with and without calcium

In the presence of either calcium ions or EGTA several polypeptides of photosystem 2 were observed to have different mobilities on polyacrylamide gels (see methods section 1.X). OGP PS2 and NaCl PS2 with calcium or with EGTA added were compared (gel 9.). Four polypeptide regions are of significance. The 47 and 43 kDa (in both NaCl PS2 and OGP PS2) migrated in two distinct bands in the gel containing 1 mM EGTA, but as one band in the presence of calcium. The D1 and D2 polypeptides both in NaCl PS2 and OGP PS2 also appear to behave differently in the two gel types. In the presence

of 1 mM calcium the D1 and D2 polypeptides are clearly visible as two distinct bands, located just above the 33 kDa extrinsic polypeptide. These polypeptides are not visible in the gel containing 1 mM EGTA. The most striking difference is the position of the LHC binding polypeptide of approximately 24 kDa found in the NaCl PS2 only. This polypeptide migrates well below the 24 kDa marker polypeptide in the presence of 1 mM calcium, exposing several polypeptides usually obscured in this region. All of the above mentioned polypeptides are considered to have regions rich in acidic amino acids which could be involved in physiological calcium binding. The presence or absence of bound calcium in these regions would be expected to affect the mobility of the polypeptide, either by some small conformational change or by electrostatic effects. Of particular interest is the fact that the position of the 33 kDa polypeptide is not altered. This polypeptide has been suggested to have an EF hand type calcium binding site, and to bind $^{45}Ca^{2+}$ when isolated on nitrocellulose (as described in the introduction). The calcium binding conformation of the 33 kDa polypeptide may be disrupted by the SDS contained in the gel. This would prevent any alteration of mobility in these gel systems associated with calcium binding polypeptides.

Gel. 9. Polyacrylamide Gel Showing the Effect of Calcium and EGTA on the Mobility of the PS2 polypeptides.

The presence of calcium or EGTA effects the mobility of calcium binding polypeptides (Gitelman S.E. & Witman G.B., 1980). The polypeptides shown are from OGP PS2 and NaCl washed PS2, both prepared under stringent calcium depletion conditions. The mobility of the 47 and 43 kDa, D1 and D2, and the 24 kDa LHC polypeptides all appeared to be altered by the presence of calcium or EGTA. This may be due to the presence of regions rich in acidic amino acids that are able to bind calcium ions. These may not neccesarily correspond to physiological binding sites. The effect on mobility is probably due to an alteration of the overall charge of the polypeptide or a conformational change. The mobility of the 33 kDa extrinsic polypeptide, suggested to have an EF hand calcium binding structure, did not appear to be altered. The EF hand calcium binding structure requires a very specific structure for tight calcium binding to occur. This structure is probably denatured in the presence of SDS, and calcium binding does not occur. (current and voltage as in gel 1).

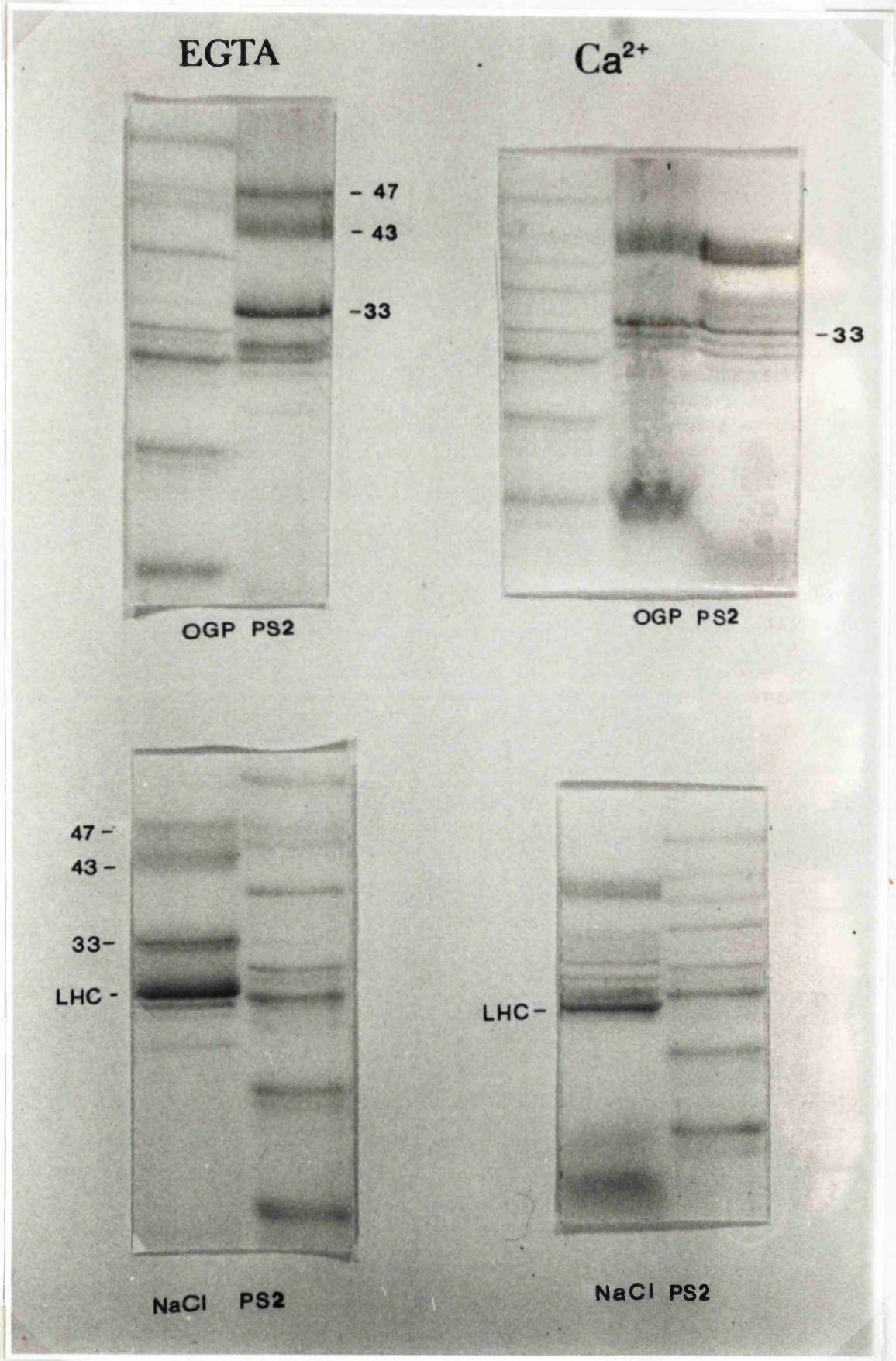
EGTA
Ca2+
- 47
- 43
-33
OGP PS2
-33
OGP PS2
47 -
43 -
33-
LHC -
NaCl PS2
LHC -
NaCl PS2

3.5.6 The Effect of Calcium Depletion on the S state cycle.

When calcium was depleted from PS2 membranes by the established methods using (1) a salt wash (in the light or dark) at pH 6.3 (Ghanotakis et al, 1984) & (Boussac . & Rutherford . . 1988) or (2) a citrate wash at pH 3.0 (Ono . & Inoue ., 1988) or (3) treatment with OGP (Ghanotakis . et al, 1987) the S_2 multiline epr signal was still formed in a sample at pH 6.3 on 200K illumination (Fig. 11. b) and (Fig.12. a and c). The signal amplitude increased slightly with calcium reconstitution (Fig. 11. c) and (Fig. 12. b and d). Oxygen evolving core complexes prepared with OGP exhibited a multiline signal which increased in amplitude with additional calcium (fig. 12. c and d). This preparation had a g = 1.8 iron semiquinone epr signal replacing the g = 1.9 epr signal seen in other PS2 preparations.

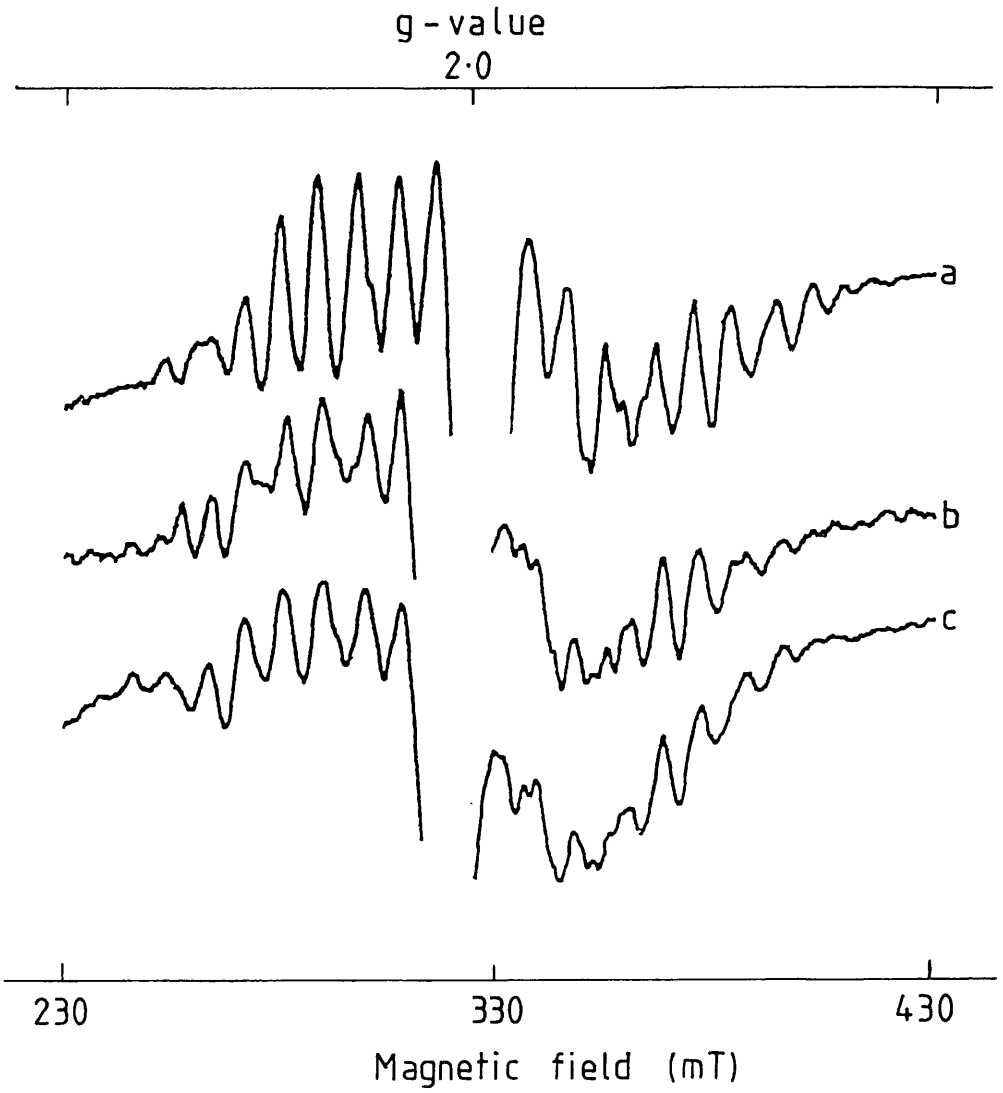

Fig. 3·11. Comparison of the conventional methods of calcium removal on the amplitude of the S_2 state multiline epr signal. S_2 induced by 200K illumination. (a) Untreated PS2 membranes (b) pH 6.3 NaCl washed PS2 membranes, (c) as in b with 20mM $CaCl_2$ added before freezing. Epr conditions as in fig. 4. Chl concentration: 4 mg/ml

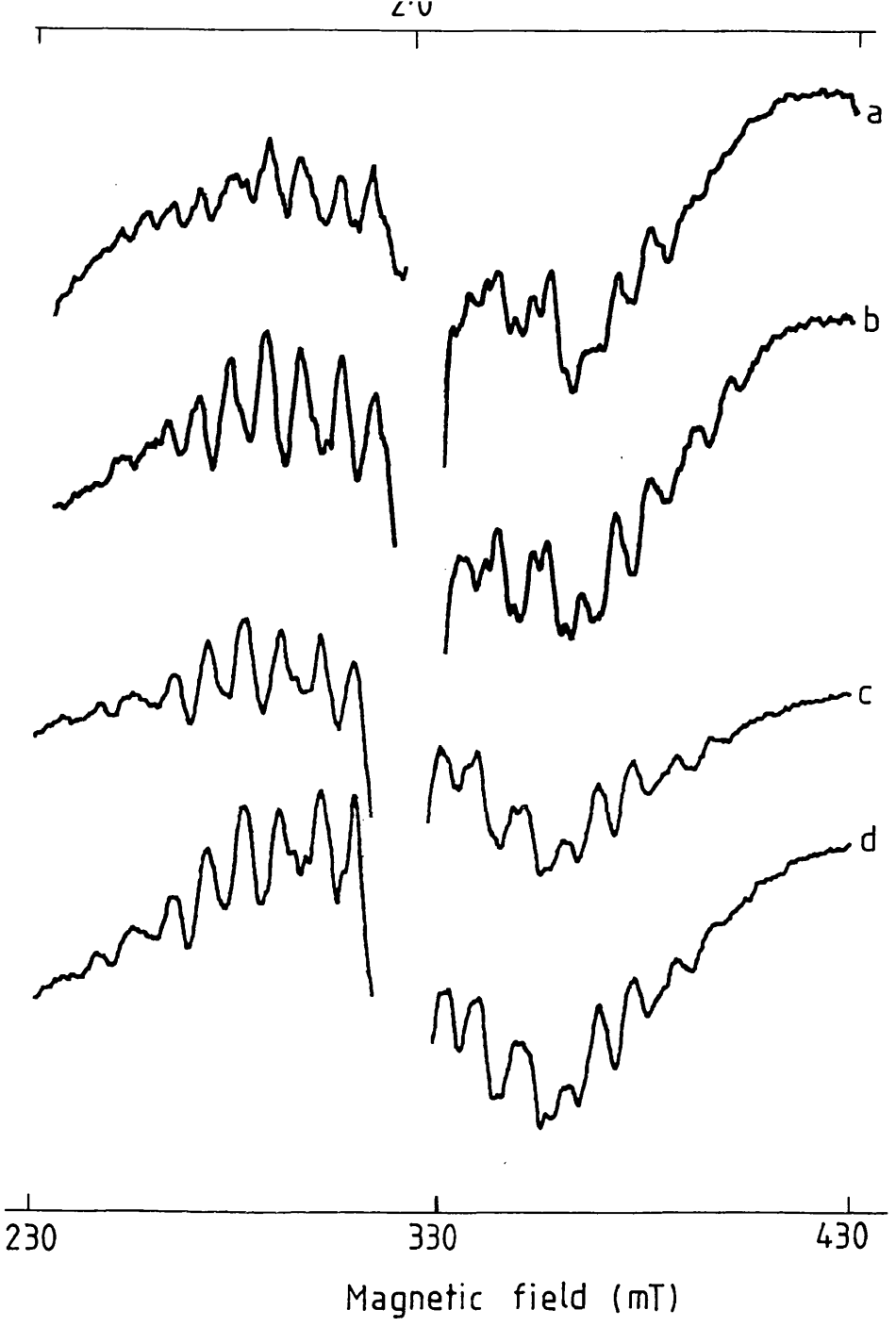

Fig. 3-12. Comparison of the S_2 state multiline epr signal from citrate washed and OGP PS2. (a) pH 3.0 citrate washed PS2 membranes, (b) as a with 20mM $CaCl_2$ added before freezing, (c) OGP treated PS2 membranes, (d) as (c) with 20mM $CaCl_2$ added. Epr conditions as in Fig. 4. Chl concentration 4 mg/ml.

3.5.7 The Role of D as an Electron Acceptor

3.5.7.1 The Characteristics of D^+ Reduction During 4 hour Dark Adaptation

In room light the S states of the oxygen evolving complex have a random distribution. At any one moment there is a 25 % population of each state. The 25 % population of the S_0 state is oxidised slowly to the dark stable S_1 state. The electrons from this process reduce the tyrosine D^+ during 4 hours in the dark. The S_0 state is more long lived than the higher S states, with oxidation complete after 4 hours in the dark.

Epr samples of untreated PS2 membranes placed in the dark, after S state randomisation of the oxygen evolving complex by illumination, showed a typical time course of reduction in the amplitude of the D^+ epr signal (Fig. 13.). The induction of the S_2 state multiline epr signal by 200 K illumination indicated the proportion of the S_1 state present.

During the first five minutes of 4 hours dark adaptation there was initially a slight increase in the D^+ epr signal, corresponding to the decay of the higher S states. This was followed by a slow reduction of D^+ with a 25% loss of signal amplitude over a period of 4 hours in the dark (fig. 14. a,b). The increase in the S_2 state multiline epr signal amplitude induced by 200 K illumination between 5 minutes in the dark and 4 hours in

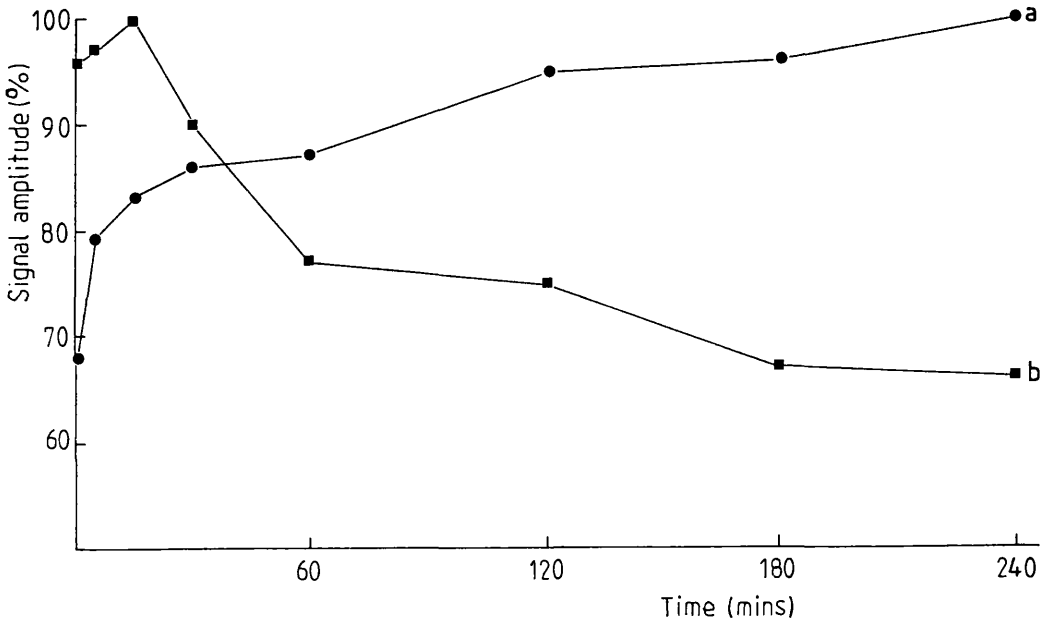

Fig. 3·13. Time course of the amplitude of the S_2 state multiline epr signal and the D^+ epr signal during dark adaptation of untreated PS2 membranes. (a) The S_2 state multiline epr signal produced by 200K illumination. (b) The D^+ epr signal. Chl concentration, 5mg/ml. Epr conditions: Multiline - power, 10 mW; temperature 8.5 K, modulation width, 1 mT. D^+ - power, 1 uW; temperature 15.0 K, modulation width, 0.2 mT.

Fig. 3·14 Changes in the epr amplitude of the S_2 state multiline signal and the D^+ signal during dark adaptation of untreated PS2 membranes. (a) D^+ amplitude in sample a before 200K illumination. (b) D^+ amplitude after 4 h dark before 200K illumination. (c) S_2 multiline signal. Sample immediately frozen in the dark then illuminated at 200K. (d) as (c) but following 4 h dark adaptation before illumination at 200K. Epr conditions as fig. 13 , the peaks used for measurement are indicated.

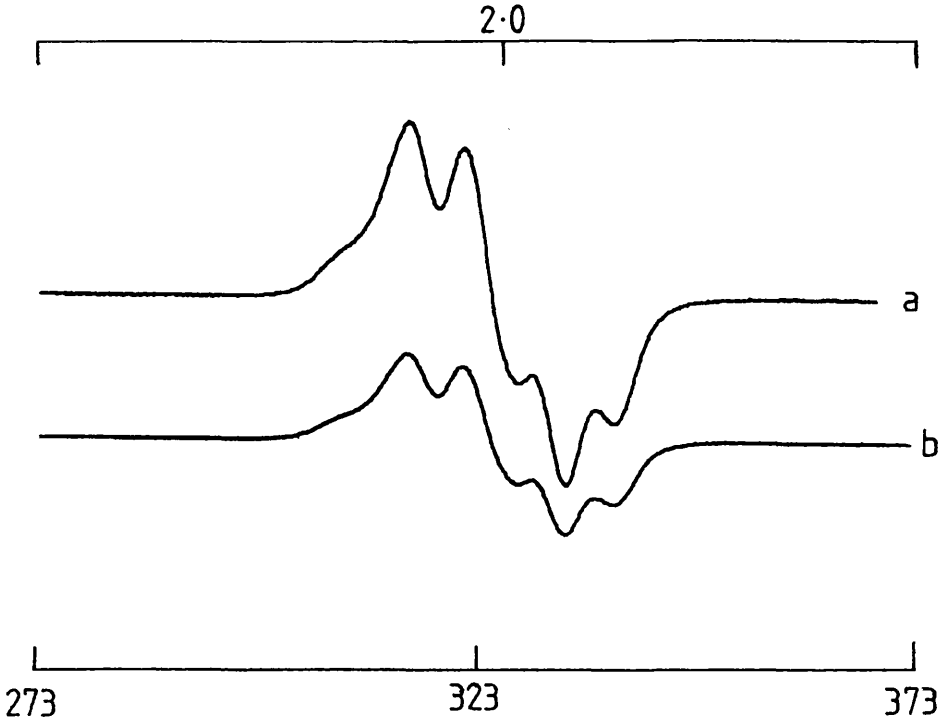
2·0
a
b
273
323
373
Magnetic field (mT)

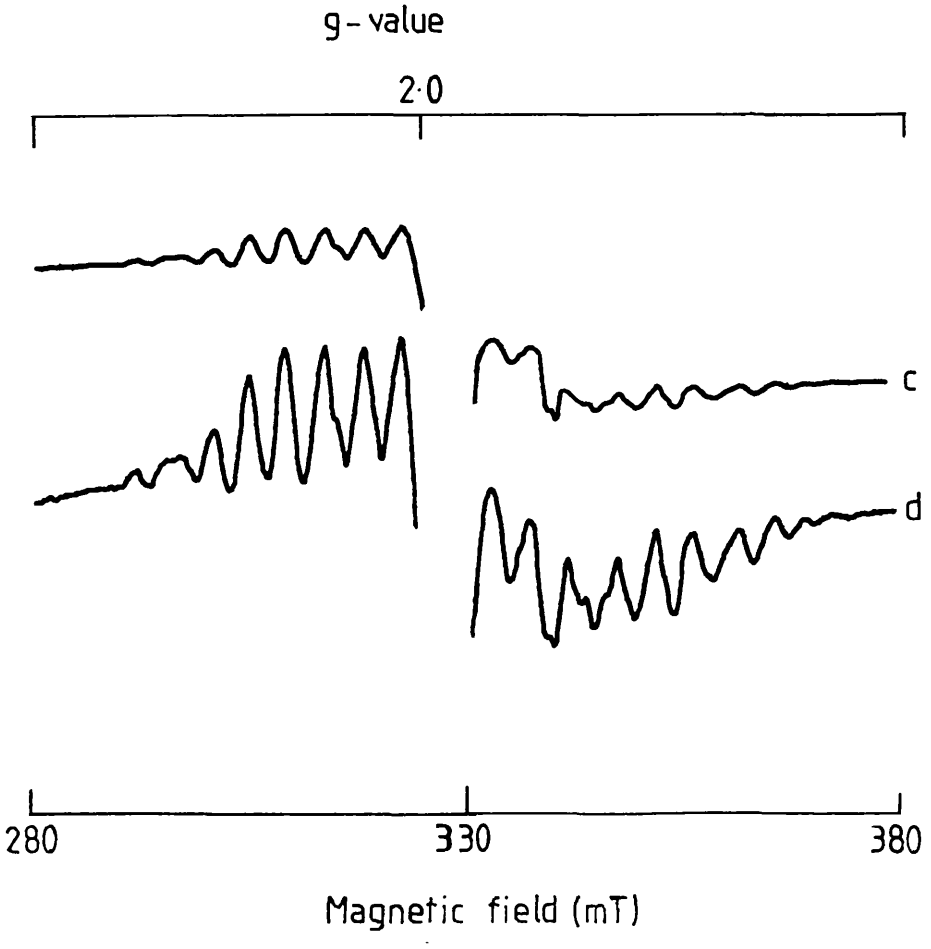
g-value
2·0
c
d
280
330
380
Magnetic field (mT)

the dark was approximately 25% of the total inducable signal. This indicated a 25% increase in the population of the S_1 state during this dark period. The S_2 state multiline signal induced on 200 K illumination however increased by more than 50% between time zero dark adaptation and 4 hours dark, with a large initial increase in the first five minutes (Fig. 14. c,d). Beck W.F. et al, 1985 have reported the existence of active and resting states of the oxygen evolving complex. The S_2 state multiline epr signal exhibits different properties in long term (4 h at 0° C) and short term (6 min at 0°C) dark adapted PS2 samples. During the initial 5 minutes of dark adaptation structural changes may occur in the oxygen evolving complex. This may explain the unusually low amount of the multiline epr signal observed during the first 5 minutes of dark adaptation.

3.5.7.2 <u>The Role of D as an Electron Donor - The Reduction of the S_2 State by D (signal II slow) at 277K</u>

Figure 15 shows the time course of the loss of the multiline epr signal and oxidation of the tyrosine D upon thawing and dark storage at 0 °C. The size of the S_2 state multiline epr signal, generated after 4 hours dark adaptation by 200 K illumination decreased rapidly when a sample was thawed and stored on ice for 3 minutes in the dark (fig. 16. c,d) and (fig 15. b). This loss of the

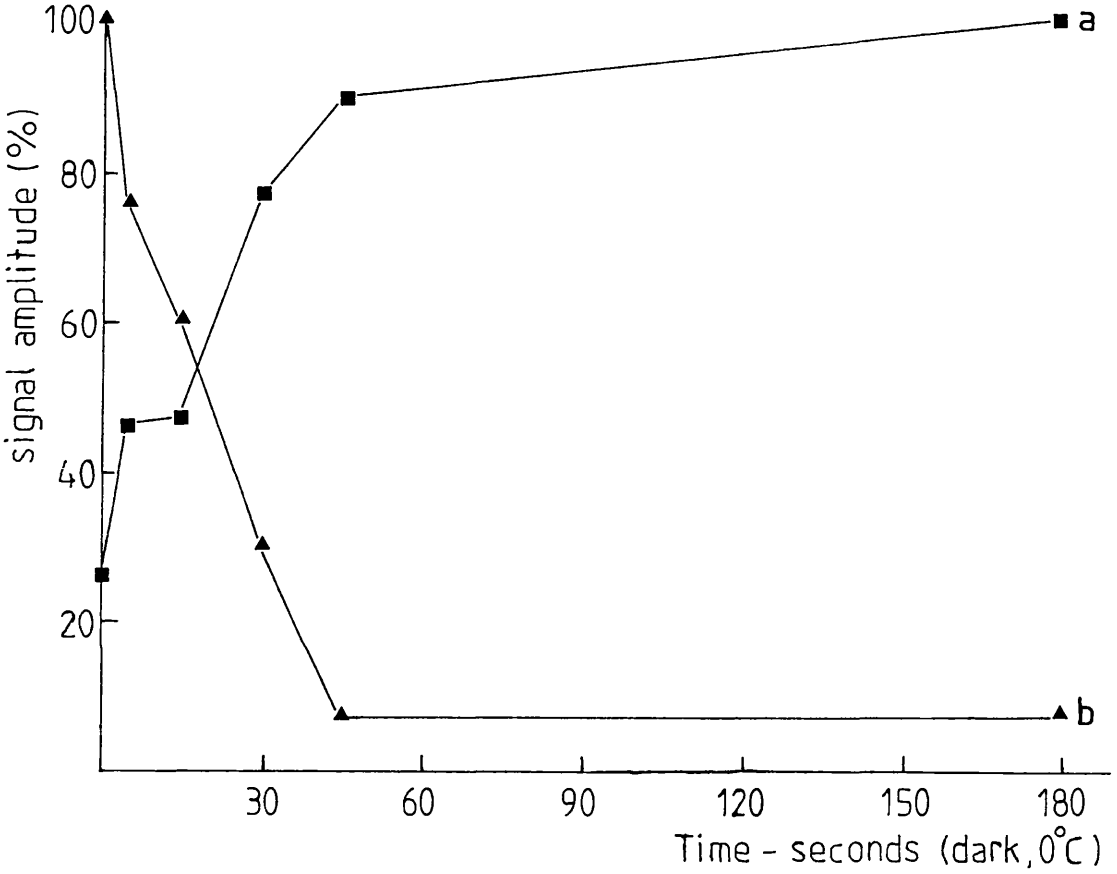

Fig.3·15. Time course of the oxidation of D^+ and reduction of the S_2 state on thawing in the dark. (a) D^+ amplitude, (b) S_2 state multiline epr signal amplitude. Chl concentration and epr conditions as in fig. 13.

Fig . 3·16. Reduction of the S_2 state by D (acting as an electron donor). (a) Amplitude of the D^+ signal II epr spectrum after D^+ depletion and 200 K illumination followed by 7 days dark at 77 K. (b) As in a, but after thawing in the dark and storage on ice in the dark for 3 minutes. (c) as a, but showing the S_2 state multiline epr signal. (d) as c, after thawing in the dark and storage on ice in the dark for 3 minutes. Chl concentration; 6 mg /ml, Epr conditions as in fig. 13.

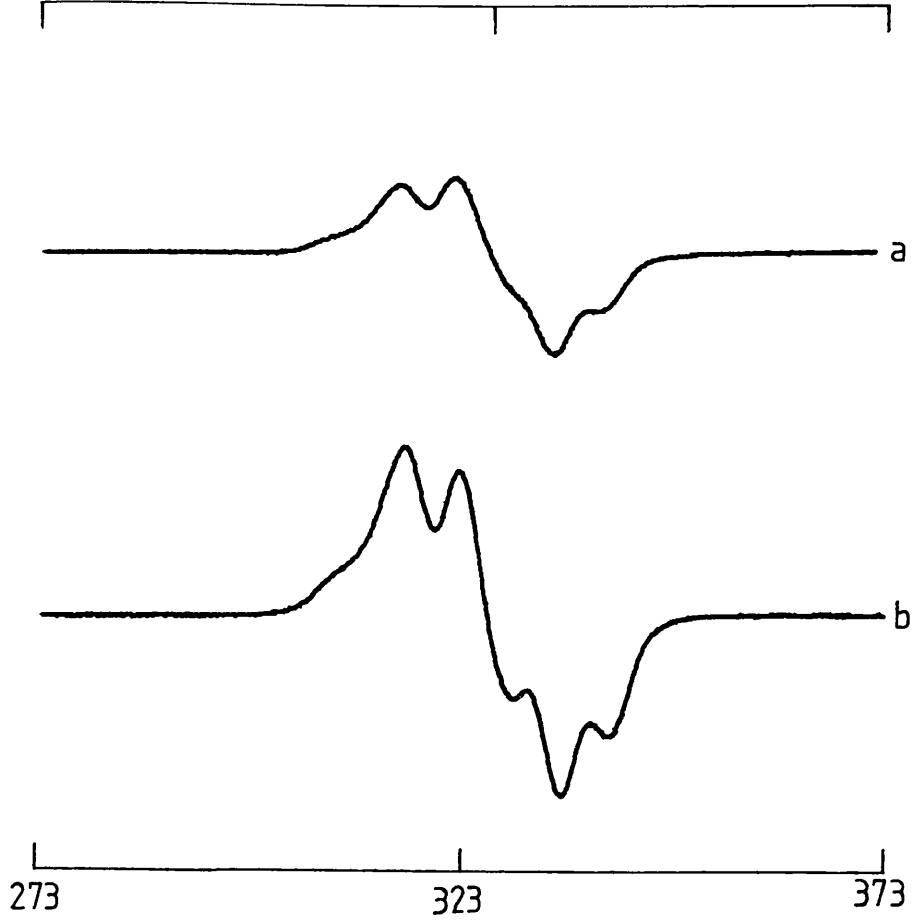
a
b
273
323
373
Magnetic field (mT)

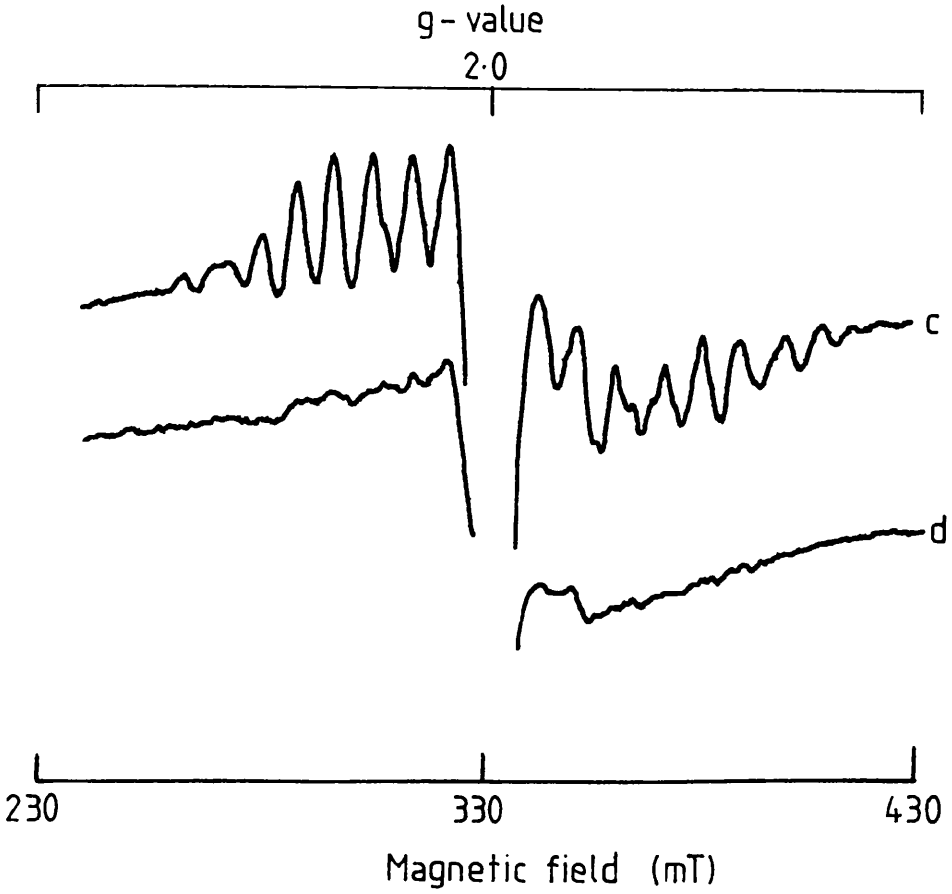
g - value
2·0
c
d
230
330
430
Magnetic field (mT)

multiline epr signal was accompanied by a large increase in the amplitude of the D^+ epr signal (fig. 15. b) and (fig. 16. a,b), providing the sample had been kept in the dark at 77K to allow the decay of the Q_A iron semiquinone epr signal. The increase in the size of D^+ was particularly marked after treatments which brought about the depletion of D^+ (Fig. 17. a,b).

The depletion (as described in the materials and methods) occured as follows. Recombination of electrons from Q_A^- to D^+ after 77 K illumination ocurred over a period of 7 days in the dark at 77 K. This was accompanied by the loss of the Q_A epr signal and a reduction in size of the D^+ epr signal (epr signal II slow). In this state the tyrosine radical D acted as the electron donor on 77 K illumination, giving rise to an increase in both the D^+ epr signal and the Q_A^- iron semiquinone epr signal.

After thawing a 7 day 77 K dark sample in the dark the S_2 state was induced by illumination at 200 K, the sample was again stored in the dark for 7 days at 77K. The iron semiquinone epr signal decayed. The electrons from the reduced iron semiquinone recombined with the oxidised D^+ tyrosine radical. This resulted in further reduction in the amplitude of D^+ (i.e. the D^+ epr signal was returned to the depleted level). After thawing of these samples in the dark and incubation on ice in the dark for 3 minutes, a 75% increase in the amplitude of

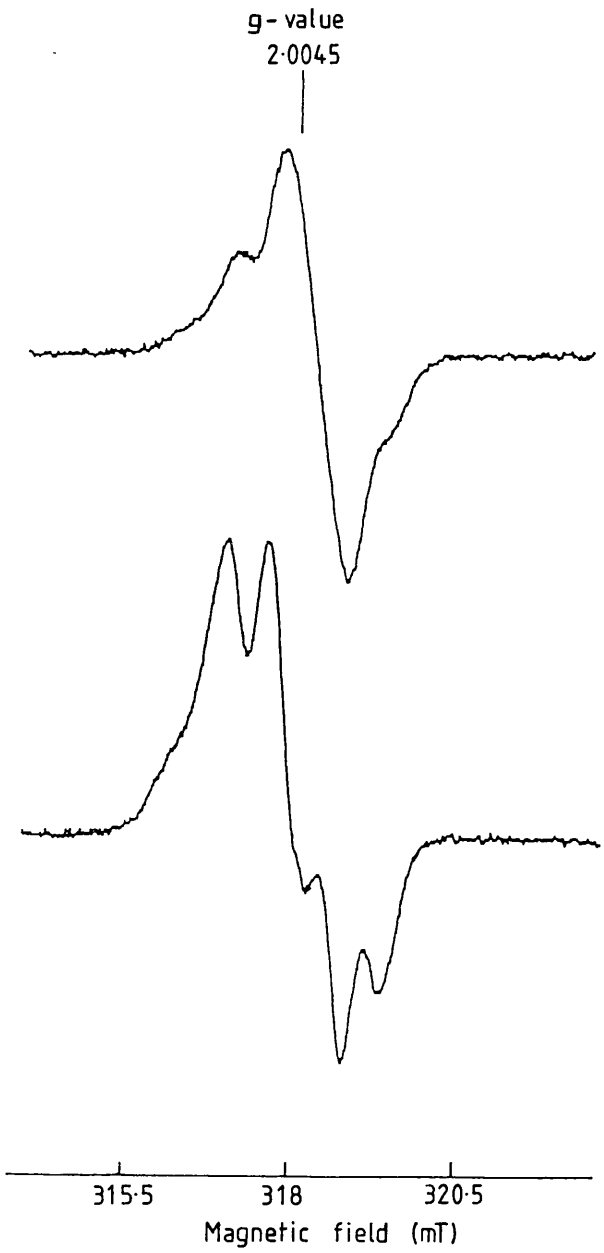

Fig. 3·17. The effect of a more efficient depletion of D^+. Difference in amplitude of the D^+ epr signal and the S_2 state multiline epr signal before and after thawing. The depletion of D^+ was as follows. (a) Untreated PS2 dark adapted for 4 h, illuminated for 5 minutes at 77K, then kept in the dark for 7 days at 77 K. The PS2 was then thawed in the dark, followed by 200 K illumination and further 7 days dark at 77 K. (b) as a, but thawed in the dark and stored on ice for 5 minutes in the dark. Chl concentration, 5 mg /ml; Epr conditions, power 1 uW; temperature, 15 K, modulation width, 0.1 mT. Chl concentration: 5 mg/ml.

the D^+ epr signal was observed (fig 15 a). The size of the S_2 state multiline epr signal dropped from 100% to zero during the thawing and 3 minute dark incubation on ice (fig 15 b). In this case D is acting as an electron donor and is oxidised in the dark by the S_2 state of the manganese cluster. This data supports the theory that D has a role of deactivating the higher S states to the stable S_1 state in the dark and thereby protecting the manganese cluster. This will be discussed further, in relation to the effect of calcium depletion on the role of D^+, during a later section. One unexplained anomaly associated with this effect is that the 100% decrease in the size of the S_2 state multiline epr signal is matched by only an approximate 75% increase in the amplitude of the D^+ epr signal. This may be explained by the presence of another electron donor.

After 4 hours dark adaptation an epr spectrum corresponding to low potential cytochrome b_{559} was observed (Fig. 18. a). Illumination at 77 K of a sample of PS2 poised in the S_1 state by 4 hour dark adaptation oxidises the high potential cytochrome b_{559}. At this temperature only the high potential cytochrome b_{559} acts as an electron donor, the S states cannot donate electrons. After illumination at 77 K the high potential form of cytochrome b_{559} was photooxidised giving rise to a g = 3.08 epr spectrum (observed as a difference spectrum) (Fig. 18. b). At 200 K the photooxidation of

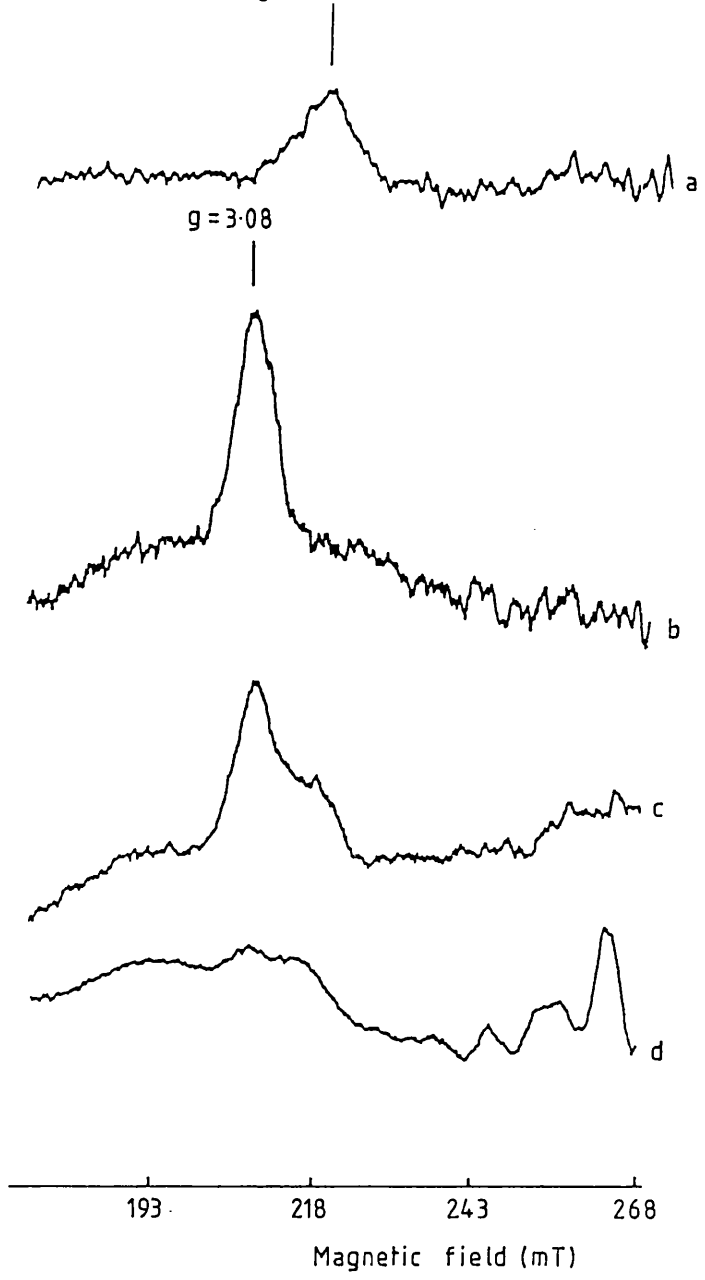

Fig. 3·18. Epr spectra at 14 K of the low - spin haem region of PS2 samples: (a) 4 h dark adapted sample showing low potential cytochrome b_{559}; (b) 5 minute illumination at 77 K minus 4 h dark adapted spectrum, showing high potential cytochrome b_{559}; (c) sample kept at 77 K in the dark for 8 days following 77 K illumination; (d) 4 h dark adapted sample illuminated at 200 K for 3 minutes. Chl concentration; a and b: 6 mg /ml; c and d: 5 mg /ml. Epr conditions: power, 4 mW; temperature, 14 K; modulation amplitude, 1mT.

the OEC to give the S_2 state replaces the photooxidation of the cytochrome. If after 77 K illumination the sample is left in the dark for 7 days at 77 K the electron from the reduced iron semi quinone reduces D^+. There was only slight loss of the g = 3.08 spectrum after 7 days in the dark at 77 K (Fig. 18. c). A further second illumination at 77 K oxidises the donor D.

In Summary:

4 hours dark, 4 °C	S_1 state	P680	Q
	D^+	cyt b_{559}	
200 K illumination	S_2 state	P680 --->	Q^-
	D	cyt b_{559}	
OR			
77 K illumination A	S_1 state	P680 --->	Q^-
	D^+	cyt b_{559}^+	
7 days dark 77 K	S_1 state	P680	Q
	D	cyt b_{559}^+	
77 K illumination B	S_1 state	P680 --->	Q^-
	D^+	cyt b_{559}^+	
7 days dark 77 K	S_2 state	P680	Q
	D	cyt b_{559}^+	

3.5.7.3 The Effect of the Redox State of the Manganese Cluster on the Power Saturation of the D^+ Epr signal

The power saturation characteristics of the D^+ epr signal reflects the relaxation properties of the signal. The manganese cluster is part of the surrounding spin lattice and hence its conformation determines how quickly and efficiently the signal can relax. Although the donor D is suggested to be 28 - 30 A^o away from the manganese cluster, located on the D2 polypeptide (Babcock , 1989) it is close enough for the relaxation properties of D to be affected by the manganese cluster.

The microwave power saturation of signal II slow arising from D^+ was measured in epr samples of PS2 membranes with different S states and different manganese coupling. The amplitude of signal II at increasing powers was measured from the outer peaks of the signal as this part of the spectrum was least likely to be affected by the presence of a narrow chlorophyll radical spectrum (see inset of fig. 19). The power saturation of Signal II slow (D^+) was measured at 120 K and is presented as a plot of log (amplitude / $power^{0.5}$) against log power. At non saturating powers, a straight line parallel with the X - axis is obtained. At high saturating powers a sloped straight line is formed. The intersection between these two straight lines corresponds to the power at half saturation ($P_{1/2}$) read from the inverse log of the X - axis value.

Fig.3-19. Measurement of microwave power saturation of the D^{+} signal II epr spectrum in the S_2 state and after pH 8.3 salt washing in the dark. (a) Power saturation of signal II from 4 h dark adapted pH 8.3 dark salt washed PS2 (no additions), power saturated at 126 uW and (b) Power saturation of signal II from untreated PS2, 4 h dark adapted and illuminated at 200K, power saturated at 141 uW. Inset - The D^{+} signal II epr spectrum measured at 1 uW and 10 mW. The peaks used for signal measurement are indicated ▼. Chl concentration, 4 mg /ml; Epr conditions, modulation amplitude 0.2 mT and temperature 120 K.

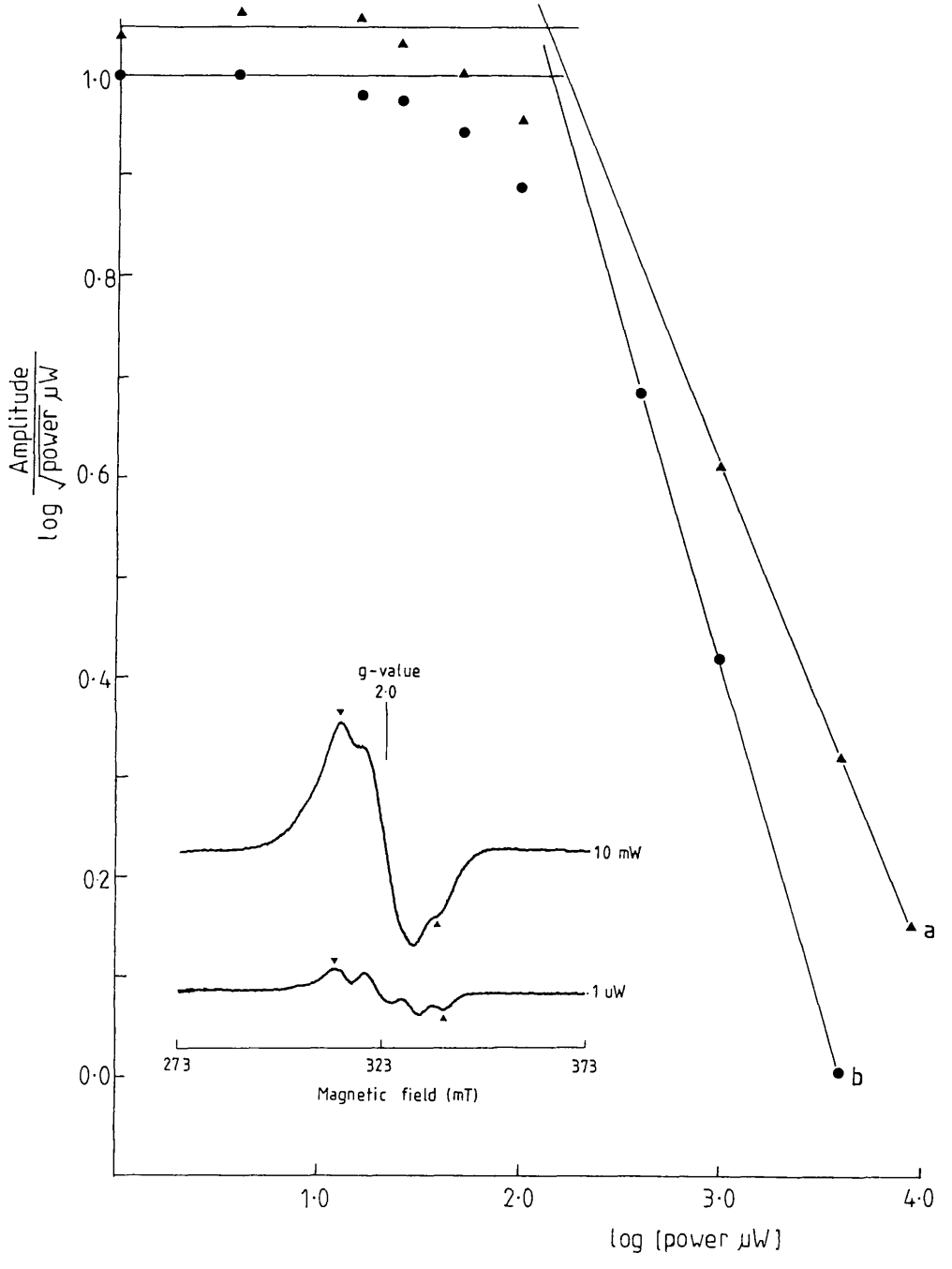
1·0
0·8
0·6
0·4
0·2
0·0
Amplitude / log √power µW
g-value
2·0
10 mW
1 uW
273
323
373
Magnetic field (mT)
a
b
1·0
2·0
3·0
4·0
log [power µW]

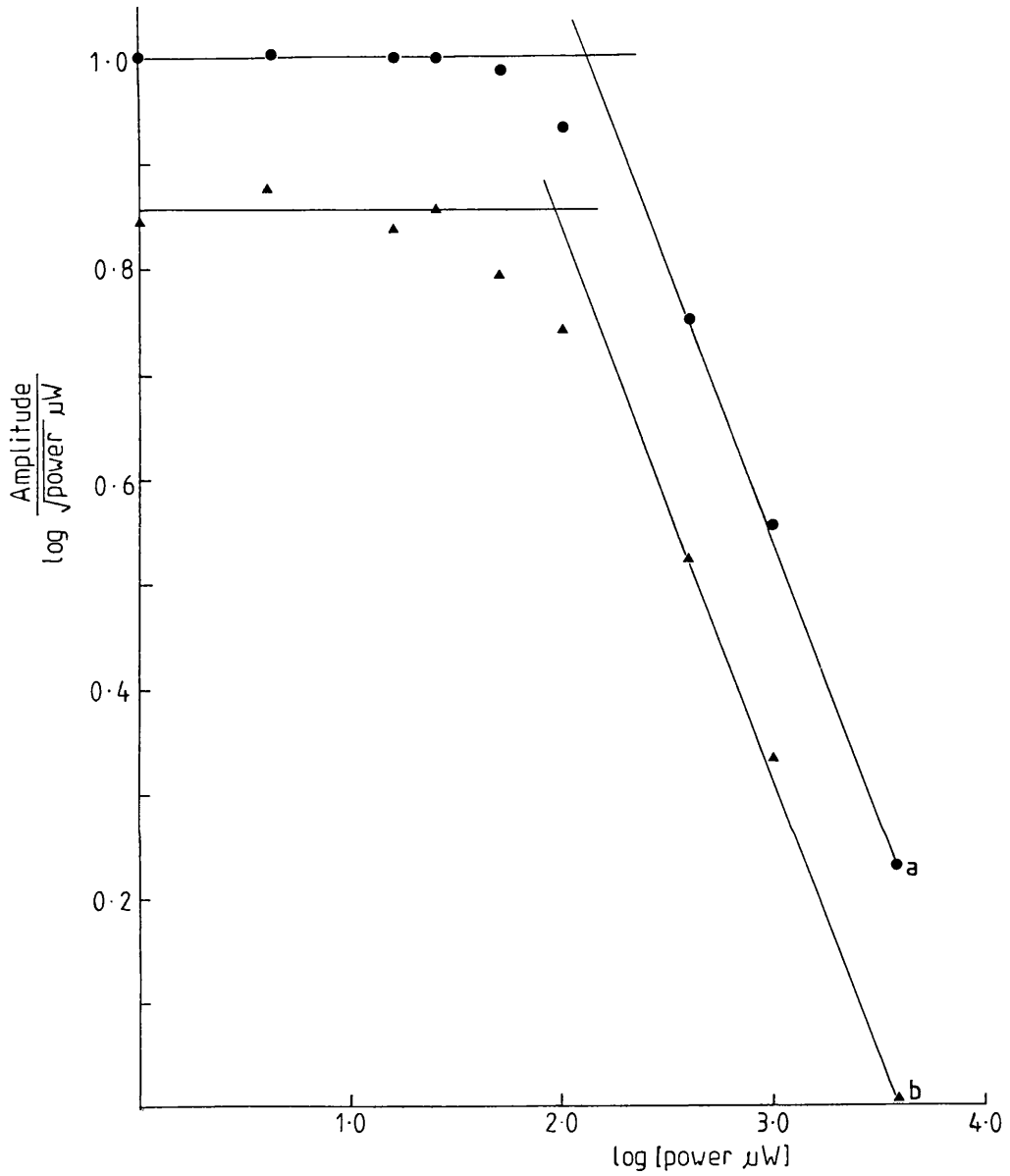

Fig.3·20. Measurement of power saturation of the D^+ signal II epr spectrum after (a) 4 h dark adaptation (pH 6.3 NaCl washed PS2) producing 100 % S_1 state, power saturated at 103 uW, and (b) 4 h dark adapted Tris washed PS2, power saturated at 87 uW. Chl and epr conditions as in fig. 19.

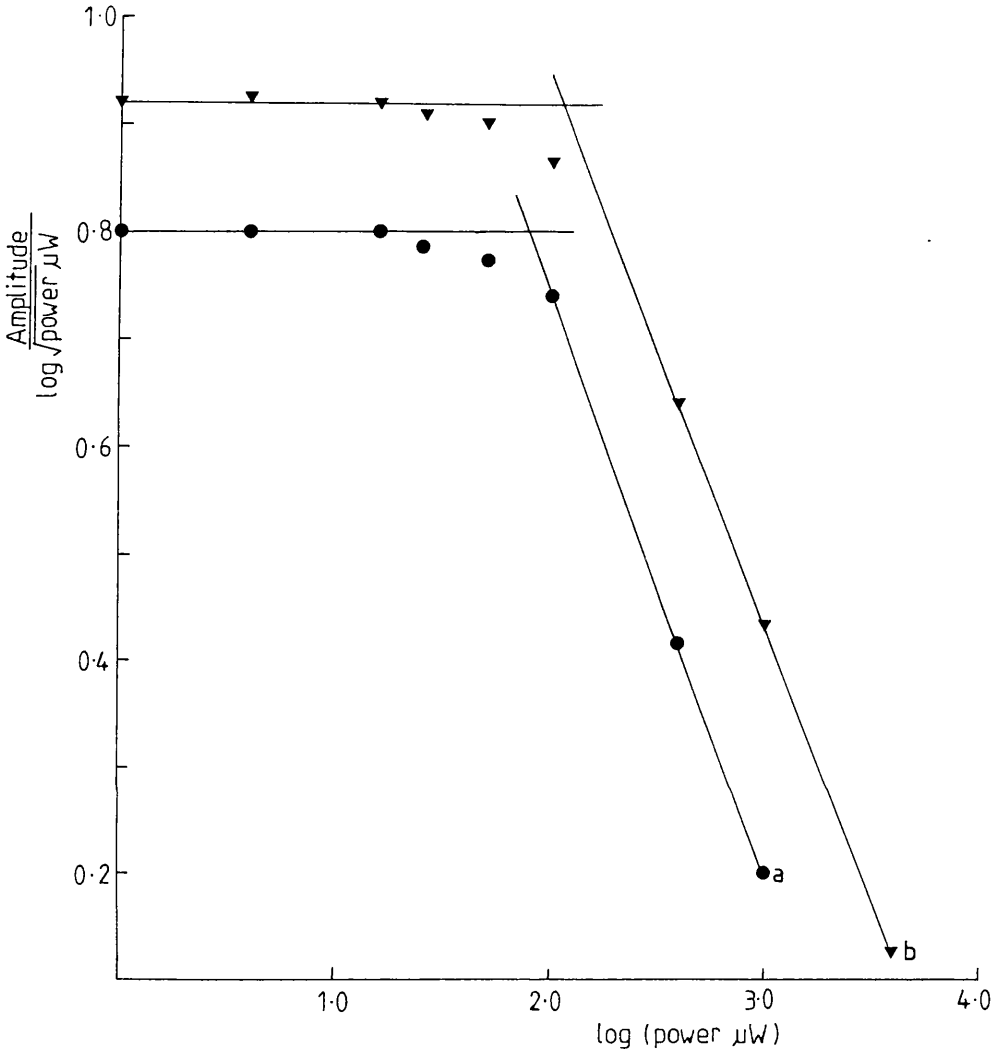

Fig. 3-21. Measurement of the power saturation of the D^+ signal II epr spectrum from Scenedesmus obliquus. (a) The LF1 mutant, power saturated at 76 uW, (b) The wild type, power saturated at 110 uW.
Chl concentration, 4 mg /ml; Epr conditions, modulation amplitude, 0.2 mT; temperature 120 K.

From figures 19, 20 and 21 it can be seen that the apparent $P_{1/2}$ of D^+ varied according to the redox state and the coupling of the manganese cluster. In the S_1 state (formed by 4 hours dark adaptation) D^+ was power saturated at lower powers than in the S_2 state (formed by 200 K illumination (Fig. 19. a and 20. a) (see materials and methods for an explanation of the power saturation phenomena). The power saturation of D^+ in the S_1 state was not affected by illumination at 77 K and was not affected by salt washing at pH 6.3. After salt washing at pH 8.3 in the dark, signal II was power saturated at higher power than in the S_1 state but at lower power than in the S_2 state (Fig. 19. b). This is what would be expected if the pH 8.3 dark salt washed PS2 membranes were inhibited in the S_0 state (see however results section on pH 8.3 salt wash). When the manganese cluster was removed, for instance by 1.0 M Tris washing, signal II slow saturated at lower powers than when the manganese cluster was present in any S state (Fig. 20. b).

In Summary:

PS2 preparation	Proposed S state	$P_{1/2}$ (power satn)
pH 6.3 NaCl washed 4 hours dark	S_1 state	103 uW
pH 6.3 NaCl washed 200 K illumination	S_2 state	141 uW
pH 8.3 NaCl washed 4 hours dark	S_0 state	126 uW
Tris washed PS2	manganese removed	87 uW

3.5.7.4 The Power Saturation of Signal II slow from the LF1 mutant and Wild Type of Scenedesmus obliquus.

The LF1 mutant is able to synthesise PS2, but the D1 polypeptide is not processed. Manganese ions are not able to bind to the oxygen evolving complex.

The amplitude of signal II slow of the LF1 mutant was not significantly different from that of signal II slow from the wild type per mg of chlorophyll. The power saturation characteristics of each however were different. In four hour dark adapted samples Signal II slow from the LF1 mutant was power saturated at lower powers than the wild type. In fig. 21 the $P_{1/2}$ of signal II slow measured at 120 K was 110 uW in the wild type (Fig. 21. b) and 76 uW in the LF1 mutant (Fig. 21. a). The absence of the manganese cluster therefore decreases the $P_{1/2}$ (as observed in Tris washed spinach PS2).

Therefore Signal II slow relaxes fastest in the higher S states giving rise to a high $P_{1/2}$. PS2 membranes in the S_1 state give rise to a slow relaxation of signal II slow. When the manganese is not present as in Tris washed PS2 and the LF1 mutant the relaxation of the D^+ signal is slowest. Therefore the manganese complex and D^+ must be close enough together for the manganese complex to affect the relaxation properties of signal II. The power saturation of the D^+ epr signal after pH 8.3 NaCl washing is consistent with a population of the S_0 state of the oxygen evolving complex.

3.6 Removal of Calcium at pH 8.3 in the dark

In untreated PS2 the approximately 25% of centres in the S_0 state was oxidised slowly to S_1 over a period of 4 hours in the dark. This corresponded to loss of D^+ during the 4 hour dark adaptation and an increase of the S_2 state multiline formed on 200 K illumination as described in section above. Illumination at 200 K allowed only a single turnover and the transition of the S_1 state to the S_2 state, giving the S_2 multiline epr signal (Fig. 22. a), no higher S states are formed. At pH 6.3 a normal multiline epr signal was induced by 200 K illumination (Fig. 22. a). Neither this signal or the alternative form of the S_2 state, (the g = 4.1 signal) was formed when the pH was raised to pH 8.3 (Fig. 22. b). When the pH of the sample was returned to pH 6.3, the ability to generate the S_2 state multiline epr signal on 200 K illumination was restored (Fig. 22. c).

Photosynthetic oxygen evolution was inhibited in untreated PS2 at pH 8.3. This effect was reversed when the PS2 was returned to pH 6.3. When calcium ions were removed from PS2 by a 2.0 M salt wash at pH 8.3 in the dark, there was almost complete loss of oxygen evolution, which was not reversed on returning to pH 6.3 (Table 4A). The rate of oxygen evolution at pH 6.3 was only restored to a maximum level on addition of mM concentrations of calcium ions. Strontium and vanadyl ions partially restored oxygen evolution (Table 4B).

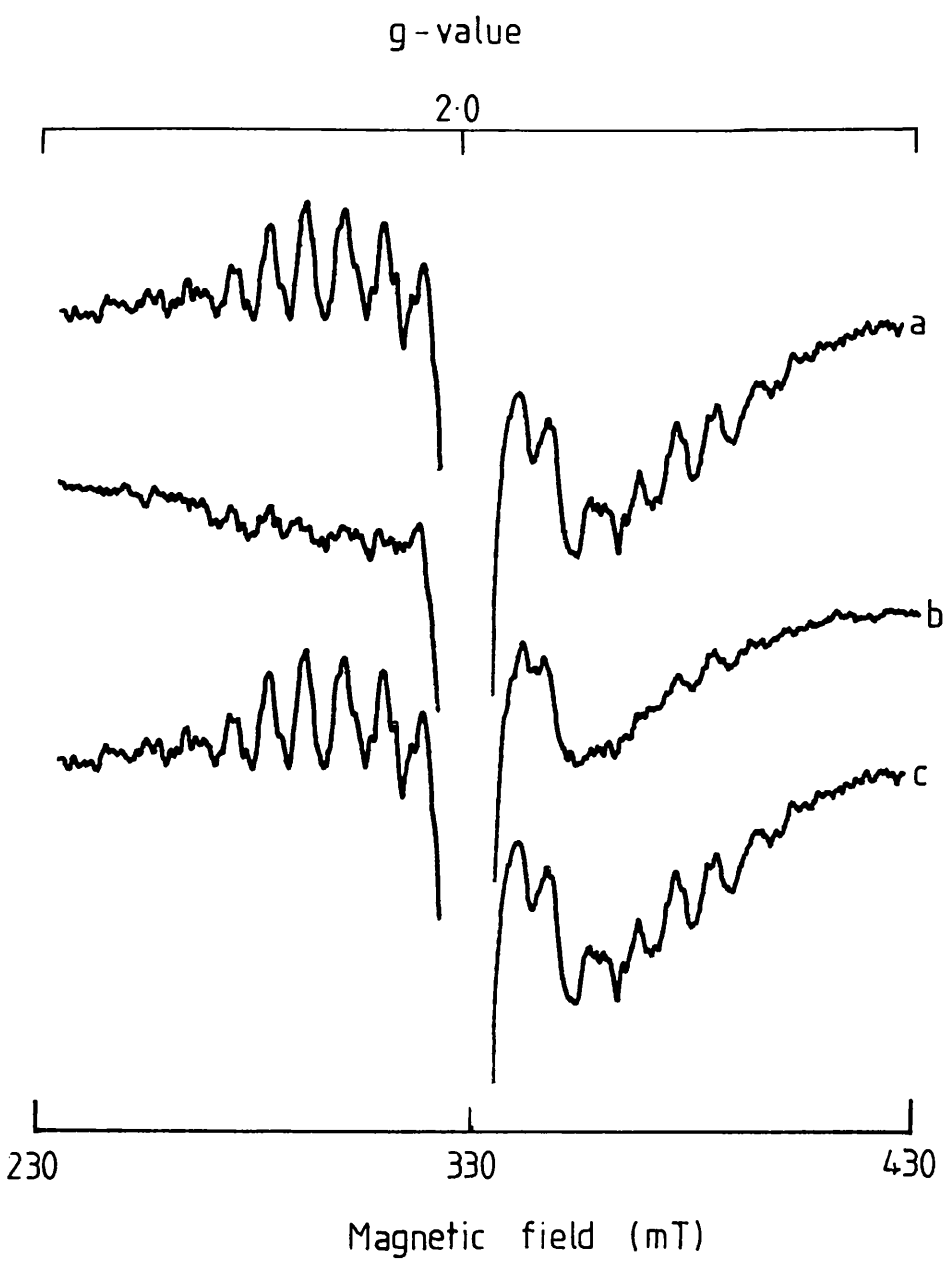

Fig. 3·22. Epr spectra of the S_2 state multiline region following 200K illumination after 4 h dark adaptation on ice. PS2 membranes (a) at pH 6.3, (b) at pH 8.3 and (c) returned to pH 6.3 from pH 8.3 . Chl concentration, 5 mg/ml. Epr conditions: power, 10 mW; temperature 8.5 K; modulation width, 1 mT.

Table 4. Rates of oxygen evolution by pH 8.3 NaCl washed PS2

Assay Conditions	Rate (umoles O_2/mg Chl/h)	
A. Untreated PS2		
No Additions pH 6.3	583	
No Additions pH 8.3	30	
No Additions (returned to pH 6.3)	520	
B. pH 8.3 NaCl washed PS2 measured at pH 6.3		% Ca^{2+} rate
(1) No Additions	35	(13.0)
(2) 20mM $CaCl_2$	265	(100.0)
(3) 20mM $SrCl_2$	176	(66.5)
(4) 20mM VO^{2+}	102	(38.5)

Other details of assay in Materials and Methods

The epr and oxygen electrode results clearly show that the normal functioning of the S state cycle of oxygen evolution was therefore perturbed at pH 8.3. It has been suggested that at pH 8.3 in the dark a uniform S_0 state is formed (see introduction). If a large fraction of the OEC were converted to the S_0 state at pH 8.3 in the dark, on returning the sample to pH 6.3 the S_0 state would have to be oxidised to the S_1 state before the S_2 state could be formed by 200 K illumination. The oxidation of the S_0 state would be expected to correspond to a large reduction in D^+. No significant reduction in

the size of the D^+ epr signal was observed when PS2 membranes were placed in the dark at pH 8.3 for 10 minutes and then returned to pH 6.3. No significant change in the characteristics of D^+ amplitude during 4 hour dark adaptation was observed when PS2 membranes were returned to pH 6.3 from pH 8.3. These results suggest the possibility that either (1) a large population of S_0 was not formed by pH 8.3 washing in the dark, or (2) the restoration of the S_1 state was rapid and therefore not detected, or (3) D was not involved in the S_0/S_1 state changes at pH 8.3 and after return to pH 6.3.

The possibility that the pH 8.3 effect may have been due to changes in the affinity of binding of the calcium cofactor was investigated. A 2.0 M salt treatment was incorporated into the pH 8.3 wash to remove calcium ions. If the S_0 state was formed at pH 8.3 in the dark the calcium binding site would have a lower affinity for calcium than in the dark in the S_1 state. (Boussac & Rutherford , 1988b).

After salt washing at pH 8.3 in the dark and returning to pH 6.3, the characteristic 25 % decay of D^+ on 4 hour dark adaptation was not seen (Fig. 23. a). This means that there was no slow oxidation of the S_0 state to the S_1 state. The epr spectrum of the 4 hour dark adapted pH 8.3 dark salt washed PS2 is shown in Figure 24.a. This shows an unusual small dark stable "multiline - like" epr signal consisting of several lines extending over 200 mT.

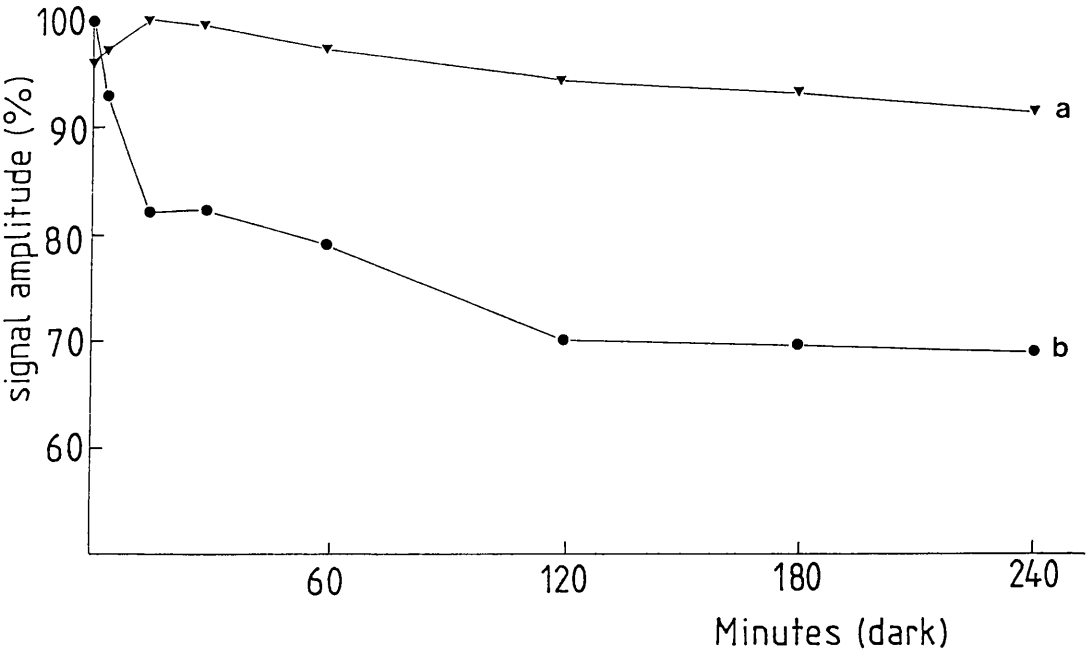

Fig. 3·23. Time course of D^+ reduction at pH 6.3 during dark adaptation after salt washing at pH 8.3 in the dark. (a) No additions, (b) 20 mM $CaCl_2$ added. Chl and epr conditions as in Fig. 13.

This suggests that the manganese complex was not in the normal epr silent S_1 state. No S_2 state multiline epr signal was generated on 200 K illumination (Fig. 24. b) and none of the g = 4.1 S_2 state epr signal was formed in its place (Fig. 8.). Therefore a situation had been created where there was irreversible inhibition of the S state cycle of oxygen evolution on returning to pH 6.3. The pH 8.3 salt wash in the dark also removes the ability to generate the normal S_2 state of the OEC.

The pH 8.3 NaCl washed PS2 membranes were depleted of the D^+ epr signal as described in 3.5.5.2. After 200 K illumination and dark storage for 7 days at 77 K (without calcium reconstitution) there was no increase in the size of the D^+epr signal upon thawing. Untreated BBYs and pH 6.3 salt washed BBYs show a large increase in the size of the D^+ epr signal after this treatment (section 3.5.5.2). This suggests that there is no S_2 state present that is to reoxidise D after pH 8.3 salt washing in the dark.

When calcium ions were reconstituted into the depleted samples there was an immediate loss of the unusual dark stable spectrum (Fig. 24. c) and an immediate rapid approximately 50% reduction of D^+. During dark adaptation of the reconstituted sample, a further fast decrease in D^+, was followed by a slow reduction of D^+ with a total 25 % loss during 4 hours dark adaptation (Fig. 23. b). After this 4 h dark period followed by 200 K illumination the normal S_2 state multiline epr signal

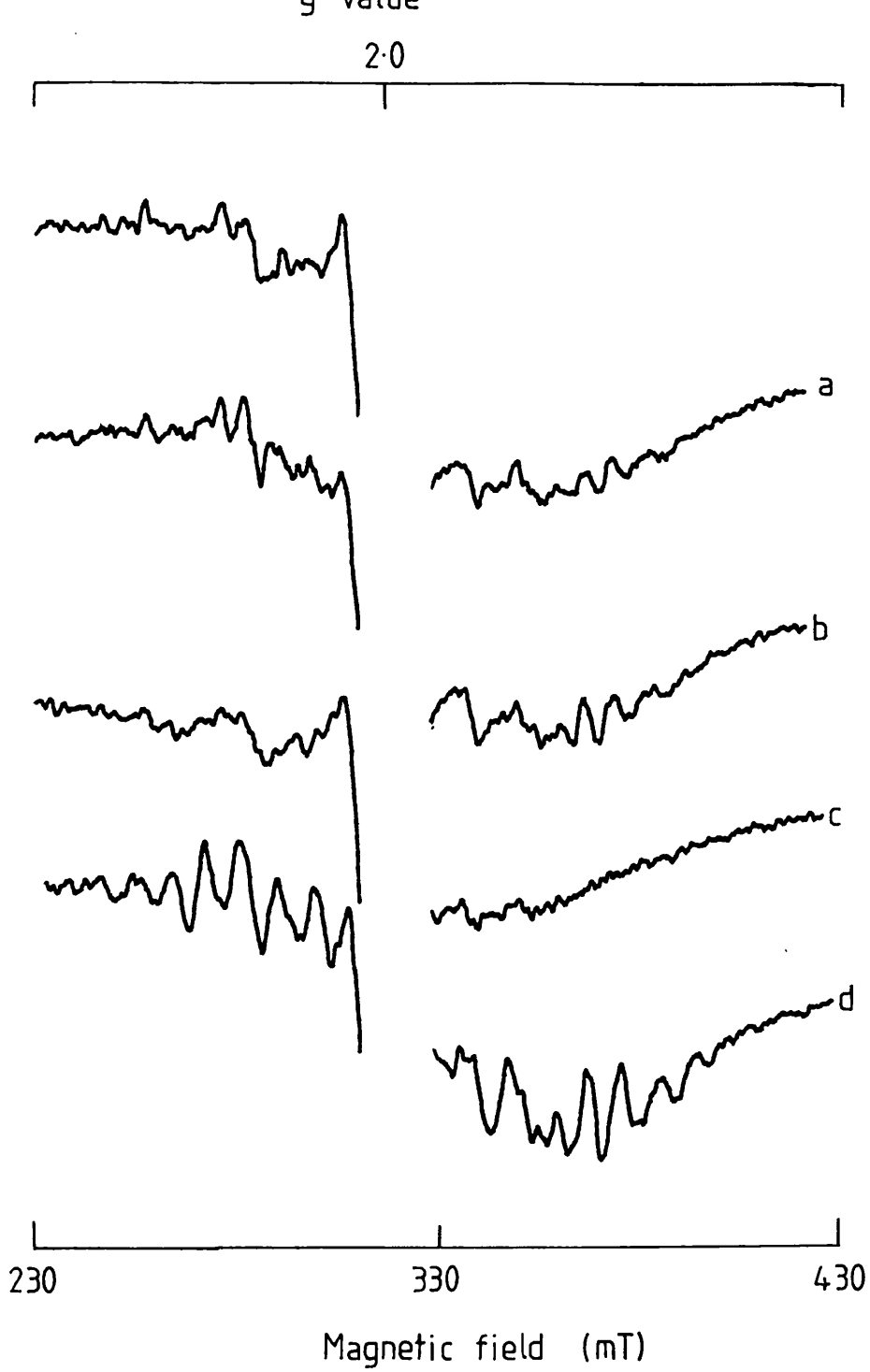

Fig.3·24. The effect of calcium depletion at pH 8.3 on the ability to induce the S_2 state multiline epr signal by 200 K illumination at pH 6.3 . (a) 4h dark, no additions (b) as (a), illuminated at 200 K (c) 4 h dark, but 20 mM $CaCl_2$ added in the dark (d) as (c), illuminated at 200 K. Chl and epr conditions as in Fig. 13.

was formed (Fig. 24.d).

These results suggest that when calcium was depleted during the pH 8.3 salt wash in the dark the S state cycle became trapped in a non-functional state. When calcium ions were reconstituted the manganese complex assumed a functional conformation, the normal S_1 state was formed which in turn lead to the ability to induce the S_2 state multiline epr signal. These experiments provide further evidence that calcium ions are essential for the process of the reduction of D^+ by oxidation of the S_0 state to the S_1 state and suggest that calcium binding influences the advance of the S state cycle.

There is therefore a clear difference between this method of calcium depletion and more conventional methods of calcium depletion which do not remove the ability to form the S_2 state multiline epr signal (see fig. 11 and 12). The PS2 depleted of calcium at pH 8.3 in the dark could be trapped in a state equivalent to the S_0 state, whilst PS2 depleted at lower pH remains in the S_1 state in the dark.

The loss of the ability for D^+ reduction to occur during 4 hours in the dark and the ability to form the multiline signal after salt washing at pH 8.3 in the dark was restored by the addition of micromolar concentrations of vanadyl ions and millimolar concentrations of strontium ions (Fig. 25.). These results provide evidence that both strontium and vanadyl ions are replacing the

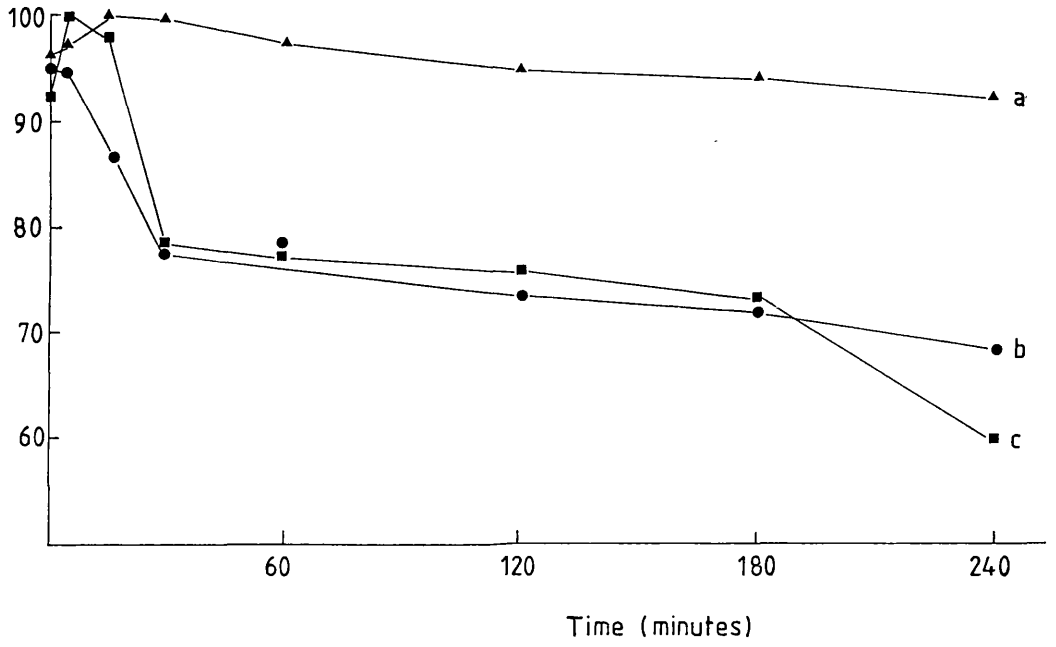

Fig. 3·25. The effect of calcium analogues on the time course of D^+ reduction at pH 6.3 after salt washing at pH 8.3 in the dark. (a) No additions, (b) 20mM $SrCl_2$ added, (c) 50 uM vanadyl (VO^{2+}) added. Chl and epr conditions as in Fig. 13.

function of calcium ions involved in oxygen evolution. Strontium ions cause hyperfine alterations in the S_2 state multiline epr signal (Fig. 10). Vanadyl ions however have not been observed to cause alterations in the S_2 state multiline epr signal.

3.7 Vanadyl Ions

3.7.1 Illumination of OGP PS2 Increased the amount of Vanadyl ion binding

Strontium and vanadyl ions partially replace calcium activity by stimulating oxygen evolution after calcium depletion in pH 6.3 salt washed PS2 (Table 2), pH 8.3 salt washed PS2 (Table 4), citrate washed PS2 (Table 3) and in OGP PS2 (Table 5). This suggests that both of these ions bind to the site of calcium binding and are able to partially replace the function of the calcium ions. Investigation of the vanadyl epr signal indicated that the ions bound more readily to PS2 during illumination. The epr signal associated with bound vanadyl increased in amplitude after illumination of the PS2 preparations.

Investigation of competitive binding of vanadyl ions and calcium ions to OGP PS2 showed that slow cycling of the S states by illumination allowed vanadyl ions to become tightly bound to OGP PS2 (Table 5). A rate of oxygen evolution approximately 40 % of the rate

associated with calcium was observed in the presence of vanadyl ions. This rate of oxygen evolution could not be stimulated to the higher rate of oxygen evolution associated with calcium by the addition of calcium (Table 5. iv and v). The binding of vanadyl ions to OGP PS2 appeared to be dark stable (Table 5. v) since after dark storage of the illuminated vanadyl treated PS2 the rate could not be stimulated to the rate of oxygen evolution associated with calcium. When both calcium and vanadyl ions were added in the dark, there was competition between the divalent cations for the calcium binding site upon illumination giving an intermediate rate between the vanadyl and calcium rate (Table 5. vi). These results suggest that vanadyl ions are competing for one or more calcium binding site involved in water oxidation.

Table 5. Rates of oxygen evolution by OGP PS2 after reconstitution with calcium and vanadyl ion ions

Assay Conditions	Rate (umoles O_2/ mg Chl/h)	% Ca^{2+} rate
(i) 5 mM $CaCl_2$	530	(100)
(ii) No additions	148	(28)
(iii) 3mM vanadyl ion (dark)	223	(42)
(iv) 3mM vanadyl ion (illuminated) then 5 mM $CaCl_2$	270	(51)
(v) 3mM vanadyl ion, (illuminated then dark 3 min) then 5 mM $CaCl_2$)	281	(53)
(vi) 3 mM vanadyl ion + 5mM $CaCl_2$ (dark)	413	(78)

Other details of assay in Materials and Methods

3.7.2 The Binding of Vanadyl Ions to the D1/D2 cytochrome b_{559} reaction centre complex.

Using epr spectrometry it was possible to detect the binding of vanadyl ions to the D1 / D2 cytochrome b_{559} reaction centre complex. A frozen solution of vanadyl ions in pH 8.3 Tris buffer (as described in the methods section) has no epr spectrum when gassed with oxygen free nitrogen (Fig. 26. a). An epr spectrum arising from vanadyl ions was detected when vanadyl ions were added to

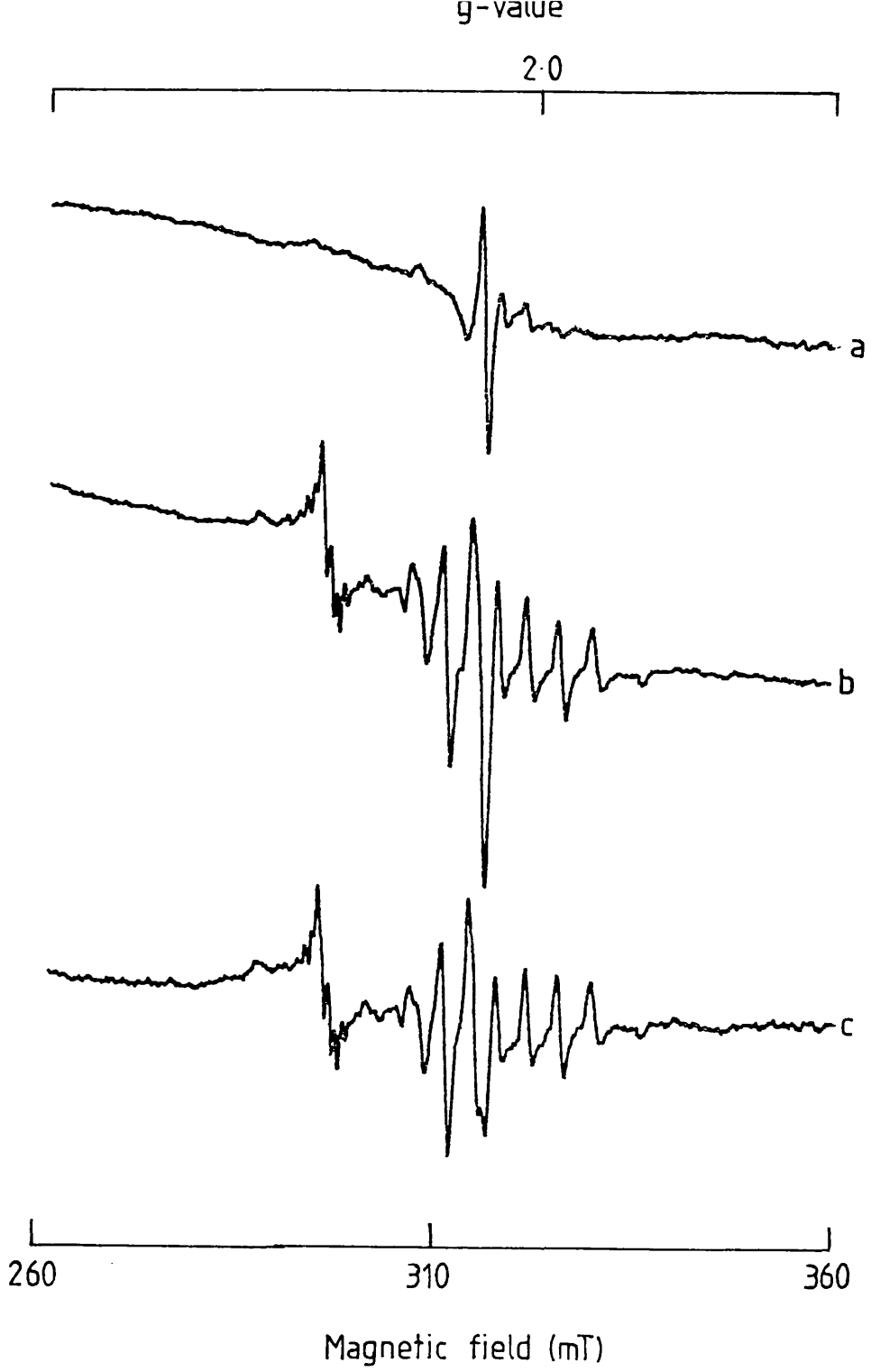

Fig. 3·26. The epr signal arising from vanadyl ions bound to the D1 /D2 cytochrome b_{559} reaction centre complex. (a) Oxygen free 25 uM vanadyl sulphate hydrate added to oxygen free Tris /HCl buffer pH 7.2. (b) As in a), but with the reaction centre complex suspended in the buffer. (c) Difference spectrum, showing the characteristic vanadyl spectrum associated with vanadyl ions bound to the reaction centre complex. Epr conditions: power, 10 mW; temperature, 185 K; modulation width, 1 mT.

a buffer containing reaction centre complexes gassed with oxygen free nitrogen to remove dissolved oxygen (Fig. 26 b and c).

When vanadyl ions were added to reaction centre complexes with calcium ions already added, competition between the two ions was observed. Calcium was added first in all cases. When calcium and vanadyl ions were added in equal proportions there was no significant decrease in the size of vanadyl epr spectrum. When 25 uM vanadyl ions were added to reaction centre complexes with 1 mM $CaCl_2$ already added, the size of the observed vanadyl epr spectrum was decreased by approximately 70 %.

This suggests that vanadyl ions are binding to the D1/D2 cytochrome b_{559} complex, and that the binding of the vanadyl ions is inhibited by the addition of excess calcium. This may be explained by the presence of a low or high affinity calcium binding site on the D1/D2 reaction centre complex. The affinity of the binding site for calcium ions and for vanadyl ions may be different. Vanadyl ions form very strong ligands with polypeptides and this might explain the high levels of calcium (mM) required to prevent the binding of uM amounts of vanadyl ions.

Chapter 4

Discussion of the Role of Calcium Ions

The investigation of the role of calcium in photosynthetic water splitting has highlighted the fact that many research groups are using slightly different PS2 preparations. This results in a very variable degree of calcium depletion and has caused inconsistencies in the results obtained by different groups. To explain these descrepancies calcium binding sites with three different affinities have recently been proposed (Kalosaka et al, 1989).

Three proposed dissociation constants for calcium binding are:

(1) Very High Affinity	Km_1	1-4 uM
(2) High Affinity	Km_2	67-97 uM
(3) Low Affinity	Km_3	2.7- 7 mM

This does not necessarily reflect the existence of three calcium binding sites, but may reflect different states of one or two sites.

When calcium has been removed by salt washing in the light or dark with EGTA added, as in this study, the formation of the S_2 state multiline epr signal is only

slightly inhibited. Kalosaka K. et al, 1989 have however used more rigorous conditions for the depletion of calcium in the dark (using a calcium ionophore A23187 and EGTA). This resulted in the loss of the ability to generate the S_2 state multiline epr signal. The OEC was inhibited in an epr silent state, presumably the S_1 state. This effect has been correlated to the depletion of the very high affinity site (Km_1 1-4 uM).

The differences between salt washing in the light or in the dark (at pH 6.3) observed in this thesis, are known to be due to the different affinities of the S states for calcium (the S_1 state having the highest affinity). These effects can be explained in relation to the three different affinities for calcium. When the 17 and 23 kDa extrinsic polypeptides are removed by a 1.8 M NaCl wash in the presence of 1 mM EGTA in the dark, only the low affinity (Km_3 2.7 - 7 mM) site might be depleted. When the same procedure is carried out in room light with the artificial electron acceptor PPBQ present, the high affinity site (Km_2 67 - 97 uM) may be depleted. This would account for the lower rates of oxygen evolution from the PS2 washed in the light. The two different affinities for calcium could be considered to be of the same calcium binding site, in different states. This interpretation is consistent with the different affinities associated with the different S states (Boussac & Rutherford , 1988b). The S_1 state may

therefore have the high or very high affinity calcium binding site and the S_3 state may have the low affinity binding site.

How do the results observed when PS2 membranes are salt washed at pH 8.3 in the dark, fit in with these theories for calcium binding site affinities?

In this thesis it is suggested that the S_0 state is formed at pH 8.3 in the dark. In this state there may be a lower affinity for calcium binding than in the S_1 state. This has also been suggested by Boussac A. and Rutherford A.W., 1988b. Calcium binding is certainly of a lower affinity than during salt washing at pH 6.3 in the dark.

A dark stable 26 line "multiline - type" epr signal has been recently reported by Boussac & Rutherford , 1989 and by Ono. and Inoue , 1989, extending over 1600 gauss, with average line spacing of 55 gauss. The signal reported by Boussac & Rutherford , 1989 is formed after salt washing in the light (in the presence of PPBQ and EGTA) followed by 80 - 85 % reconstitution with the 17 and 23 kDa extrinsic polypeptides. The signal reported by Ono & Inoue , 1989 is formed by a similar procedure but without polypeptide reconstitution.

An epr signal stable at room temperature in the dark that is similar to the S_2 state multiline epr signal is also present after a pH 8.3 salt wash in the dark. The

main difference between the dark stable signal reported by Boussac & Rutherford , 1989, Ono and Inoue ., 1989 and the dark stable multiline signal reported in this thesis is the pH and illumination conditions.

Boussac & Rutherford , 1989 have also reported the appearance of another new epr signal at g = 2.004, extending over 164 gauss. The signal has characteristics which are typical of a magnetic interaction between an organic free radical and the manganese cluster. This epr signal is formed when a sample displaying the dark stable multiline epr signal is illuminated at 0 °C. The signal replaces the dark stable "multiline - type" epr signal. When the light is turned off this signal decays away and the dark stable "multiline - type" epr signal returns. This characteristic and the kinetic characteristics of the two signals upon calcium reconstitution suggests that the g = 2.004 signal is from a modified S_3 state and the dark stable signal is from a modified S_2 signal (Fig. 1.).

If the model for the redox state of the manganese cluster from the introduction (Fig. 6) is recalled, it is tempting to suggest that this signal arises from an interaction of an oxidised histidine (formed in the S_3 state of model 6. a) and the manganese cluster. The method of calcium removal in the light by Boussac & Rutherford ., 1989 suggests that calcium may be removed in the higher S states probably the S_3 state.

Fig 1. Scheme for the Formation of the Various Modified and Normal Epr Signals Associated with the pH 6.3 NaCl wash

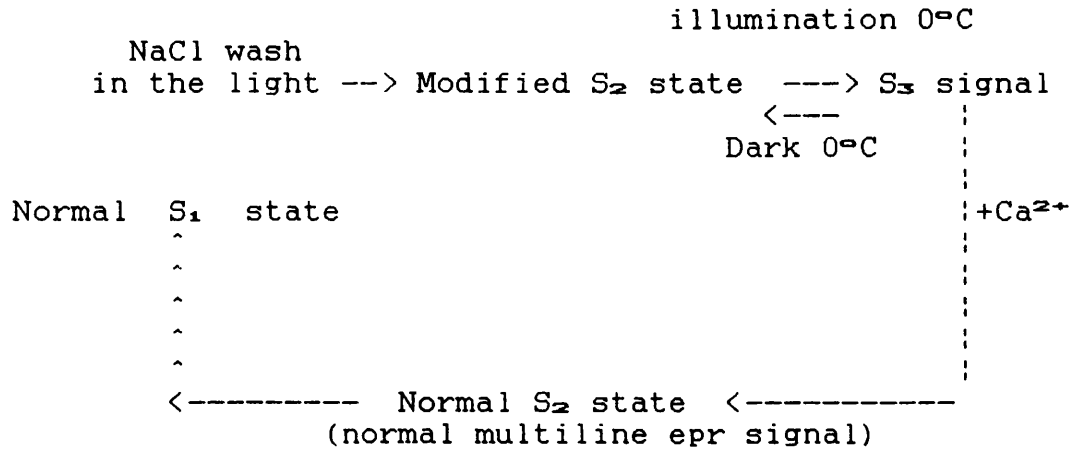

Calcium depletion by the method of Boussac . & Rutherford . ., 1989 inhibits the formation of the S_1 state in the dark. An abnormal dark stable S_2 state is observed. During illumination at 0 °C a modified S_3 state is formed, which decays back to the dark stable S_2 state in the dark. The effect of calcium reconstitution is shown.

It has been suggested that calcium acts by providing the substrate water and chloride ions at the right moment during the S state cycle of oxygen evolution (Rutherford , 1989). In this model chloride ligands could affect the redox properties of the manganese complex. Manganese liganded to chloride ions would be more difficult to oxidise. This would prevent water oxidation at states formed before the S_4 state. Therefore the chloride ligands could help to control the oxidation of the manganese complex. The calcium ions could function by forming ligands to the chloride ions when they are not liganded to the manganese complex. This would maintain the chloride ions close to the manganese complex ready to form ligands to the manganese complex again after water oxidation had occured. It is then possible to imagine that substrate water molecules might occupy the ligands to the calcium ions when chloride was bound to the manganese complex. The calcium ions could therefore act by switching chloride ligands for water molecules, when the S_4 state was formed, allowing manganese oxidation and water splitting to occur.

The decay charcteristics of the dark stable "mulitline - type signal we observe following a pH 8.3 dark 2.0 M NaCl wash and also the D^+ kinetics observed on readdition of calcium both suggest that this calcium depletion method forms a dark stable S_0 state.

It is possible that part of the large reduction of

D^+ associated with the readdition of calcium could be due to the recombination of dark stable Q_B^- or Q_A^-. This however seems unlikely and certainly does not explain all of the D^+ reduction observed (approximately 75 %). The reasons for this are (1) there is little or no dark stable iron semiquinone epr signal after the dark pH 8.3 salt wash and (2) the large reduction of the D^+ radical is not observed upon calcium reconstitution of PS2 membranes salt washed at pH 6.3 in room light.

The S_2 state multiline epr signal is not formed after chloride extraction (Ono . et al, 1986) or after fluoride substitution (Casey . and Sauer , 1984). Instead of the S_2 state multiline epr signal, the S_2 state g = 4.1 epr signal is formed. The results described in this thesis were not due to the depletion of chloride. No g = 4.1 epr signal or multiline epr signal was observed after the dark pH 8.3 NaCl wash, and high levels of chloride ions (40 mM) were maintained to prevent chloride depletion.

Final Conclusion

Calcium ions have a vital role in water oxidation. After removal of calcium in the S_0 state the S state cycle appears to be completely inhibited and it is not possible to advance from the S_0 state. When calcium ions are removed in the S_1 state, the S_2 state multiline epr signal was still formed on 200 K illumination. No oxygen evolution occured. This suggests that the S state cycle was unable to advance further than the S_3 state.

Calcium ions therefore appear to be vital for the cycling the S states. Calcium is particularly essential to advance from the S_0 state and from the S_3 state.

CHAPTER 5 : REFERENCES

Abramowicz D.A. & Dismukes G.C. (1984) Biochim. Biophys. Acta 765, 318-328.

Akerlund H.E., Andersson B. & Albertsson P.A. (1976) Biochim. Biophys. Acta 449, 525-535.

Akerlund H.-E., Jansson C. & Andersson B. (1982) Biochim. Biophys. Acta. 681, 1-10.

Anderson J.M. & Andersson B. (1982) Trends. Biochem. Sci. 6, 289-292.

Arnon D.I. & Tang G.M.-S. (1988) Proc. Natl. Acad. Sci. 85, 9524-9528.

Babcock G.T. (1987) in New Comprehensive Biochemistry: Photosynthesis, ed Amesz, J. (Elsevier, Amsterdam) 125-158.

Babcock G.T. & Sauer K. (1973) Biochim. Biophys. Acta 325, 483-519.

Babcock G.T. & Sauer K. (1975) Biochim. Biophys. Acta 376, 315-344.

Barber J., Chapman D.J. & Telfer A. (1987) FEBS Lett. 220, 67-73.

Barry B.A. & Babcock G.T. (1987) Proc. Natl. Acad. Sci. 84, 7099- 7103.

Barry B.A. & babcock G.T. (1988) Chemica Scripta 28A 117-122.

Beck W.F., de Paula J.C. & Brudvig G.W. (1985) Biochemistry 24, 3035-3043.

Beck W.F., de Paula J.C. & Brudvig G.W. (1986) J. Am. Chem. Soc 108, 4018-4022.

Beck W.F. & Brudvig G.W. (1988) Chemica Scripta 28A, 93-98.

Berthold D.A., Babcock G.T. & Yocum C.F. (1981) FEBS Lett. 134, 231-234.

Bishop N.I. (1971) Methods of Enzymology, San Pietro, A.ed, 23B 130-143.

Bishop N.I. & Senger H. (1972) Plant Cell Physiol 13, 937-953.

Boardman N.K. & Anderson J.M. (1964) Nature 203, 166-167.

Boussac A. & Rutherford A.W. (1988a) Biochemistry U.S.A. 27, 3476-3483.

Boussac A. & Rutherford A.W. (1988b) FEBS Letts. 236, 432-436.

Boussac A. & Rutherford A.W. (1988c) Chemica. Scripta. 28A, 123-126.

Boussac A. & Rutherford A.W. (1989) VIIIth International Congress on Photosynthesis, Stockholm, poster 771.

Boussac A., Maison-Peteri B., Vernotte C. & Etienne A.L. (1985) Biochim. Biophys. Acta. 808, 231-234.

Briantais J.M., Vernotte C., Lavergne J. & Arntzen C.J. (1977) Biochim. Biophys. Acta 462, 61-74.

Brudvig G.W., Casey J.L. & Sauer K. (1983) Biochim. Biophys. Acta 723, 366-371.

Brudvig G.W. & Crabtree R.H. (1986) Proc. Natl. Acad. Sci. U.S.A. 83, 4586-4588.

Cammarata K. & Cheniae G. (1987) in Progress in Photosynthesis Research (Biggins J. ed) 1, 617-620.

Cannon J.D. & Chasteen N.D. (1975) Biochemistry 14, 4573-4577.

Casey J.L. & Sauer K. (1984) Biochim. Biophys. Acta 767, 21-28.

Chapman D.J., De Felice J., Davis K., Barber J. (1989) Biochem J. 258, 357-362.

Chasteen N.D. (1981) in Biological Magnetic Resonance (Berliner J.L. & Reuben J. Eds) Plenum New York. 3, 53-119.

Christou G. & Vincent J.B. (1987) Biochim. Biophys. Acta 895, 259-274.

Chua N.M. & Bennoun P. (1975) Proc. Natl. Acad. Sci. U.S.A. 72, 2175-2179.

Chua N.M. (1979) Methods of Enzymology 69, 434-446.

Cohn D.E., Cohen W.S. & Bertsch W. (1975) Biochim. Biophys. Acta 376, 97-104.

Cole J., Boska M., Blough N.V. & Sauer K. (1986) Biochim. Biophys. Acta 848, 41-47.

Cole J. & Sauer K. (1987) Biochim. Biophys. Acta. 891, 40-48.

Colman W.J. & Govindjee (1987) Photosynth. Res. 13, 199-224.

Commoner B., Heise J.J., & Townsend J. (1956) Proc. Natl. Acad. Sci. U.S.A. 42, 710-718.

Davis D.J. & Gross E.L. (1975) Biochim. biophys. Acta 387, 557-567.

Debus R.J., Barry B.A., Babcock G.T. & Mcintosh L. (1988) Proc. Natl. Acad. Sci. 85, 427-430.

Dekoch R.J., West D.J., Cannon J.C. & Chasteen N.D. (1974) Biochemistry 13, 4347-4354.

De Groot A., Plitjer J.J., Evelo R., Babcock G.T. & Hoff A.J. (1986) Biochim. Biophys. Acta 848, 8-15.

Deisenhofer J., Epp O., Miki K., Huber R. & Michel H. (1985) Nature 318, 618-624.

Dekker J.P., Ghanotakis D.F., Plitjer J.J., Van Gorkom H.J. & Babcock G.T. (1984) Biochim. Biophys. Acta 767, 515-519.

Dekker J.P., van Gorkom H.J., Wessink J. & Ouwehand L. (1984) Biochim. Biophys. Acta 767, 1-9.

Demetriou C., Lockett C.J. & Nugent J.H.A. (1988) Biochem. J. 252, 921-924.

Diner B.A., Ries D.F. Cohen B.N. & Metz J.G. (1988) J. Biol. Chem. 263, 8972-8980.

Dismukes G.C. & Siderer Y. (1980) FEBS Lett. 121, 78-80.

Dismukes G.C. & Siderer Y. (1981) Proc. Natl. Acad. Sci. U.S.A., 78, 274-278.

Dismukes G.C., Ferris K. & Watnick P. (1982) Photochem. Photobiophys. 3, 243-256.

Dismukes G.C. (1986) Photochem. Photobiol. 43, 99-105.

Dismukes G.C. (1988) Chemica Scripta 28A, 921-924.

Dunahay T.G., Staehelin L.A., Seibert M., Ogilvie P.D. & Berg S.P. (1984) Biochim. Biophys. Acta 764, 179-193.

England R.R. & Evans E.H. (1983) Biochem. J. 210, 473-476.

England R.R. & Evans E.H. (1985) Biochim. Biophys. Acta 808, 323-327.

Evans E.H., McColl S., Tramontini L.S. & Keskin S. (1988) Proc. 6TH Int. Cogr. Photosyn. Prokaryotes, Noordwijkerhout, The Netherlands p.42.

Evans M.C.W., Diner B.A. & Nugent J.H.A. (1982) Biochim. Biophys. Acta 682, 97-105.

Feher G., Allen J.P., Okamura M.Y. & Rees D.C. (1989) Nature 339, 111-116.

Fitzgerald J.J. & Chasteen N.D. (1974) Biochemistry 13, 4338-4347.

Ford R.C. & Evans M.C.W. (1983) FEBS Lett. 160, 159-163.

Forster V. & Junge W. (1985) Photochem. Photobiol. 41, 183-190.

Forster V. & Junge W. (1988) Chemica Scripta 28A, 111-116.

Ghanotakis D.F., O'Malley P.J., Babcock G.T. & Yocum C.F. (1983) in Oxygen Evolving System of Photosynthesis, ed. Inoue, Y. (Academic, Tokyo) 91-101.

Ghanotakis D.F., Babcock G.T. & Yocum C.F. (1984a) Biochim. Biophys. Acta. 765, 388-398.

Ghanotakis D.F., Babcock G.T. & Yocum C.F. (1984b) FEBS lett. 167, 127-130.

Ghanotakis D.F., Babcock G.T. & Yocum C.F. (1985) Biochim. Biophys. Acta 809, 173-180.

Ghanotakis D.F. & Yocum C.F. (1986) FEBS Lett. 197, 244-248.

Ghanotakis D.F., Demetriou D.M. & Yocum C.F. (1987) Biochim. Biophys. Acta. 891, 15-21.

Gitelman S.E. & Witman G.B. (1980) J. Cell Biol. 87, 764-770.

Gounaris K., Barber J. & Harwood J.L. (1986) Biochem. J. 237, 313-326.

Gounaris K., Chapman D.J. & Barber J. (1988) FEBS Lett. 240, 143-147.

Govindjee & Van Rensen J.J.S. (1978) Biochim. Biophys. Acta 505, 183-213.

Hansson O. & Andreasson L.-E. (1982) Biochim. Biophys. Acta. 679, 261-268.

Hannsson O., Andreasson L.-E. & Vanngard T. (1986) FEBS Lett. 195, 151-154.

Hansson O., Aasa R. & Vanngard T. (1987) Biophys J. 51, 825-832.

Homann P.H. (1988a) Biochim. Biophys. Acta 934, 1-13.

Homann P.H. (1988b) Plant. Physiol. 88, 194-199.

Hunziker D., Abramowicz D., Damoder R. & Dismukes G.C. (1987) Biochim. Biophys. Acta 890, 6-10.

Ianuzzi M.M. & Rieger P.H. (1975) Inorg. Chem. 14, 2895-2899.

Ikeuchi M. & Inoue Y. (1988) Plant Cell Physiol. 29, 1233-1239.

Ikeuchi M., Takio K. & Inoue Y. (1989) FEBS Lett. 242, 263-269.

Imaoka A., Yanagi M., Akabori K. & Toyoshima Y. (1984) FEBS Lett. 176, 341-345.

Innes J.B. & Brudvig G.W. (1989) Biochemistry 28, 1116-1125.

Isogai Y., Nishimura M., Iwaki M. & Itoh S. (1988) Biochim. Biophys. Acta. 936, 259-268.

Kalosaka K., Beck W.F., Brudvig G. & Cheniae G. (1989) VIIIth International Congress on Photosynthesis, Stockholm, poster 773.

Kohl D.H. & Wood P.M. (1969) Plant Physiol. 44, 1439-1445.

Koike H., Mamada K., Ikeuchi M. & Inoue Y. (1989) FEBS lett. 244, 391-396.

Kok B., Forbush B. & McGloin M. (1970) Photochem. photobiol. 11, 457-475.

Kuwabara T. & Murata N. (1983) Plant Cell Physiol. 24, 741-747.

Kuwabara T., Miyao M., Murata T. & Murata N. (1985) Biochim. Biophys. Acta. 806, 283-289.

Laemmli U.K. (1970) Nature 227, 680-685.

Lavergne J. (1986) Photochem. Photobiol. 43, 311-323.

Lavergne J. (1987) Biocim. Biophys. Acta 894, 91-107.

Ljungberg U., Akerlund H.-E. & Andersson B. (1984) FEBS. Lett. 175, 255-258.

Lockett C.J., Demetriou C., Bowden S.J. & Nugent J.H.A. (1989) submitted to BBA.

Lubbers K. & Junge W. (1989) VIIIth International Congress on Photosynthesis, Stockholm. Poster 813.

McTavish H., Picorel R. & Seibert M. (1989) Plant. Physiol. 89, 452-456.

Metz J.G. & Bishop N.I. (1980) Biochim. Biophys. Res. Commun. 94, 560-566.

Metz J.G., Wong J. & Bishop N.I. (1980) FEBS lett. 114, 61-66.

Metz J.G. & Seibert M. (1984) Plant Physiol 76, 829-832.

Meyer B., Schlodder E., Dekker J.P. & Witt H.T. (1989) Biochim. Biophys. Acta 974, 36-43.

Michel H. & Deisenhofer J. (1986) photosynthesis III (Staehelin L.A. & Arntzen C.J. Eds.) 371-381.

Michel H. & Deisenhofer J. (1988) Biochemistry 27, 1-7.

Miller K.R. & Lyon M.K. (1985) Trends. Biochem. Sci. 219-222.

Minami E. & Watanabe A. (1985) Plant Cell Physiol. 26, 839-849.

Mitchell P. (1977) FEBS Lett. 78, 1-20.

Miyao M. & Murata N. (1983) Biochim. Biophys. Acta. 725, 87-93.

Miyao M. & Murata N. (1984) FEBS lett. 170, 350-354.

Miyao M. & Murata N. (1985) FEBS Lett. 180, 303-308.

Miyao M., Murata N., Lavorel J., Maison-Peteri B., Boussac A. & Etienne A.-L. (1987) Biochim. Biophys. Acta 890, 151-159.

Murata N. & Miyao N. (1985) Trends. Biochem. Sci. 10, 122-124.

Nanba O. & Satoh K. (1987) Proc. Natl. Acad. Sci. U.S.A. 84, 109-112.

Nieves J., Kim L., Puett D. & Echegoyen L. (1987) Biochemistry 26, 4523-4527.

Nugent J.H.A. & Evans M.C.W. (1980) FEBS Lett. 112, 1-4.

Nugent J.H.A., Diner B.A. & Evans M.C.W. (1981) FEBS Lett. 124, 241-244.

Nugent J.H.A., Evans M.C.W. & Diner B.A. (1982) Biochim. Biophys. Acta 682, 106-114.

Nugent J.H.A. (1987) Biochim. Biophys. Acta 893, 184-189.

Nugent J.H.A., Demetriou C. & Lockett C.J. (1987) Biochim. Biophys. Acta 894, 534-542.

Nugent J.H.A., Corrie A.R., Hubbard J.A.M., Bowden S.J., Demetriou C., Lockett C.J. & Evans M.C.W. (1988) (in press).

Nugent J.H.A., Corrie A.R., Demetriou C., Evans M.C.W. & Lockett C.J. (1988) FEBS lett. 235, 71-75.

Oh-oka H., Wada K., Kuwabara & Murata N. (1986) 197, 1, 2, 63-66.

Okamura M.Y., Feher G. & Nelson N. (1982) in Photosynthesis ed. Govindjee (Academic, New York) 195-272.

O'Malley P.J., Babcock G.T., & Prince R.C. (1984) Biochim. Biophys. Acta. 766, 283-288.

Ono T.A. & Inoue Y. (1983) FEBS Lett. 164, 255-260.

Ono T.A. & Inoue Y. (1986) Biochim. Biophys. Acta 850, 380-389.

Ono T.A. & Inoue Y. (1988) FEBS Lett. 227, 147-152.

Ono T.A. & Inoue Y. (1989a) Biochim. Biophys. Acta. 973, 443-449.

Ono T.A. & Inoue Y. (1989b) VIIIth International Congress on Photosynthesis, Stockholm, poster 778.

Ono T.A., Zimmermann J.-L. Inoue Y. & Rutherford A.W. (1986) Biochim. Biophys. Acta. 851, 193-201.

Packham N.K. & Barber J. (1984) Biochim. Biophys. Acta 764, 17-23.

Petrouleas V. & Diner B.A. (1986) Biochim. Biophys. Acta 849, 265-275.

Plitjer J.J., de Groot A., van Dijk M.A. & van Gorkom H.J. (1986) FEBS Lett. 195, 313-318.

Prince R.C. (1988) Trends. Biochem. Sci. 13, 286-288.

Reimer S. & Trebst A. (1975) Biochem. physiol. Pflanz 168, 225-232.

Reisfeld A., Mattoo A.K. & Edelman M. (1982) Eur. J. Biochem. 124, 125-129.

Regitz G. & Ohad I. (1976) J. Biol. Chem. 251, 247-252.

Renger G., Hagemann R. & Fromme R. (1986) FEBS Lett. 203, 210-214.

Renger G., Fromme R. & Hagemann R. (1988) Biochim. Biophys. Acta 935, 173-183.

Renger G. & Hanssum B. (1988) Photosyn. Res. 16, 243-259.

Renger G. (1988) Chemica Scripta 28A 105-109.

Rolfe S.A. & Bendall D.S. (1989) Biochim. Biophys. Acta. 973, 220-226.

Rutherford A.W. & Zimmermann J.L. (1984) Biochim. Biophys. Acta 767, 168-175.

Rutherford A.W., Seibert M. & Metz J.G. (1988) Biochim. Biophys. Acta 932, 171-176.

Rutherford A.W. (1989a) Trends. Biochem. Sci. 14, 227-232.

Sakurai H., Hirata J. & Michibata H. (1987) Biochem. Biophys. Res. Comm. 149, 411-416.

Sandusky P.O. & Yocum C.F. (1984) Biochim. Biophys. Acta. 766, 603-611.

Sandusky P.O. & Yocum C.F. (1986) Biochim. Biophys. Acta 849, 85-93.

Saphon S. & Crofts A.R. (1977) Z. Naturforsch 32C, 617-626.

Sauer K., Guiles R.D., Mcdermott A.E. & Cole J.L. (1988) Chemica. Scripta. 28A, 87-91.

Saygin O & Witt H.T. (1987) Biochim. Biophys. Acta 893,

452-469.

Shen J.-R., Satoh K. & Katoh S. (1988a) Biochim. Biophys. Acta. 933, 358-364.

Shen J.-R., Satoh K. & Katoh S. (1988b) Biochim. Biophys. Acta 936, 386-394.

Staehelin L.A. & Arntzen C.J. (1983) J. Cell Biol. 97, 1327-1337.

Stewart A.C., Ljunberg U., Akerlund H.E. & Andreasson B. (1985a) Biochim. Biophys. Acta 808, 353-362.

Stewart A.C., Sickowski M. & Ljunberg U. (1985b) FEBS Lett. 193, 175-179.

Styring S.A. & Rutherford A.W. (1988) Biochemistry 27, 4915-4923.

Swartz H.M., Bolton J.R. & Borg D.C. (1972) Biological Applications of Electron Spin Resonance, Wiley-Interscience.

Tamura N. & Cheniae G.M. (1987) Biochim. Biophys. Acta 890, 179-194.

Tamura N., Ikeuchi M. & Inoue Y. (1989) Biochim. Biophys. Acta 973, 281-289.

Taylor M.A., Nixon P.J., Todd C.M., Barber J. & Bowyer J.R. (1988) FEBS Lett. 235, 109-116.

Trebst A. (1987) Z. Naturforsch 42c 742-750.

Trebst A., Depka B., Kraft B. & Johanningmeier U. (1988) Photosynthesis Res. 18, 163-177.

Vermaas W.F.J., Renger G. & Dohnt G. (1984) Biochim. Biophys. Acta 764, 194-202.

Vermaas W.F.J., Rutherford A.W. & Hansson O. (1988) Proc. Natl. Acad. Sci. 85, 8477- 8481.

Volker M., Eckert H.-J. & Renger G. (1987) Biochim. Biophys. Acta. 890, 66-76.

Wales R., Newman B.J., Pappin D. & Gray J.C. (1989) Plant Mol. Biol. in press.

Warden J.T., Blankenship R.E. & Sauer K. (1976) Biochim. Biophys. Acta 423, 462-478.

Weaver E.C. (1962) Arch. Biochem. Biophys. 99, 193-196.

Webber A.N. & Gray J.C. (1989) FEBS Lett. 249, 79-82.

Wille B. & Lavergne J. (1982) Photochem. Photobiophys. 4, 131-144.

Williams J.C., Steiner L.A., Ogden R.C., Simon M.I. & Feher G. (1983) Proc. Natl. Acad. Sci. U.S.A. 80, 6505-6509.

Williams J.C., Steiner L.A., Feher G. & Simon M.I. (1984) Proc. Natl. Acad. Sci. 81, 7303-7307.

Wraight C.A. (1985) Biochim. Biophys. Acta 809, 320-330.

Yachandra V.K., Guiles R.D., McDermott A., Britt R.D., Dexheimer S.L., Sauer K. & Klein M.P., (1986) Biochim. Biophys. Acta 850, 324-332.

Youvan D.C., Bylina B.J., Alberti M., Begusch H. & hearst J.E. (1984) Cell 37, 949-957.

Zimmermann J.-L. & Rutherford A.W. (1984) Biochim. Biophys. Acta 767, 160-167.

Zimmermann J.-L. & Rutherford A.W. (1986) Biochim. Biophys. Acta 851, 416-423.

Zurawski G., Bohnert H., Whitfield P.R. & Bottomley W. (1982) Proc. Natl. Acad. Sci. U.S.A. 79, 7699-7703.